IDENTIFICATION AND FUNCTIONAL VALIDATION OF CALDESMON AS A POTENTIAL GASTRIC CANCER METASTASIS-ASSOCIATED PROTEIN

HOU QIAN

NATIONALUNIVERSITY OF SINGAPORE

2013

IDENTIFICATION AND FUNCTIONAL VALIDATION OF CALDESMON AS A POTENTIAL GASTRIC CANCER METASTASIS-ASSOCIATED PROTEIN

HOU QIAN

B. Sc. (*Hons.*), NTU

A THESIS SUBMITTED

FOR THE DEGREE OF

DOCTOR OF PHILOSOPHY

DEPARTMENT OF BIOCHEMISTRY

NATIONALUNIVERSITY OF SINGAPORE

2013

DECLARATION

I hereby declare that the thesis is my original work and it has been written by me in its entirety.

I have duly acknowledged all the sources of information which have been used in the thesis.

This thesis has also not been submitted for any degree in any university previously.

_____

Hou Qian

31 July 2013

ACKNOWLEDGEMENTS

I wish to thank those people who have assisted me throughout my PhD project. First of all, I would like to express my greatest gratitude to my supervisor, A/P Maxey Chung Ching Ming who has provided me the wonderful opportunity to perform the research in his lab. With his constant guidance, help and advice for the past 4 years, this project was made possible. I have benefited tremendously during the journey of my PhD under his supervision.

I would like to thank Dr Tan Hwee Tong for his invaluable mentoring, discussion and help during the past 4 years, thank Dr Tony Lim and Ms Avery Khoo from Singapore General Hospital for the collaboration work done with their mentoring and help. I would also like to thank our lab's former research assistants Ms Cynthia Liang and Ms Tan Gek San for their guidance and assistance. I am also greatly indebted to Dr Lin Qingsong and Mr Lim Teck Kwang for helping me in 2-D LC MALDI-TOF/TOF MS analysis for my samples.

My seniors:Dr Zubaidah, Mr Vincent Lau, Mr Hendrick Loei have helped me in my lab techniques. My labmates: Qifeng, Seow Chong, Wu Wei, Yee Jiun have been wonderful colleagues and friends in our journeys towards PhD. Here I would like to express my gratitude to them.

My parents have encouraged me to pursue a postgraduate degree and I would like to thank them for their support. I would also like to thank my husband Lichuan who has been with me through this wonderful journey.

JOURNAL PUBLICATION AND CONFERENCES ATTENDED

Published:

Hou Q, Tan HT, Lim KH, Lim TK, Khoo A, Tan IB, Yeoh KG, Chung MC. (2013) Identification and Functional Validation of Caldesmon as a Potential Gastric Cancer Metastasis-associated Protein. *J Proteome Res.*, 12(2):980-90.

Conference poster presented in 6th International Conference on Structural Biology & Functional Genomics, December 6-8, 2010.

Hou Q, Tan HT, Lim TK, Chung MC. Unraveling the Molecular Basis of Gastric Cancer Metastasis by Comparative Proteome Analyses of Gastric Cancer Cell Lines

Conference poster presented in FAOBMB Student Symposium, 7 October, 2011.

Hou Q, Tan HT, Lim KH, Chung MC. Role of Fascin and Caldesmon in Gastric Cancer Metastasis.

Conference poster presented in YLLSoM 2nd Annual Graduate Scientific Congress, 15 February, 2012. (Best Poster Presentation Award)

Hou Q, Tan HT, Lim KH, Chung MC. Role of Fascin and Caldesmon in Gastric Cancer Metastasis.

Conference poster presented in the 11th Annual HUPO World Congress, 9-13 September, 2012.

Hou Q,Tan HT; Lim TK,Lim KH, Chung MC. Identification of Caldesmon as a Potential Gastric Cancer Metastasis Regulator by Comparative Proteome Analyses of Gastric Cancer Cell Lines.

Conference poster presented in Singapore Gastric Cancer Consortium 6th Annual Scientific Meeting, 25 – 26 July, 2013.

Hou Q, Tan HT, Lim KH, Lim TK, Khoo A, Tan IB, Yeoh KG, Chung MC. Identification and Functional Validation of Caldesmon as a Potential Gastric Cancer Metastasis-associated Protein.

Table of Contents

ABSTRACT

Gastric cancer is the fourth most common cancer in the world and the second most common cause of cancer-related death. The rate of metastasis is high in gastric cancer patients. During cancer metastasis progression, the tumor cells underwent a plethora of molecular and morphological changes to become motile and invasive for the malignant transformation. Thus discovery of the molecules that were involved in metastasis progression is critical for early diagnosis and prognosis for gastric cancer patients. In this study, we aim to identify biomarkers for gastric cancer metastasis using a quantitative proteomics approach. The proteins extracted from a panel of 4 gastric cancer cell lines, two derived from primary cancer (AGS, FU97) and two from lymph node metastasis (AZ521, MKN7) were labeled with iTRAQ (8-plex) reagents and analyzed by 2D - LC MALDI-TOF/TOF MS. In total, 641 proteins were identified with at least a 95% confidence. Using cutoff values of >1.5 and <0.67, 19 proteins were found to be up-regulated and 33 were down-regulated in the metastatic *versus* primary gastric cancer cell lines respectively.

Among these dysregulated proteins, fascin and UCHL1 expressions were increased while caldesmon expression decreased in the metastasis-derived cancer cell lines as verified by western blotting. The trend of expression of fascin and caldesmon in the metastasis-derived cell lines were further confirmed by the analysis of a panel of eleven gastric cancer cell lines. Furthermore, immunohistochemical staining of 9 pairs of primary gastric cancer tissues and the matched lymph node metastasis tissue also corroborated this observation. Tissue microarray analysis showed that fascin expression was correlated with gastric cancer serosal invasion and lymph node metastasis. In patients with well-differentiated gastric cancer, positive expression of fascin is associated with poorer survival. On the other hand, the expression of caldesmon in tumor tissues was scarce. Pericellular caldesmon expression is correlated with serosal invasion.

As caldesmon is a novel target associated with gastric cancer, we studied its function in gastric cancer cell lines. Knockdown of caldesmon using siRNA in AGS and FU97 gastric cancer cells resulted in an increase in cell migration and invasion, while the over-expression of caldesmon in AZ521 cells led to a decrease in cell migration and invasion, and increase in cell adhesion. To elucidate caldesmon interacting partners, co-immunoprecipitation coupled to in-gel digestion experiment identified myosin, tropomyosin and other actin cytoskeleton regulating proteins as caldesmon interacting proteins. This study has thus established the potential role of caldesmon in gastric cancer metastasis.

LIST OF TABLES

TABLE

LIST OF FIGURES

FIGURE

LIST OF ABBREVIATIONS

2D-GE	Two-dimensional gel electrophoresis
ACN	Acetonitrile
AFP	Alpha-fetoprotein
ALDH1A3	Aldehyde dehydrogenase
BSA	Bovine serum albumin
CAFs	Cancer-associated fibroblasts
CagA	Cytotoxin-associated gene A
CAPZB	F-actin capping protein subunit beta
CA19-9	Carbohydrate antigen 19-9
CCL	Chemokine Ligand
CDC-2	Cell division control protein 2
CDK	Cyclin-dependent kinase
CEA	Carcinoembryonic antigen
Co-IP	Co-Immunoprecipitation
Cov	Coverage
Ctrl	Control
DIGE	Difference –in- gel electrophoresis
ECM	Extracellular matrix
EDTA	Ethylenediaminetetraacetic acid
EEF1D	Eukaryotic elongation factor 1-delta
EGFR	Epidermal growth factor receptor
EIF5A2	Eukaryotic initiation factor 5A2
EMR	Endoscopic mucosal resection
EMT	Epithelial-mesenchymal transition
ECF	Epirubicin, Cisplatin and Fluorouracil
EPPK1	Epiplakin
ESD	Endoscopic submucosal dissection
FA	Formic acid
FDA	Food and Drug Administration
F-actin	Filamentous actin
FH	Fumarate hydratase
GALNT2	N-acetylgalactosaminyltransferase 2
GAPDH	Glyceraldehyde-3-phosphate dehydrogenase
GC	Gastric cancer
GO	Gene ontology
GSTP1	Glutathione S-transferase P
h-Cald	High-molecular weight caldesmon
HCC	Hepatocellular carcinoma
hCG	Human chorionic gonadotropin
HER2	Human epithelial growth factor receptor 2
HIF-1α	Hypoxia-inducible transcription factor 1α
HMW	High molecular weight

HRP	Horseradish peroxidase
ICAT	Isotope-coded affinity tag
ICC	Immunocytochemical
IDH1	Isocitrate dehydrogenase 1
IEF	Isoelectric focusing
IF	Intermediate filament
IHC	Immunohistochemistry
IP	Immunoprecipitation
IPA	Ingenuity Pathway Analysis
IPI	International Protein Index
iTRAQ	Isobaric tags for relative and absolute quantitation
LC	Liquid chromatography
l-Cald	Low-molecular weight caldesmon
LDH	Lactate dehydrogenase
LMW	Low molecular weight
LDHA	Lactate dehydrogenase
LN	Lymph node
MALDI	Matrix-assisted laser desorption/ionization
MMPs	Matrix metalloproteinases
MMTS	Methyl methanethiosulfonate
MS	Mass spectrometry
MT1-MMP	Membrane-binding matrix metalloproteinases
MTT	3-(4,5-dimethylthiazol-2-yl)-2,5- diphenyltetrazolium bromide
MYH10	Myosin 10
NH4HCO3	Ammonium bicarbonate
NSGCTs	Nonseminomatous germ cell tumors
OD	Optical density
OE	Over-expression
OPN	Osteopontin
PAI-1	Plasminogen activator inhibitor
PBS	Phosphate-buffered saline
PDA	Pancreatic ductal adenocarcinoma
PDGF	Platelet-derived growth factor
PDGFR-β	PDGF receptors
PET	Polyethylene terephthalate
PFTK1	Cyclin-dependent kinase 14
PG	Pepsinogen
pI	Isoelectric points
PLA2G2A	Phospholipase A2, membrane associated
PRC2	Polycomb repressive complex 2
PRDX1	Peroxiredoxin 1
PTEN	Phosphatase and tensin homolog
RhoGDI2	Rho GDP dissociation inhibitor 2
RT	Reverse-Transcriptase
RT-PCR	Reverse-Transcription Polymerase Chain Reaction

S/N	Signal to noise
SCX	Strong cation exchange
SELDI	Surface-enhanced laser desorption/ionization
SD	Standard deviations
SDHA	Succinate dehydrogenase
SDS-PAGE	Sodium dodecyl sulfate polyacrylamide gel electrophoresis
SERPINB1	Leukocyte elastase inhibitor
SILAC	Stable-isotope labeling by amino acids in cell culture
siRNA	Small interfering RNA
SLC3A2	4F2 cell-surface antigen heavy chain
STRAP	Software Tool for Researching Annotations of Proteins
STRAP	Software Tool for Researching Annotations of Proteins
TBS-T	Tris buffered saline
TCA	Tricarboxylic acid cycle
TCEP	Tris-2-carboxyethyl phosphine
TEAB	Triethylammonium bicarbonate
TFA	Trifluoroacetic acid
TGF-β	Transforming growth factor beta
TIMPs	Tissue inhibitors of MMP
TMA	Tissue microarray
TOF	Time of flight
TPM	Tropomyosin
UCHL1	Ubiquitin carboxy-terminal hydrolase L1
uPA	Urokinase plasminogen activator
VEGF-A	Vascular endothelial growth factor A
VEGF-C	Vascular endothelial growth factor-C
VEGFR	Vascular endothelial growth factor receptor
WASP	Wiskott-Aldrich syndrome protein
WIP	WASP-interacting protein

CHAPTER 1 INTRODUCTION

1.1 GASTRIC CANCER

1.1.1 Gastric Cancer Epidemiology

Gastric cancer is a malignancy that usually arises from the inner epithelial linings of the stomach. In 2008, with approximately 990,000 new cases and 738,000 cancer related death around the globe, GC ranked as the fourth most common malignancy and the second leading cause of cancer related death in the world (Jemal *et al.*, 2010). The incidence rates of gastric cancer are high in Asia, Eastern Europe and parts of Central and South America. The disease incidence rates are about twice as high in males compared to females (Garcia *et al.*, 2007). In Singapore, from 2006-2010, gastric cancer is the 5th most common cancer in male (account for 6% of 25,087 total cancer cases) and the 7th most common cancer in female (4% of 26,570 total cancer cases) (Singapore Cancer Registry).

Despite a decreasing incidence rate of gastric cancer around the world in the recent 30 years (Garcia *et al.*, 2007), the survival rate of gastric cancer remains poor. About 74% of people who were diagnosed with gastric cancer died of this disease in 2000 (Hartgrink *et al.*, 2009). The 5-year survival rates for gastric cancer patients are only around 24% in US and Europe (Brenner *et al.*, 2009; Garcia *et al*., 2007). In Singapore, the post-resection 2-year survival rates are only 40% (Look *et al.*, 2001). The poor prognosis rate of gastric cancer poses a health burden and there is a pressing need to develop novel methods for gastric cancer diagnosis and prognosis.

1.1.2 Gastric Cancer Risk Factors

The best established risk factor for gastric cancer, especially the distal gastric cancer is *Helicobacter pylori* infection (Brenner *et al*., 2009). In 1994, the International Center for Cancer Research officially recognized *Helicobacter pylori* as a carcinogen for gastric cancer (Ito *et al*., 2009). *Helicobacter pylori* is a Gram-negative bacterium which localized mainly extracellularly within the gastric lumen. It is estimated to be present in over 50% of the human population and it is highly adaptable in colonizing the stomach epithelium (Piazuelo *et al.*, 2010), leading to gastritis and chronic infection which may eventually develop into gastric cancer. The attributable risk for gastric cancer conferred by *Helicobacter pylori* is approximately 75% (Polk & Peek, 2010). A large scale clinical trial involving 2-weeks antibiotic treatment to eradicate *Helicobacter pylori* followed by 7 years of dietary vitamin supplement reduced gastric cancer risk over a follow-up period of 15 years (Ma *et al*., 2012).

Other risk factors associated with gastric cancer include smoking (Catalano *et al.*, 2009), and high salt intake (in excess of the WHO recommended maximum of 5 gram of salt intake per day) (Peleteiro *et al.*, 2011). For example, a meta-analysis of over a hundred epidemiology studies found that approximately 50% of the increased risk of gastric cancer was associated with the intake of high-salt pickled vegetables, especially in China and Korea (Ren *et al.*, 2012). Consumption of several types of meat, high-fat dairy foods, starchy food and sweets ("unhealthy" diet) also increased the risk of gastric cancer by 50%, whereas consumption of large quantity of fruits and non-starchy vegetables, including allium vegetables (garlic, onions *etc*.) (prudent/healthy diet) may decrease the risk of gastric cancer by 25% (Bertuccio *et al*., 2013; Catalano *et al*., 2009).

Age, gender, and ethnicity may also be related to gastric cancer risk. In Singapore, the Chinese males have higher risk of gastric cancer compared to the Malay and Indian counterparts. The incidence rates of gastric cancer also rise with age (Look *et al.*, 2001).

1.1.3 Gastric Cancer Histological classifications

Two types of gastric cancer have been defined by Lauren's classification based on the tumor histology (Lauren, 1965): the intestinal type and the diffuse type. The intestinal type has retained well-defined glandular structures surrounded by stroma and resembled the adenocarcinoma arising in the intestinal tract (Catalano *et al*., 2009). It is often associated with a multi- step neoplastic development which started with *Helicobacter pylori* infection induced chronic gastritis, intestinal metaplasia, dysplasia and eventually adenocarcinoma (Hartgrink *et al.*, 2009; Polk & Peek, 2010). The diffuse type consists of individual infiltrating neoplastic cells that do not form glandular structures (Polk & Peek, 2010) and have low cell-cell adhesions (Catalano *et al*., 2009).

Gastric cancer can be defined as well/moderately- , or poorly-differentiated subtypes based on the degree of glandular differentiation (Broders, 1925). The well/moderately-differentiated gastric cancers are often classified into intestinal type, whereas the poorly-differentiated subtype usually corresponds to diffuse type in Lauren's classification (Tahara, 2004).

Gastric cancer may also be classified into two types based on different growth and invasion patterns: the expanding type which contains discrete tumor nodules, may arise from intestinal metaplasia, and have better prognosis; and the infiltrating type which contains individual invading cells, of which the prognosis is poor (Catalano *et al*., 2009; Ming, 1977).

1.1.4 Screening and Diagnostic Tools for Gastric Cancer

The stomach epithelial lining undergo precancerous changes which were often long and asymptomatic (averaging 44 months) (Tsukuma *et al*., 2000) before gastric cancer development. For early gastric cancer cells, it was observed that their doubling time is approximately 16.6 months (Haruma, 1991). Hence, screening and early diagnosis of gastric cancer is necessary for disease intervention. *Helicobacter pylori* screening and treatment for positive cases, endoscopic screening of pre-malignant gastric lesions are commonly used diagnostic tools for the early detection and prevention of gastric cancer (Areia *et al.*, 2013) In Japan, the high risk population was screened annually with barium meal or endoscopy for possible gastric cancer (Leung *et al*., 2008). However, these detection methods were limited by the size of the tumor (barium study) and the skills of the endoscopists.

A measurement of serum pepsinogen level combined with *Helicobacter pylori* antibody status may be a useful non-invasive serological screening method (Leung *et al*., 2008). Pepsinogen (PG) is an inactive precursor of pepsin: a gastrointestinal enzyme produced in the gastric mucosae. Approximately 1% PG entered the blood circulation and a reduction of serum PGI as well as PG I/II ratio was correlated with gastric mucosal atrophy progression. The patients who tested positive in the pepsinogen test with progression of chronic atrophy gastritis have higher risk of developing into gastric cancer, thus might be classified into high-risk group and are monitored closely (Enomoto *et al.*, 2010). However, the serum pepsinogen test is limited in the detection of intestinal-type gastric cancer which started with chronic atrophy gastritis (Leung *et al*., 2008).

1.1.5 Treatment Options for Gastric Cancer

The therapeutic options for gastric cancer are endoscopic mucosal resection (EMR), endoscopic submucosal dissection (ESD), surgical gastrectomy and chemotherapy (Katoh, 2005). Randomized clinical trials have shown that a combination of pre-operative radiotherapy combined with surgery improved the patients' survival (Hartgrink *et al*., 2009). The overall survival in patients with resectable gastric cancer has been significantly improved with use of either post-operative chemo-radiation or peri-operative ECF (Epirubicin, Cisplatin and Fluorouracil) (Knight *et al*., 2013). For the inoperable advanced stage gastric cancer which consisted of 80-90% of total cases, chemotherapy based on drug combinations, like 5-FU/platinum drug combinations, as well as irinotecan and docetaxel-combination are current treatment options (Wagner *et al*., 2010). 5-FU is a pyrimidine analogue which blocks thymidine synthesis and subsequent DNA replication by inhibiting thymidilate synthethase. The platinum-containing drugs Cisplatin and oxaliplatin crosslink DNA, which leads to the apoptosis of cancer cells. Irinotecan exerts the anti-cancer effect by acting as a DNA topoisomerase inhibitor, whereas docetaxel inhibits cancer cell division by preventing the depolymerization of microtubules (Wagner *et al*., 2010). The administrations of these cytotoxic drugs have adverse effects on normal cells as well and patients often suffer from severe side effects with poor prognosis: the 5-year survival rates are only approximately 20% (Catalano *et al*., 2009).

Besides the conventional anti-cancer therapies, research on targeted therapy which involves monoclonal antibodies or small molecules specifically inhibiting certain oncogenes has been underway. It is believed that the targeted therapy will be focused on eliminating only the cancer cells with minimal side effects on the normal cells. The identification of the oncogenic pathways and gastric cancer biomarkers are critical in this context. Investigation of targeted therapy to gastric cancer is under clinical Phase II trials with monoclonal antibodies targeting oncogenes such as ERBB2, VEGF (Hartgrink *et al*., 2009). Recently Trastuzumab,

a monoclonal antibody against Human epidermal growth factor receptor 2 (HER2), has been approved by the FDA to use in combination with chemotherapy for treating the metastatic gastric adenocarcinoma with HER2- over-expression (Saghier *et al.*, 2013).

1.1.6 Molecular Patterns and Biomarkers for Gastric Cancer

Gastric cancer is a heterogeneous disease. It has been estimated that 80-90% gastric cancers were developed sporadically, 10-20% occurred in family clusters, and 1-3% have genetic susceptibility (Saghier *et al.*, 2013). Identification of these molecules that were involved in the carcinogenesis is critical for the early detection of disease, and stratification for the appropriate treatment and disease prognosis. The most widely used cancer-associated antigen, carcinoembryonic antigen (CEA) and carbohydrate antigen 19-9 (CA19-9) are found to be elevated in only 30-40% of primary gastric cancer patients (Catalano *et al*., 2009).

A recent study has found human epithelial growth factor receptor 2 (HER2), a member of the human epidermal growth factor receptor family, is over-expressed in approximately 9-38% of gastric cancer (Gravalos & Jimeno, 2008), especially in the intestinal type of gastric cancer. Over-expression of HER2 in intestinal type gastric cancer is also correlated with poorer survival (Chua & Merrett, 2012). A large scale Phase III clinical trial (ToGA) using Trastuzumab (Herceptin) combined with chemotherapy in HER2 positive gastric cancer patients has effectively improved the patients' 5-year survival by 3 months (Hu *et al*., 2012; Saghier *et al*., 2013). It is recommended to conduct HER2 screening at the initial gastric tumor diagnosis for targeted therapy (Rüschoff *et al*., 2012).

Cell cycle regulators have also been found to be dysregulated in gastric cancer. Cyclin E over-expression has been identified in 15-20% of gastric cancer patients. A reduction of $p27^{Kip1}$, a cyclin-dependent kinase (CDK) inhibitor is associated with advanced stage gastric cancer (Yasui *et al*., 2005).

Cell adhesion molecules are associated with gastric cancer progression. It has been observed that increased expression of β-catenin which was involved in cell-cell adhesion and gene transcription activation expressed in up to 50% of gastric cancer. The increased β-catenin could be attributed to the translocation of *Helicobacter pylori* cytotoxin-associated gene A (CagA) protein which induced

nuclear accumulation of β-catenin and subsequent gene transcription upon the bacteria infection (Polk & Peek, 2010).

Patients with germ-line mutation of CDH1 (gene encodes for E-cadherin expressed at the adherence junction) had a high chance of developing into familial diffuse type gastric cancer (Katoh, 2005). The expression level of CD44, a membrane-bound glycoprotein involved in cell adhesion may be associated with gastric cancer lymph node metastasis (Hsieh *et al.*, 1999).An immunohistochemical study has established a combination of CD44 and epithelial-mesenchymal transition related proteins Snail-1, vimentin and E-cadherin have prognostic significance in predicting the gastric cancer patients' survival (Ryu *et al.*, 2012).

The 4 gastric cancer cell lines AGS, AZ521, FU97 and MKN7 used in this study have been adopted in various gastric cancer biomarker researches. The AGS cell line, derived from a specimen of human stomach adenocarcinoma, possess some characteristics of normal gastric epithelial cell such as epithelial-like morphology (Zheng *et al.*, 1996). AGS cells expressed PLA2G2A phospholipase which has an anti-invasion effect, while MKN7 and FU97 did not express this protein (Ganesan *et al*., 2008). The expressions of metastasis-related proteins have been studied in gastric cell lines. A loss of expression of E-cadherin, a marker for epithelial cell adherence junction, has been observed in AZ521 (Yonemura *et al*., 2000). Vascular endothelial growth factor-C (VEGF-C), a risk factor associated with gastric cancer metastasis, has been found to be expressed in AZ521 but not in MKN7 (Yonemura *et al*., 1999). Using a panel of gastric cancer cell lines including AGS, MKN7, AZ521, EZH2, a critical component of polycomb repressive complex 2 (PRC2) was identified to have increased expression levels associated with gastric cancer progression (Cheng *et al*., 2012). A large scale genomics profiling of 37 gastric cancer cell lines have identified two major genomic subtypes coined as G-INT and G-DIF which is partially associated with Lauren's histopathologic classification. AGS was in the G-INT group, while FU97, MKN7 and AZ521 were classified into G-DIF group (Tan *et al*., 2011).

1.2 CANCER METASTASIS

1.2.1 TNM Staging of Tumor, Lymph Node Metastasis

Cancer staging provides histological summary of the tumors and is useful for decision on treatment as well as prognosis of disease. The TNM classification for gastric cancer has been widely adopted (Sobin and Wittekind, 2002). The TNM staging criteria for gastric cancer are listed in Table 1.1 below (adapted from Catalano *et al*., 2009). T is used to describe the size and invasion depth of tumor. Tx or T_0 is defined as no evidence of primary tumor. T_{is} is defined as carcinoma *in situ*. T_1 tumor has invaded lamina propria/submucosa. T_2 tumor penetrated muscularis propria or submucosal. T_3 tumor invaded stomach serosa, while T_4 tumor has invaded stomach adjacent structures including spleen, colon, liver, diaphragm, pancreas, abdominal wall, adrenal gland, kidney, small intestine, retroperitoneum *etc.* N defined the tumor involvement of regional lymph nodes. Nx or N_0 meant no lymph node metastasis. N_1 tumor has metastasized to 1-6 regional lymph nodes, N_2 to 7-15 regional lymph nodes, and N_3 to more than 15 regional lymph nodes. M defined the status of distant metastasis. Mx or M_0 has no distant metastasis, while M_1 tumor has metastasized to distant organs.

TNM Stage	Description
T	**Size, invasion depth of tumor**
T_X	Primary tumor cannot be assessed
T_0	No evidence of primary tumor
T_{is}	Carcinoma *in situ*: intraepithelial tumor without invasion of the lamina propria
T_1	Tumor invaded lamina propria or submucosa
T_2	Tumor invaded muscularis propria or submucosa
T_{2a}	Tumor invaded muscularis propria
T_{2b}	Tumor invaded submucosa
T_3	Tumor invaded serosa without invasion of adjacent structures
T_4	Tumor invaded adjacent structures (Spleen, transverse colon, liver, diaphragm, pancreas, abdominal wall, adrenal gland, kidney, small intestine, retroperitoneum)
N	**Involvement of regional lymph nodes (a minimum of 15 lymph nodes examined)**
N_X	Regional lymph node cannot be assessed
N_0	No regional lymph node metastasis
N_1	Metastasis in 1-6 regional lymph nodes
N_2	Metastasis in 7-15 regional lymph nodes
N_3	Metastasis in more than 15 regional lymph nodes
M	**Distant metastasis**
M_X	Presence of distant metastasis cannot be assessed.
M_0	No distant metastasis.
M_1	Distant metastasis.

Table 1.1 TNM staging classification of gastric cancer.

1.2.2 Metastasis Is a Multi-Step Process

Metastasis, the spread of tumor from the primary organ to a distant part of the body (Talmadge & Fidler, 2010), is responsible for as much as 90% of cancer-related death (Chaffer & Weinberg, 2011). The ability of tumor cells to activate invasion and metastasis is coined as one of the hallmarks of cancer (Hanahan & Weinberg, 2011).

The growth of primary tumor was slow. To reach a 1cm diameter (minimum size for detection with current imaging tools) which has approximately 10^9 cells, at least 30 doublings (average 12 years) of the tumor cells were required. However the tumor only required 10 doublings to grow from 1 cm diameter to the size of 1000 cm^3 which was lethal (Talmadge & Fidler, 2010). Therefore a better understanding of the metastasis mechanism and its molecular phenotype is required for early detection of cancer and prediction of disease outcome.

In order for metastasis to occur, tumor cells undergo a series of progressions consisting of detachment of tumor cells, local invasion and angiogenesis, gaining motility to enter the circulation, vessel invasion, adhesion to endothelial cells and extravasation, and growth in distant organs (Yasui *et al*., 2005).

It is hypothesized that metastasis may have occurred prior to tumor diagnosis. Studies have found that metastases exhibit substantial differences in the gene expression profiles when compared to that of the primary tumors (Sleeman & Steeg, 2010). It has thus been proposed that the ectopically residing tumor cells may have disseminated in the early stage and developed independently into metastases in parallel with the primary tumor development (Stoecklein & Klein, 2010). Genome-wide analysis of 4 breast cancer samples: primary tumor, peripheral blood, brain metastasis and xenograft developed from primary tumor isolated from the same patient discovered that tumor metastases has retained the

mutations existed in primary tumor with higher frequency, and carried *de novo* mutation not found in the primary tumor (Ding *et al*., 2010). This finding confirmed that tumor metastases may arise from a subset of primary cancer cells.

1.2.3 Molecular Features of Metastasis

The expressions of many proteins and metabolites are perturbed during metastasis progression. These dysregulations probably resulted from the increased energy demand, gaining of motility and invasiveness of the metastasizing cancer cells. These molecular features might serve as potential biomarkers for metastasis.

Activation of oncogenic signaling pathways is an important feature for cancer progression and metastasis. Amplification of tyrosine kinase MET has been observed in certain gastric cancer (Gherardi *et al.*, 2012). Activation of Notch signaling promoted gastric tumor growth and metastasis via activation of STAT3 and Twist mediated signaling cascade (Hsu *et al*., 2012).

Increased expression of metabolic proteins involved in glycolysis, the citric acid cycle, oxidative phosphorylation, β-oxidation, the glutathione system, and the pentose pathway were observed in breast cancer metastasis, implying that the metastatic cancer cells gain energy mainly through glycolysis (Chou & Chan, 2012). Studies have found that differentially-expressed metabolites between metastatic and non-metastatic gastric cancer include those involved in glycolysis (lactic acid, alaine), nucleotide metabolism (pyrimidine), and fatty acid metabolism *etc.* The increased production of lactic acid in metastatic cancer may reflect the increased energy demand for tumor progression (Chen *et al*., 2010).

Decreased cell-cell adhesion, re-arrangement of the actin cytoskeleton, and increased motility and cell invasiveness are distinct characteristics of metastatic cancer cells compared to the normal epithelial cells (Katoh, 2005; Voulgari & Pintzas, 2009). Actin cytoskeleton mediates cell morphology, cell migration and cell-cell attachment. During metastasis, gaining of motility in cancer cells has been observed for the cancer cells to breach through the basement membrane with actin filament-enriched cellular processes (Bravo-Cordero *et al.,* 2012). Invadopodia, an actin-enriched cellular protrusion that degraded the extracellular matrix, facilitate the invasion of metastatic cancer cells (Bravo-Cordero *et al*.,

2012). The expression perturbations of proteins which regulate actin polymerization, actin bundling and invadopodia formation are present in metastasis. Reduction of E-cadherin, an increase of RhoA/ROCK-mediated actin cytoskeleton re-organization signaling networks have been observed in cancer cell migration (Spano *et al.*, 2012). Actin bundling protein fascin is often seen as up-regulated in metastatic cancer, and up-regulation of non-muscle myosin's activity which mediated cell contractility and stiffness has been observed in advanced stage cancer (Stevenson *et al.*, 2012).

Proteins which are involved in tissue remodeling in inflammation, like osteopontin (OPN), an inflammatory cytokine, and SPARC, a stress-response protein (Chiodoni *et al.*, 2010), proteolytic enzymes like matrix metalloproteinases (MMPs) which may play a role in degrading the basement membrane (Brooks *et al*., 2010) were found to be expressed in metastatic cancer cells. The expressions of specific adhesion molecules involved in crosstalks between migrating cancer cells and their microenvironment were also observed (Chaffer & Weinberg, 2011). The over-expression of chemokine ligands (CCLs) CCL7 and CCL21 in gastric cancer was correlated with lymph node metastasis and poor survival. It was postulated that over-expression of CCLs may recruit myeloid cells which expressed chemokine ligand receptor and produced MMPs to the tumor invasive front (Hwang *et al*., 2012).

1.3 PROTEOMICS: A HIGH-THROUGHPUT METHOD IN UNDERSTANDING THE MECHANISMS OF CANCER

1.3.1 Proteomics in Cancer Marker Discovery

Protein biomarkers for cancer diagnosis and prognosis are valuable tools that complement traditional cancer staging methods. They may improve the effectiveness of clinical intervention, stratify the patients to the most appropriate treatment, and predict cancer recurrence after treatment (Tainsky, 2009). Currently the cancer biomarkers used in clinics include serum-based markers Alpha-fetoprotein (AFP), human chorionic gonadotropin (hCG), and lactate dehydrogenase (LDH) for patients with metastatic nonseminomatous germ cell tumors (NSGCTs); human epidermal growth factor receptor 2 (HER-2), urokinase plasminogen activator (uPA), and plasminogen activator inhibitor (PAI-1) for breast cancer prognosis (Duffy & Crown, 2008). However, these biomarkers may have limited diagnostic power with sensitivity and specificity that are not optimal.

Proteomics refers to the study of entire protein complement expressed by the genome. It involves the large-scale identification, quantitation and characterization of proteins expressed in cells or tissues in a given condition (He & Chiu, 2003). In cancer cells, both the transcriptional programs and the post-translational protein modifications are altered for cancer cells to gain the growth and motility advantage. The challenge to capture these global changes in protein expression has been met by high-throughput proteomics approach (Chen & Yates, 2007). Studies have found that while the current gastric cancer marker carcinoembryonic antigen (CEA) has only 49% sensitivity, a panel of peptide mass fingerprinting identified with surface-enhanced laser desorption/ionization (SELDI) proteomics with gastric cancer serum samples yielded 83% sensitivity and 95% specificity (Cho, 2007; Poon *et al*., 2006). However, many still remain to be understood for cancer progression, and biomarkers which can better predict

cancer occurrence, diagnose early cancer and predict patients' survival are urgently in need.

The samples for cancer proteomics studies vary from cancer cell lines, tumor tissues or body fluids/plasma. Cancer cell lines have high degree of homogeneity and are easy to handle. They can be genetically manipulated for functional studies. However they are prone to genotypic and phenotypic drifts over prolonged culturing time, and thus may not resemble 100% of the original tumor from which they were isolated. Tumor tissues and body fluids/plasma are good models for subsequent clinical applications, however the tumor samples are often limited and inherent variance exist among different patients. The complexity in plasma sample and the dynamic range in protein concentrations may also pose a problem for biomarker identification (Chen & Yates, 2007).

1.3.2 Proteomics Techniques: Gel-based platforms

The two-dimensional gel electrophoresis (2D-GE), a gel-based technique, is a classic proteomics approach. The proteins are fractioned on the first dimension based on their isoelectric points (p*I*) using isoelectric focusing (IEF), followed by separation by molecular weight via sodium dodecyl sulfate polyacrylamide gel electrophoresis (SDS-PAGE) (Görg *et al*., 2000). Difference – in- gel electrophoresis (DIGE) method allows for quantification with incorporation of CyDye fluors (Cy2, Cy3, and Cy5) by covalently labeling the ε-amino group of lysines in two different samples. Equal amount of the two samples are combined and run in a single first dimensional IEF gel. The same protein labeled with any of the fluors will be resolved as the same spot and the relative expression across samples is reflected when comparing intensity of the spots (Wu *et al*., 2006). Several inherent problems are associated with 2D-GE and DIGE approach: Proteins of low abundance, extreme p*I* and molecular weight cannot be identified due to the detection limit of 2D-GE. Proteins of similar p*I* and size may co-migrate to the same spot, and the gel-to-gel variation between batches may confound quantification of the proteins (Lilley, Razzaq, & Dupree, 2001).

1.3.3 Proteomics Techniques: LC-based platforms

LC-based proteomics methods choose a variety of stationary and mobile phases to resolve complex biological samples. Generally, the proteins are first digested into peptides, followed by separation with strong cation exchange and then with reverse phase chromatography (Wu *et al*., 2006). Quantitative methods involved in LC-based approach include Stable-isotope labeling by amino acids in cell culture (SILAC), cleavable Isotope-coded affinity tag (cICAT) labeling, and isobaric tags for relative and absolute quantitation (iTRAQ).

In the SILAC approach, cells are grown in media with normal amino acids (^{12}C) or in the media with non-radioactive, isotope-coded form of specified amino acids (^{13}C). The isotopic labeling can be achieved in 4-5 cell doubling times and the temporal dynamics of proteins can be quantified based on the light-to-heavy isotope ratio (Chen & Yates, 2007). The SILAC method can only be applied in cell line models but not tissue samples.

In the cICAT approach, proteins from two states on cysteinyl residues are labeled with light and heavy isotopes ($^{12}C/^{13}C$) carrying a biotin moiety. The labeled proteins are then mixed, digested and affinity purified using avidin (Chaerkady & Pandey, 2007). Peaks corresponding to the same peptide are identified as doublets in the mass spectra due to the mass difference between light and heavy isotopes. The peak intensities of the peptides correlate with the relative abundance of the proteins in the two states. Due to the affinity purification step involved, cICAT technique can only identify proteins containing cysteinyl residues (Wu *et al*., 2006).

In iTRAQ approach, 4-plex or 8-plex isobaric tags consisting of reporter mass of 114-117 (4-plex) or 113-121 (excluding 120, 8-plex), a corresponding balance group and an amine-reactive group are used to label primary amino group in peptides. The labeled samples are pooled, fractionated and subjected to mass spectrometry whereby MS/MS fragmentation release the reporter ions which

would reflect the relative abundance of the proteins (Chaerkady & Pandey, 2007). The iTRAQ approach allows for multiplexing of up to 8 samples. In a recent study, the proteome of 2 distinct panels of isogenic prostate cancer cells with varying growth and metastatic potential were profiled with 8-plex iTRAQ analysis. Of the 245 proteins identified and quantified, 17 proteins were significantly differential expressed and potentially associated with metastasis progression (Glen *et al*., 2010).

These three quantitative proteomics approaches: DIGE, cICAT and iTRAQ have been compared recently in regard to their sensitivity (number of peptides detected for each protein) and proteins profiling using six-protein mixture and cancer cell lysates. It is found that while DIGE is as sensitive as cICAT approach, iTRAQ has a higher sensitivity than the cICAT and DIGE method, and may have a higher chance of identifying low abundance proteins. The three methods covered cell lysates protein profiles which have little overlaps, suggesting that these methods may complement each other (Wu *et al*., 2006).

1.3.4 Proteomics in Gastric Cancer Biomarker Discovery

There have been several publications that used proteomics approach to identify potential gastric cancer biomarkers. Many of them focused on markers that differentiate the early cancer from the normal gastric tissues, whereas those directed towards unraveling the proteome differences between metastatic and primary gastric cancers were relatively scarce.

In a 2D-GE approach, 152 human gastric cancer tissue samples were analyzed (Cho *et al*., 2009), and it was reported that Rho GDP dissociation inhibitor 2 (RhoGDI2) to be positively linked to tumor growth and invasion, which was confirmed by tissue immunohistochemistry, cell-based functional assays and tumor growth study in nude mice. In one study, up-regulation of heat shock proteins, glycolytic enzymes, cytokeratin 8 and tropomyosin isoform, and down-regulation of cytokeratin 20 were observed via analyzing 10 paired tumors *versus* normal tissue samples in a 2D-GE approach (He *et al*., 2004). In another DIGE study, 13 dysregulated proteins involved in protein synthesis, metabolism and cytoskeleton were found in a highly metastatic gastric cancer cell MKN-45-P compared to its parental cell line MKN-45 (Takikawa *et al*., 2006). The proteome difference between a well-differentiated, non-metastatic gastric cancer cell line SC-M1 and its metastatic counterpart TMC-1 were compared using isotope-coded affinity tagging (ICAT) analysis, and several dysregulated proteins including up-regulation of vimentin and galectin-1 were identified and verified in the same cell line (Chen *et al*., 2006). In a recent study, iTRAQ analysis of a gastric cancer cell line MKN7 and a normal gastric epithelium cell line HFE145 identified SLC3A2 cell membrane protein to be a potential gastric cancer biomarker (Yang *et al*., 2012). However, few of these studies performed functional validations of the targets to substantiate their involvement in gastric cancer metastasis.

1.4 OBJECTIVES

Cancer metastasis is a major cause of death in cancer patients. The molecular events underlying gastric cancer metastasis remains to be discovered. In this study, we aim to identify the potential biomarkers for gastric cancer metastasis and also to investigate the functional roles of these proteins. We analyzed the cellular proteome of 4 different gastric cancer (GC) cell lines with isobaric tags for relative and absolute quantitation (iTRAQ) technology and MALDI-TOF/TOF MS. These GC cell lines consisted of 2 primary (AGS, FU97) and2 lymph node metastatic (AZ521, MKN7) gastric cancer cells. In addition, among these 4 cell lines, we have also included the two major histological subtypes of gastric cancer: (a) well/moderately differentiated (AGS, MKN7) and (b) poorly differentiated (FU97, AZ521) for proteome analyses with the view to identify the dysregulated proteins involved in gastric cancer metastasis in both histological subtypes. With the benefit of iTRAQ multiplexing, a panel of 4 cell lines with their technical replicates was incorporated in this study. This is in contrast to the previous gastric cancer cell line-based proteomics studies that compared only 2 cell lines. In order to discover the dysregulated proteins in gastric cancer metastasis and to understand their functional roles in metastasis, we plan to carry out the following:

1. In the proteomics discovery phase, iTRAQ technology is used to perform comparative proteomics of four gastric cancer cell lines: two from primary cancer and two from lymph node metastasis, with paired differentiation subtype. The expression of dysregulated proteins would be verified by Western blotting and tissue immunohistochemistry.

2. Functional studies to correlate the protein expression differences with the metastatic phenotype. Identify potential target involved in gastric cancer metastasis from the findings from the proteomics study. Perform

functional studies based on gene knockdown and over-expression as well as cell-based assays to examine the function of potential biomarkers identified in gastric cancer.

Chapter 2 MATERIAL AND METHODS

2.1 CELL CULTURE

The gastric cancer cell lines used in this study include AGS, NCI-N87 (American Type Culture Collection (ATCC), Manassas, VA); AZ521, FU97, MKN7, MKN74 (Japanese Collection of Research Bioresources (JCRB), Osaka, Japan); and SNU16 (ATCC), YCC1, YCC2, YCC3, YCC9 (Yonsei Cancer Center, Seoul, South Korea) which were a kind gift from Prof Sun-Young Rha (Yu *et al*., 2008). The isolation sources of these cell lines and descriptions of the stomach tumor pathology were listed in Table 2.1. The cells were cultured in RPMI-1640 media (Sigma, St. Louis, MO) supplemented with 10% (v/v) heat-inactivated fetal bovine serum (Gibco, Grand Island, NY) and 1 mM sodium pyruvate (Invitrogen, Carlsbad, CA) in a humidified incubator (37 °C, 5% CO_2). Upon reaching 90% confluency, the cells were harvested with 0.05% (v/v) trypsin – 0.53 mM EDTA solution (Gibco). The cells were pelleted by centrifuging at 1,000 g for 5 min at 15 °C. The cell pellets were washed thrice in phosphate-buffered saline (PBS) before cell lysis.

Cell line	Source	Description of tumor pathology
AGS	Stomach	Moderately-differentiated gastric adenocarcinoma
FU 97	Stomach	Poorly differentiated adenocarcinoma
MKN 7	Stomach lymph node	Well differentiated adenocarcinoma
AZ 521	Stomach lymph node	Poorly differentiated adenocarcinoma
MKN 74	Stomach cancer liver metastasis.	Moderately differentiated adenocarcinoma
NCI-N87	Stomach cancer liver metastasis	Well differentiated adenocarcinoma
SNU 16	Stomach cancer ascites	Poorly differentiated adenocarcinoma
YCC 1	Stomach cancer ascites	Adenocarcinoma
YCC 2	Stomach cancer ascites	Adenocarcinoma
YCC 3	Stomach cancer ascites	Adenocarcinoma
YCC 9	Stomach cancer ascites	Adenocarcinoma

Table 2.1 Cell lines used in this study. The table displays information of the location and histology of the tumors from which the cell lines were isolated from.

2.2 QUANTITATIVE PROTEOMICS USING ITRAQ

2.2.1 Cell Lysates Preparation

The harvested cells were lysed in iTRAQ labeling buffer (Sadowski *et al*., 2006) that comprised of 25 mM Triethylammonium bicarbonate (TEAB), 8 M urea, 2% Triton X-100, 0.1% SDS, 50 µg/ml DNase I, 50 µg/ml RNase A, and 1×Halt protease inhibitor cocktail (Pierce, Rockford, IL), and centrifuged at 18,800 × *g* for 1h at 15 °C.

The supernatants were then collected, and their protein concentrations were determined using the Coomassie Plus Protein Assay reagent kit (Pierce, Rockford, IL), and bovine serum albumin (BSA) as the calibration standard. The absorbance of the dye-protein complex was measured at 595 nm in a microtitre plate.

2.2.2 iTRAQ Labeling

The samples were labeled with iTRAQ reagents according to the manufacturers' instructions shown in Figure 2.1. Duplicates of 100 µg of proteins from each of the 4 cell lines (AGS, FU97, AZ521 and MKN7) were reduced with 5 mM tris-(2-carboxyethyl phosphine (TCEP) at 20 °C for 1 h, followed by alkylation with 10 mM methyl methanethiosulfonate (MMTS) for 10 min at room temperature. The samples were diluted 10 fold with 50 mM TEAB to reduce the SDS and urea concentrations, and subjected to trypsin (10 µg each) digestion at 37 °C for 16 h with constant shaking.

iTRAQ reagents (8-plex) (AB SCIEX, Foster City, CA) were each reconstituted in 50 µl of isopropanol. Each tryptic digest was labeled with iTRAQ reagents for 2 h at room temperature based on the following: AGS labeled with 113 and 117, AZ521 labeled with 114 and 118, FU97 labeled with 115 and 119, and MKN7 labeled with 116 and 121. After labeling, the samples were pooled

together and passed through a strong cation exchange (SCX) cartridge as recommended by the manufacturer (AB SCIEX), followed by desalting with a reverse phase Sep-Pak C18 cartridge (Millipore, Marlborough, MA). The sample was vacuum dried and reconstituted for 2D-LC.

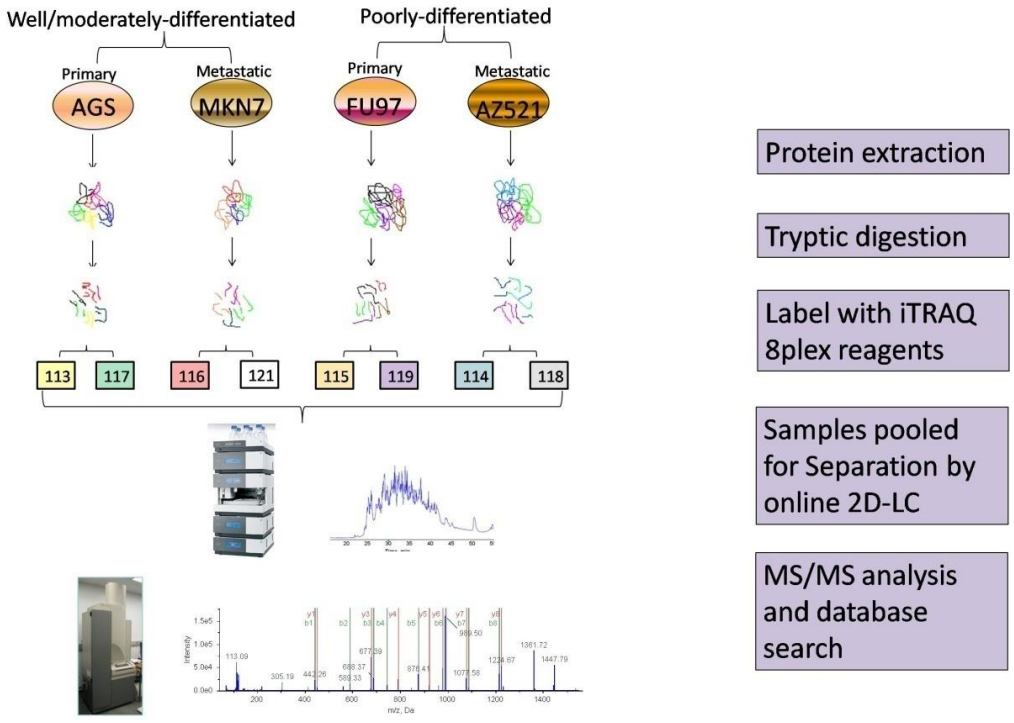

Figure 2.1 Experimental workflow. The cell pellets from 4 gastric cancer cell lines: AGS, MKN7, FU97 and AZ521 were lysed and protein was extracted. 100 µg of proteins were digested by trypsin and were labeled with iTRAQ 8 plex reagents. The samples were pooled and separated on 2D-liquid chromatography and subject to MALDI-TOF/TOF MS analysis. The protein IDs were searched against International Protein Index (IPI) human database (v. 3.72) with Protein Pilot ^{TM} software 2.0.1 and quantitation information was obtained.

2.3 TWO-DIMENSIONAL LIQUID CHROMATOGRAPHY

The iTRAQ-labeled peptide mixture was separated by the Ultimate^{TM} 3000 LC system (Dionex-LC Packings, Bannockburn, IL) (Hou *et al*., 2013; Tan *et al*., 2008). A 2-D LC separation was performed as follows: the labeled peptide mixture was dissolved in 2% acetonitrile (ACN) with 0.05% trifluoroacetic acid (TFA) and injected into a strong cation-exchange (SCX) column (Dionex-LC Packings) for the first dimensional separation. The mobile phase A and B were 5 mM KH_2PO_4 buffer, pH 3, with 5% ACN and 5 mM KH_2PO_4 buffer, pH 3, with 5% ACN and 100 mM KCl, respectively. 10 fractions were obtained using step gradients of mobile phase B: unbound, 0-2, 2-4, 4-6, 6-10, 10-20, 20-30, 30-40 and 40-100% B. The eluting fractions were captured alternatively onto two trap column (Dionex-LC Packings) and eluted with an organic solvent gradient in a reverse-phase column (Dionex-LC Packings). The mobile phase A and B used for the second-dimensional separation were 100% H_2O with 0.05% TFA and 100% ACN with 0.04% TFA, respectively. The gradient elution step was 0-60% B in 15 min. The LC fractions were mixed directly with MALDI matrix solution (7 mg/ml α-cyano-4-hydroxycinnamic acid and 130μg/ml ammonium citrate in 75% ACN) via a 25-nl mixing tee (Upchurch Scientific, Oak Harbor, WA) before they were spotted onto a 1232-well stainless steel MALDI target plate (AB SCIEX) using a Probot Micro Precision Fraction collector (Dionex-LC Packings). 50 fmol of 4700 Proteomics Analyzer Calibration Mixture 1 (AB SCIEX, Foster City, CA) was used for mass calibration.

2.4 MALDI-TOF/TOF MS

The sample spots were analyzed using a 4800 MALDI TOF/TOF^{TM} Analyzer (AB SCIEX). MS/MS analysis was achieved with air as collision gas at collision energy of 1kV and collision gas pressure of $1X10^{-6}$Torr. 1000 laser shots were accumulated from each sample well and the precursor ions were selected

from MS spectra ranging from 920 Da to 3900 Da with a minimum signal to noise (S/N) ratio of 40. MS/MS analyses were performed for the seven most abundant precursor ions per well. 5000 shots were accumulated for each MS/MS spectrum.

All MS/MS spectra were searched by the Protein Pilot ^{TM} software v. 2.0.1 (AB SCIEX, Foster City, CA) for relative quantification and protein identification against the International Protein Index (IPI) human database (version 3.72, 17,2772 sequences) (Kersey *et al*., 2004). Protein identification and relative iTRAQ quantification were performed with the Protein Pilot Software 2.0.1 (AB SCIEX) using the Paragon algorithm. The search parameters allowed for cysteine modification by methyl methanethiosulfonate, and biological modifications set by the algorithm. The detected protein threshold (Unused ProtScore) in the software was set to 1.3 to achieve a 95% confidence. The identified proteins were grouped by the ProGroup algorithm in the software to minimize redundancy. All protein groups reported were based on MS/MS spectra of at least two peptides. No identification was based on PMF alone.

2.5 MS DATA ANALYSIS

The results were exported into Microsoft Excel for data curation. Peptides which were unique for a specific protein group were incorporated in the relative quantitation by the ProGroup algorithm. Those peptides of low identification confidence (<15%), shared MS/MS or no iTRAQ modification were excluded from the quantitative analysis. The average ratios for the proteins were calculated using the Protein Pilot software with the following equation:

$$\text{Average Ratio} = \frac{10(Weighted\,Average\,of\,Log\,Ratios)}{Bias}$$

Where Bias is automatically calculated and Weighted Average of Log Ratios= $\frac{\sum_{i=1}^{N} w_i \times x_i}{\sum_{i=1}^{N} w_i}$

x_i= log(peptide ratio$_i$), w$_i$=1/%Error$_i$, the weight for the ith observation

The *p* values which represents the probability of the observed ratio is different than 1 by chance were also reported.

The geometric mean of the 4 iTRAQ ratios of each pair of cell lines range from 0.94 to 1. The standard deviation of log ratios of the 4 iTRAQ ratios of each pair of cell lines range from 0.28-0.36.

An iTRAQ ratio of >1.5 was taken to be a significant change for up-regulated proteins, and <0.67 for down-regulated proteins. These values represent 95% confidence (2 standard deviations) based on MS/MS analysis of two equivalent protein standards (Tan *et al*., 2008). Proteins that meet the cutoff value must also show consistent changes in both replicate samples, and have iTRAQ ratios' *p* values <0.05 in at least one of the data set to be considered as differentially expressed.

For Gene Ontology annotations, the protein lists were mapped to their associated localizations, biological processes and molecular functions using the Software Tool for Researching Annotations of Proteins (STRAP), obtaining the respective information from UniProtKB and EBI GOA databases (Bhatia *et al.*, 2009). The ID list and differentially-expressed protein list were uploaded to the Ingenuity Pathway Analysis (IPA) software (Ingenuity Systems, Redwood City, CA) to identify the associated networks based on scores that showed the relevance of networks according to *p* values.

2.6 WESTERN BLOTTING

10 µg of proteins from each gastric cancer cell line lysate was first resolved by SDS-PAGE at a constant current of 15 mA/gel in 10% (v/v) polyacrylamide gel and then were electroblotted onto a PVDF membrane at a constant voltage of 100 volt. The membranes were blocked in 5% milk (w/v) in Tris buffered saline (TBS-T) with 0.1% Tween 20 (USB, Cleveland) for 2 hours. Primary antibodies were used, with dilution factors and incubation times according to the manufacturer's recommendation, in 1% (w/v) milk in TBS-T. Primary antibodies used were mouse monoclonal anti-L-caldesmon (1:5000) (BD Biosciences, San Jose, CA), mouse monoclonal anti-fascin (1:5000) (Abcam, Cambridge, UK), rabbit anti-UCHL1 (1:5000) (Millipore, Marlborough, MA), mouse anti-tropomyosin (1:1000) (Sigma, St. Louis, MO), and rabbit anti-myosin10 (1:1000) (Cell Signaling Technology, Danvers, MA) antibodies. Mouse anti-α-actin (1:10,000) (Abcam, Cambridge, UK) and rabbit anti-glyceraldehyde-3-phosphate dehydrogenase (GAPDH) (1:10,000) (Santa Cruz Biotechnology, Santa Cruz, CA) were used as loading controls. Secondary antibodies used were HRP- conjugated goat anti-rabbit IgG (1:5000) (Pierce, Rockford, IL), HRP-conjugated goat anti-rabbit IgG (1:5,000) (Santa Cruz Biotechnology, Santa Cruz, CA) and HRP-conjugated sheep anti-mouse IgG (1:5000) (GE Healthcare, Little Chalfont, Buckinghamshire, United Kingdom). The membrane was washed three times with TBS-T in between each antibody incubation step. Subsequent visualization was performed using the SuperSignal West Dura Extended Duration Substrate (Pierce, Rockford, IL) and developed using the Kodak developer and X-ray film, or visualized with the ChemiDoc™ MP System (Bio-Rad, Hercules, CA). The intensity of the bands was quantified by the Quantity One software (GE Healthcare).

2.7 IMMUNOCYTOCHEMISTRY, TISSUE IMMUNOHISTOCHEMISTRY

2.7.1 Immunocytochemistry (ICC) Sample Preparation

The 4 gastric cancer cell lines: AGS, AZ521, FU97 and MKN7 were each cultured as described above. The cells were pelleted by centrifuging at 1000 × g for 10 min, and fixed in Bouin's solution. The cell pellets were transferred for formalin processing and embedded in paraffin cell, and sectioned at 5 µm thickness using a microtome.

2.7.2 Tissue Immunohistochemistry (IHC) Sample Preparation

The tissue samples from 9 patients admitted to Singapore General Hospital between 2004 and 2007 were embedded in paraffin and sectioned for hematoxylin and eosin staining. The tumor regions were reviewed and determined by a pathologist. 5 µm sections from the tissue blocks were made with a microtome. Tissue microarray (TMA) of gastric cancer was constructed with a manual tissue arrayer (Beecher instruments, Silver springs, MD). Cylindrical cores of 1 mm diameter were taken from tissue blocks from 240 patients admitted to Singapore General Hospital between 1998 and 2008, and two cores were taken for each case. Among the 240 patients, 37.8% patients were diagnosed in early tumor stage (T1-T2), while 62.2% were in T3-T4. 25% patients had no lymph node metastasis (N0), and 75% had lymph node metastasis (N1-N3). 85.7% patients had no distant metastasis (M0), 14.3% had distant metastasis (M1)

2.7.3 Immunostaining

The cell block and gastric tumor tissue sections were de-waxed using xylene and ethanol. Antigen retrieval was performed using Tris-EDTA solution (pH = 9) for L-caldesmon, and citrate solution (pH = 6) for fascin with a multifunctional microwave histoprocessor (Milestone, Italy) for 10 minutes. H_2O_2 solution (Dako, Glostrup, Denmark) was added to the tissue sections for 10 min to block endogenous hydrogen peroxidase. Excess reagents were removed from the slides by washing with TBS thrice, each for 3 minutes.

Mouse monoclonal anti-L-caldesmon (BD Biosciences, San Jose, CA) and mouse monoclonal anti-fascin (Abcam, Cambridge, UK) were used as primary antibodies at a dilution of 1:400. The slides were incubated with the primary antibodies for 1 h and subsequently stained with Dako's Real EnVision Detection Kit (Dako, Glostrup, Denmark) following the manufacturers' instruction. The slides were counterstained with hematoxylin (Merck, Darmstadt, Germany). The stained tissue images were scanned and viewed using the ImageScope software (Aperio, CA).

The intensity of the immunocytochemical (ICC) and immunohistochemical (IHC) staining and percentage of positive cells were evaluated by a pathologist. The staining intensity score was rated as follows: 0: no staining, 1+: weak staining, 2+: moderate staining, 3+: strong staining. % positive represents the percentage of positively stained tumor cells. Staining index was calculated as the sum of intensity scores and the percentage of positively stained cells. Wilcoxon signed rank test was used in statistical analysis of paired lymph nodes and primary tumors. Fisher's exact test was used to determine the association between the staining index and the tumor clinical features. The software used for statistical analysis is GraphPad Prism version 5 (San Diego, CA).

2.8 SIRNA-MEDIATED CALDESMON KNOCKDOWN

AGS and FU97 cells were seeded into 6-well plates at a density of 3×10^5 cells per well, and cultured for 24 hours prior to transfection. 10 nM ON-TARGETplus siRNA SMART pool which contained a mixture of 4 siRNA specific for *CALD1* gene (Dharmacon Inc., IL) was introduced to the cells by transfection using 2.5 µl Lipofectamine™ RNAiMAX Transfection Reagent (Invitrogen, Carlsbad, CA) per well. In addition, 10 nM ON-TARGETplus Non-targeting Control pool (Dharmacon) was transfected to control cells for comparison to rule out any off-target effects. 48 hours after transfection, the cells were harvested for immunoblotting to confirm the knockdown of *CALD1*.

2.9 REVERSE-TRANSCRIPTION POLYMERASE CHAIN REACTION (RT-PCR) FOR IDENTIFICATION OF CALDESMON ISOFORMS

2.9.1 RNA Isolation

Total RNA of AGS, AZ521, FU97 and MKN7 cell lines were isolated with TRIZOL Reagent (Invitrogen) according to the manufacturer's instruction. The cell pellets were lysed with 1 ml TRIZOL Reagent. 0.2 ml chloroform was added to each tube and the phase separation was achieved by centrifuging at 4 °C, 12,000 g for 15 min. The upper aqueous phase was transferred to a fresh tube and the RNA was precipitated with 0.5 ml isopropyl alcohol, and washed with 70% ethanol. The extracted RNA was quantified with Nanovue spectrophotometer (GE Healthcare).

2.9.2 cDNA synthesis

SuperScript^{TM}III First-Strand Synthesis System (Invitrogen) was used for first strand cDNA synthesis according to the manufacturer's protocol. 2 µg RNA was mixed with 1 µl 50 µM oligo$(dT)_{20}$ primer and 1 µl 10 mM dNTP, and incubated at 65 °C for 5 min for denaturing. The sample tube was then placed on ice for 1 min. 10 µl cDNA synthesis mix (containing 2 µl 10×RT buffer, 2 µl 0.1 M DTT, 4 µl 25 mM $MgCl_2$, 1 µl RNaseOUT™ and 1 µl SuperScript III RT) were added to the tube and incubated at 50 °C for 50 min. The cDNA synthesis reaction was terminated by incubation at 85 °C for 5 min, briefly chilled on ice and the RNA was removed by 1 µl RNase H at 37 °C for 20 min.

2.9.3 Reverse-Transcription Polymerase Chain Reaction (RT-PCR)

Forward and Reverse primers for caldesmon (Table 2.2) (1stBASE, Singapore) were used to differentiate the isoforms of caldesmon (Figure 2.2)

(Okamoto *et al*., 2000). 2 µl cDNA template was mixed with 10 µM forward and reverse primers, 0.3 µl dNTP, 3 µl 5×PCR buffer, 0.075 µl Taq DNA polymerase (Invitrogen) and topped up to 15 µl. with H_2O. The thermal cycling parameters were set as: 95 °C for 30 sec, 60 ^{0}C for 40 sec, 72 °C for 30 sec for 35 cycles. The reaction was terminated at 72 °C for 5 min. β-actin was used as an internal control to check the efficiency of cDNA synthesis and PCR amplification. The PCR product was separated by 1% agarose gel electrophoresis.

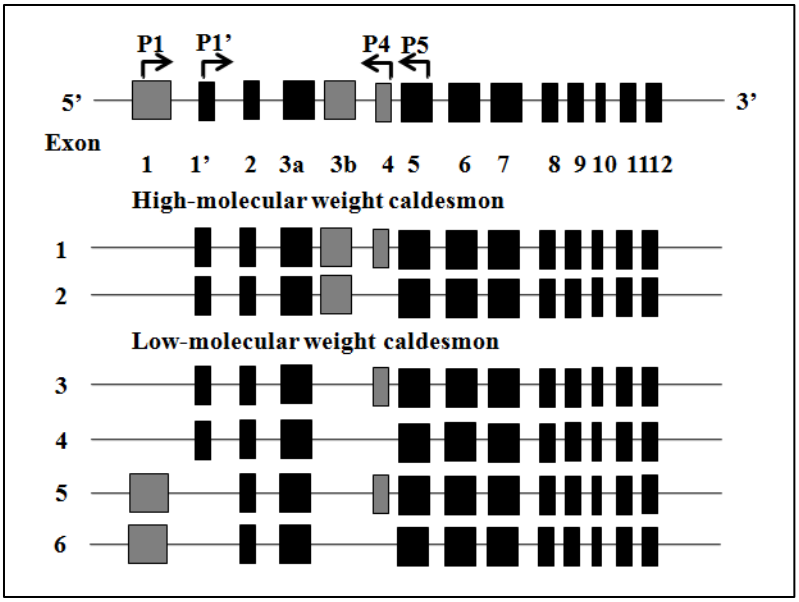

Figure 2.2 The structure of human caldesmon gene consists of at least 14 exons. The arrows indicate the position of the primers used for PCR amplification to identify the isoforms. The six isoforms were shown here. Isoform 1 and 2 are h-caldesmons which are expressed in muscle cells. Isoforms 3 and 4 can be distinguished from isoforms 5 and 6 by primer P1 or P1'. The difference between isoforms 3 and 4, isoform 5 and 6 is the presence of exon 4(78 bp), which can be differentiated by primer P4. (Figure adapted from Okamoto *et al*., 2000).

Gene Target	Forward Primer	Reverse Primer	Expected product length
Caldesmon isoform with exon 1 and exon 5	P1: 5'-GCACCGTGCATTTCAGCCAC-3'	P5:5′-GTTTAAGTTTGTGGGTCATGAATTCTCC-3	851 and 929
Caldesmon isoform with exon 1'and exon 5	P1':5′-CACCATGGATGATTTTGAGCG-3′	P5:5′-GTTTAAGTTTGTGGGTCATGAATTCTCC-3	691 and 752
Caldesmon isoform with exon 1 and exon 4	P1:5'-GCACCGTGCATTTCAGCCAC-3'	P4:5′-GAAGGTAGGCTTGTCTTCTTGGAGCTTTTC-3′	790
Caldesmon isoform with exon 1' and exon 4'	P1':5′-CACCATGGATGATTTTGAGCG-3′	P4:5′-GAAGGTAGGCTTGTCTTCTTGGAGCTTTTC-3′	691
β-actin	5'-TCCATCATGAAGTGTGACGT-3'	5'-TACTCCTGCTTGCTGATCCAC-3'	245

Table 2.2 The list of primers that were used to differentiate the isoforms of caldesmon transcripts and the product length that were amplified.

2.10 STABLE OVER-EXPRESSION OF CALDESMON

Stable over-expression of caldesmon was achieved in AZ521 cells which have low intrinsic expression level of caldesmon. 3×10^4 cells were seeded in a 24-well plate for 24 h. 800 ng of an expression clone encoding human caldesmon 1 transcript variant 3 (also containing puromycin resistance gene) (Genecopoeia, Rockville, MD) was transfected using 2 µl Lipofectamine™ 2000 Transfection Reagent (Invitrogen). After 24 h incubation, the cells were trypsinized and seeded in 1:10 dilution with 1 µg/ml puromycin (Sigma, St. Louis, MO) as the selection reagent. Mock transfection of the empty vector was done in parallel as the negative control. The culturing media was changed every 2-3 days with fresh puromycin. After 2-3 weeks, most of the cells without stable gene integration died and those with stable gene integration grew as individual colonies. These colonies were picked with brief trypsinization and were serial diluted in 96-well plate to obtain single cell per well. Each single cell-generated colony was maintained in puromycin-containing media and their expression levels of caldesmon were checked by Western blotting.

2.11 CELL ASSAYS

2.11.1 Cell Proliferation Assay

$1x10^4$ cells were seeded per well in a 24-well plate (Day 0). After 24, 48 and 72 h, 5 mg/ml of 20 µl 3-(4,5-dimethylthiazol-2-yl)-2,5- diphenyltetrazolium bromide (MTT) (Invitrogen) dissolved in phosphate buffer saline were added to the wells and incubated at 37 °C for 2 h. The insoluble purple color formazan formed from the reduction of tetrazolium MTT by viable cells were solubilized by 200 µl dimethyl sulfoxide (Sigma, St. Louis, MO) and the OD were recorded at 550 nm.

2.11.2 Wound Healing Assay

Wound healing assays were performed with ibidi silicone-insert (ibidi GmbH, Martinsried, Germany). 7×10^5 cells were seeded in both reservoirs of the insert for 24 h. Upon removal of the insert, the closure of the gap was monitored under a light microscope. Triplicate experiments were performed. The images were taken with a 10×objective lens.

2.11.3 Transwell Migration Assay and Matrigel Invasion Assay

Transwell migration assays were carried out using 8.0 micron PET cell culture insert (BD Biosciences, San Jose, CA) coated with 10 µg/ml fibronectin (Sigma, St. Louis, MO) overnight. 3×10^4 cells in media containing 10% FBS were seeded into each insert. Invasion assays were performed with the BioCoat Matrigel Invasion chambers (BD Biosciences, San Jose, CA) using 5×10^4 cells. After 48 h, the cells that had not migrated across the insert pores were removed with a cotton swab. The cells that had migrated through the pores and adhered to the other side of the insert were fixed with 3% paraformaldehyde and stained with crystal violet. The migrated cells were quantified by dissolving the crystal violet dye intake in 1% SDS, and the absorbance was measured at 595 nm. The images were captured with a light microscope and were processed with ImageScope software (Aperio, CA). The experiments were repeated 3 times.

2.11.4 Cell Attachment Assay

Cell attachment assay was performed in 96-well plate. The wells were coated with fibronectin for 1 h at 37 °C, followed by blocking with 0.5% BSA in medium for 1 h. The wells were then washed with 0.1% BSA in medium. 2×10^4 Cells were seeded into the wells for 35 min and the non-attached cells were

washed away by phosphate buffer saline (PBS). The cells were fixed with 3% paraformaldehyde and stained with crystal violet. The experiment was performed in triplicate.

2.12 CO-IMMUNOPRECIPITATION

2.12.1 Caldesmon Co-Immunoprecipitation

The co-immunoprecipitation experiment was performed with Classic IP kit (Pierce, Rockford, IL) according to the manufacturer's instruction. FU97 cells were grown in T175 flask till confluent. The cells were washed twice with cold phosphate buffer saline (PBS) and a cell scrapper was used to detach the cells. The cells were pelleted at 1,000 g for 5 min. 500 µl IP lysis/wash buffer (0.025 M Tris, 0.15 M NaCl, 0.001 M EDTA, 1% NP-40, 5% glycerol, pH 7.4)with 2.5 µl Halt protease inhibitor cocktail (Pierce, Rockford, IL) was used to lyse the cells on ice for 10 min. The lysate was centrifuged at 13,000 g, 4 °C for 30 min and the protein concentration in the supernatant was determined by Coomassie Plus Protein Assay reagent kit (Pierce, Rockford, IL). 1 mg of the protein lysates was incubated with 2.5 µg anti-caldesmon antibody (BD Biosciences, San Jose, CA) in a total volume of 400 µl overnight with gentle end-over-end mixing.

After the incubation step, 20 µl protein A/G agarose beads were washed twice with 100 µl IP lysis/wash buffer in a spin column, and the lysates were added to the beads and incubated for 2 h with gentle end-over-end mixing for the immunocomplex to bind to the agarose beads. The beads were washed thrice with 200 µl IP lysis/wash buffer and once with 100 µl conditioning buffer, before the immunocomplex was eluted thrice with 20 µl elution buffer. The low pH of the eluate was neutralized with 0.5 µl 1M Tris, pH 9.5. A control experiment was performed with an equal amount of lysates incubating with the agarose beads only, and washed and eluted as described above. The presence of caldesmon in the eluate was checked with Western blotting.

2.12.2 Silver Staining

8 µl of the lysates, eluates and control eluate from IP were resolved by SDS-PAGE at a constant current of 15 mA/gel in 10% (v/v) polyacrylamide gel. The gel was silver-stained based on a modified Vorum protocol (Mortz *et al*., 2001). The gel was fixed in 50% (v/v) methanol, 12% (v/v) aceticacid and 0.05% (v/v) formalin for 2 h, followed by washing thrice in 35% (v/v) ethanol, each 20 min. The gel was then sensitized in 0.02% (w/v) sodium thiosulphate for 2 min. The gel was rinsed thrice with water for 5 min, followed by incubation in 0.2% (w/v) silver nitrate and 0.076% (v/v) formalin for 20 min. The gel was washed twice with water, each 1 min, then developed in 6% (w/v) sodium carbonate, 0.004% (w/v) sodium thiosulphate with 0.05% (v/v) formalin. Upon reaching the desired density, the gel was incubated for 20 min in 1.46% (w/v) sodium ethylenediaminetetraacetic acid (EDTA) to stop the development. Lastly, the gel was washed thrice with water, 5 min each time. Every step was conducted with constant shaking.

2.12.3 In-Gel Tryptic Digestion

The protein bands of interest were excised from the silver stained gel. Each band was soaked in 150 µl of 50% HPLC grade acetonitrile (ACN) (ThermoScientific, Bremen, Germany) with 2.5 mM ammonium bicarbonate (NH_4HCO_3) (Sigma) washing buffer for 24 h at 4 °C. Fresh washing buffer of 150 µl of 50% ACN, 2.5 mM NH_4HCO_3 was added and the bands were incubated at 37 °C for 10 min. The bands were vacuum dried for 10 min before 20 µl of 10 mM dithiothreitol (DTT) (Bio-Rad, Hercules, CA) in 100 mM NH_4HCO_3 was added for protein reduction at 56 °C for 1 h. The DTT solution was then removed and the bands were incubated with 20 µl of 55 mM iodoacetamide (IAA) (Fluka, Buchs, Switzerland)) in 100 mM NH_4HCO_3 for 45 min at room temperature in the dark. The bands were then soaked in 100 mM NH_4HCO_3 at 37 °C for 10min, followed by incubation in 100 µl ACN for 10 min at room temperature. These two steps were repeated. The bands were then vacuum dried. 0.1 µg of sequence grade modified trypsin (Promega, Madison, WI) was added to each band and

trypsinization was performed at 37 °C for 16 h. After that, the peptide extraction was further enhanced by the addition of 10 µl of 0.1% formic acid (FA) (Fluka) in 50% ACN to each band and the tubes were sonicated for 20 min in an ultrasonic water bath.

The digested samples were desalted with Sep-Pak tC_{18} µElution Plate (Waters, Milford, MA) according to the manufacturer's instruction. The plate was activated with 400 µl 100% ACN with 0.05% formic acid twice with a full vacuum pressure by a vacuum manifold, followed by equilibration with 400 µl 2% (v/v) ACN with 0.05% FA in H_2O twice. The digested samples were topped up to 250 µl with 2% (v/v) ACN with 0.05% FA in H_2O and loaded to the plate with half vacuum pressure for binding. The unbound fractions was washed away with 200 µl 2% (v/v) ACN with 0.05% FA in H_2O. The peptides were eluted by 100 µl 80% ACN with 0.05% FA in H_2O thrice. The eluate was vacuum dried and redissolved in 10 µl 2% (v/v) ACN with 0.05% FA in H_2O for mass spectrometry analysis.

2 µl sample was loaded onto ChromXP C18-CL, 3 µm 120 A trap column (Eksigent, Dublin, CA) and eluted on an analytical column (Eksigent) with increased organic phase gradient at a flow rate of 300 nl/min on an Eksigent nanoLC Ultra and ChiPLC-nanoflex system. The MS spectra were acquired on a TripleTOF 5600 system (AB SCIEX) across a mass range of 400-1250 m/z in high resolution mode (>30000). A maximum of 10 precursors per cycle were chosen for fragmentation from each MS spectrum. Tandem mass spectra were performed in high sensitivity mode (resolution >15000). All MS/MS spectra were searched by the Protein Pilot ^{TM} software v. 4.0 (AB SCIEX) against UniProt database for protein identification.

CHAPTER 3 RESULTS

3.1 ITRAQ ANALYSIS OF METASTATIC *VERSUS* PRIMARY GASTRIC CANCER CELL PROTEOMES

From the iTRAQ results, a total of 641 proteins were identified with 95% confidence. To obtain the Gene Ontology information (The Gene Ontology Consortium., 2000) of these proteins, we used the Software Tool for Researching Annotations of Proteins (STRAP), an open-source C# application which annotates gene functions based on gene ontology (GO) terms associated with Uniprot protein IDs (Bhatia, 2009). The proteins identified from the iTRAQ results covered a wide range of cellular locations: 24% from nucleus, 21% from cytoplasm, 7% from mitochondria, 7% from cytoskeleton and 8% from plasma membrane (Figure 3.1).

For each of the proteins identified, the relative expressions between well/ moderate-differentiated metastatic (MKN7) *versus* primary cell line (AGS), and poorly-differentiated metastatic (AZ521) *versus* primary cell line (FU97) were represented by 8 iTRAQ ratios. With cutoff value of 1.5-fold applied, the proteins were considered to be up-regulated when 6 out of 8 iTRAQ ratios were above 1.5, and at least one ratio with $p<0.05$ and down-regulated when 6 of the 8 iTRAQ ratios < 0.67, and at least one ratio has $p<0.05$. The list of these differentially-expressed proteins (19 up- and 33 down-regulated) was shown in Table 3.1. Up-regulation of proteins involved in the transcriptional regulation and translational regulation were observed in the metastatic cell lines. The up-regulation of proteins involved in glycolysis (LDHA) and down-regulation of proteins in tricarboxylic acid cycle (IDH1, FH, SDHA) may be associated with the cancer cells' increasing demand for energy and switching from normal oxidative phosphorylation to glycolysis during metastasis progression (Pani *et al.*, 2010).

The analysis of these 52 differentially-expressed proteins using the Ingenuity Pathway Analysis (IPA) software showed that the top networks were related to cell death, cellular movement, cell growth and proliferation. The top-ranking network, with 16 of the regulated proteins mapped to it, was presented in Figure 3.2. Several proteins associated with this network have been reported in previous studies to predict cancer metastasis. For example, high expression level of aldehyde dehydrogenase ALDH1A3 has been proposed to predict breast cancer metastasis (Marcato *et al*., 2011). Leukocyte elastase inhibitor SERPINB1, a matrix metalloproteinase inhibitor, was found to have lower expression level in tumors as compared to normal tissues (Chen *et al*., 2007). In addition, it was noted that cell motility-related cytoskeleton proteins, such as caldesmon, were also associated with this network.

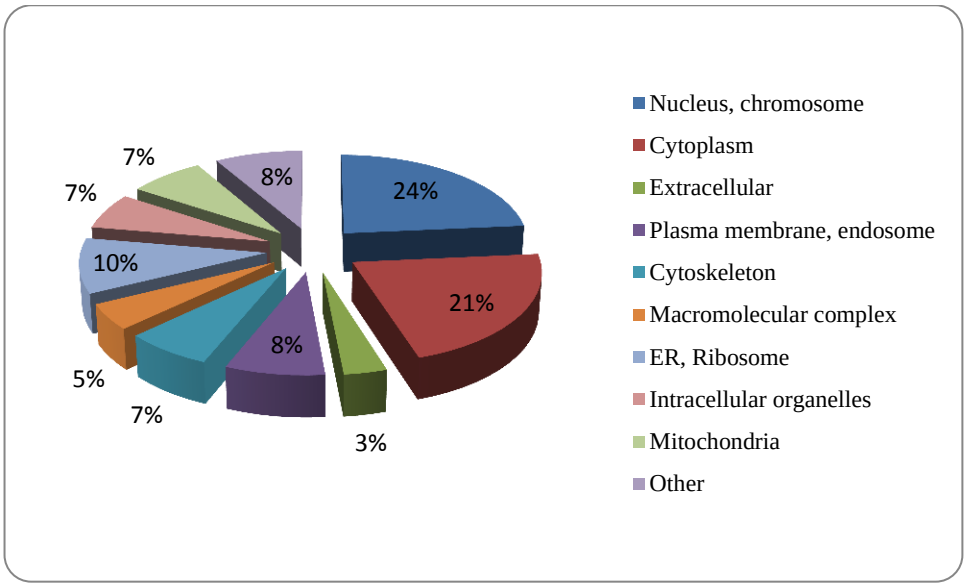

Figure 3.1 Gene Ontology classification of the cellular component of total proteins identified by iTRAQ.

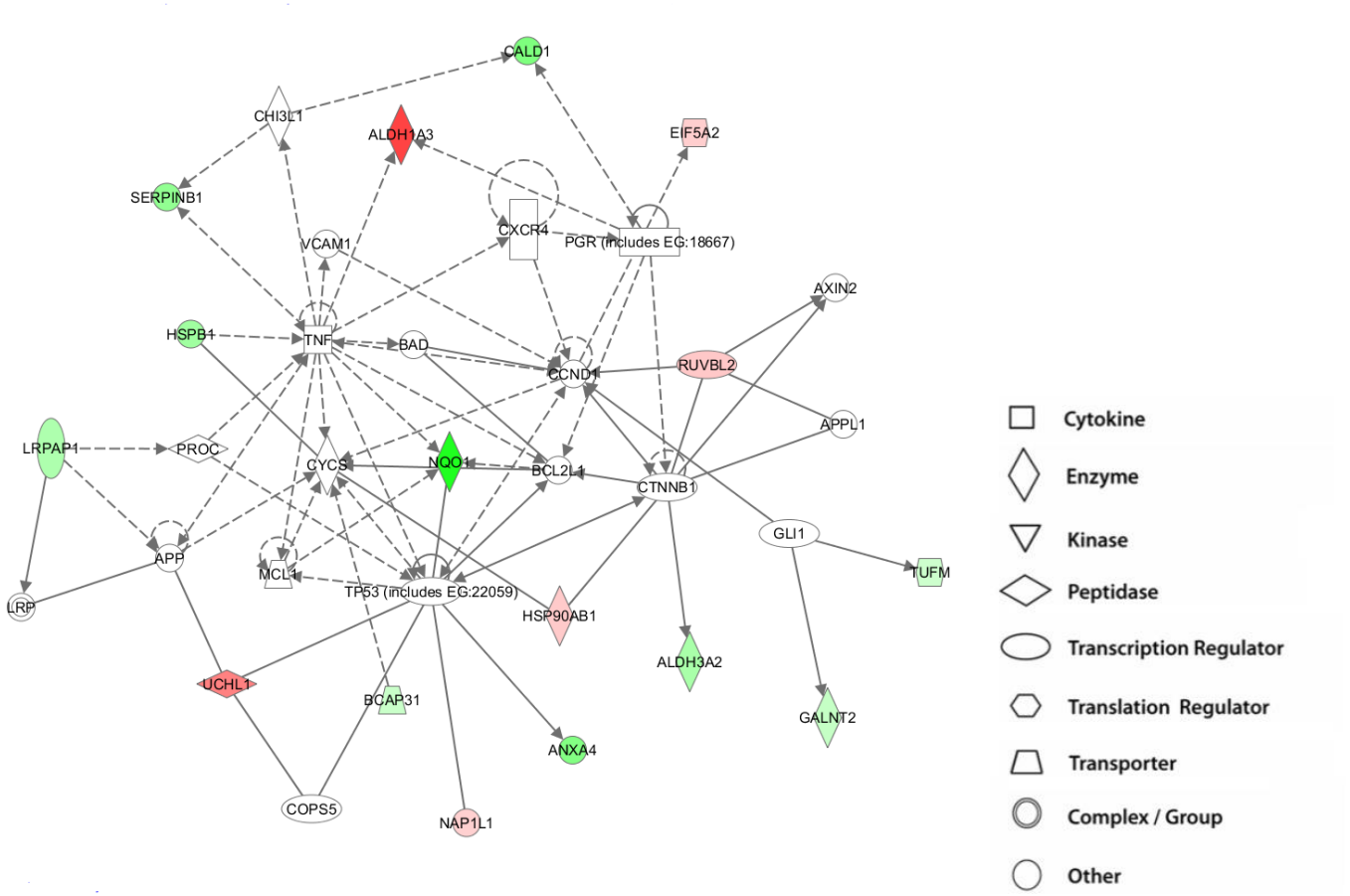

Figure 3.2 Top network for the differentially expressed proteins in gastric cancer metastasis. Green: down-regulated proteins, red: up-regulated proteins in metastasis.

Up-regulation in metastasis							
IPI accessions	**Unused Score**	**Gene symbols**	**Protein Name**	**Function**	**MKN7:AGS**	**AZ521:FU97**	***P* Value**
IPI00396485.3	40.03	EEF1A1	Elongation factor 1-alpha 1	Protein biosynthesis, Transcription regulation	1.49	1.69	0
IPI00789435.2	6	EEF1D	Elongation factor 1-delta isoform 3		2.53	1.95	0.02
IPI00738381.2	17.88	EEF1G	Elongation factor 1-gamma		1.60	1.63	0
IPI00946642.1	4.77	EIF5A2	Eukaryotic translation initiation factor 5A2		1.46	1.84	0
IPI00299573.12	2.8	RPL7A	60S ribosomal protein L7a	Structural constituent of ribosome, RNA binding, Translation	1.79	2.93	0.002
IPI00027270.1	2.11	RPL26	60S ribosomal protein L26		1.89	3.76	0.0036
IPI00927658.1	2.17	RPL32	Ribosomal protein L32		1.72	3.16	0.006
IPI00794894.1	2.03	RPL23A	RPL23A Protein		2.02	3.91	0.036
IPI00414676.6	66.97	HSP90AB1	Heat shock protein HSP 90-beta	Molecular chaperone, Stress response	1.66	1.87	0
IPI00026663.2	7.66	ALDH1A3	Aldehyde dehydrogenase family 1 member A3	Catalyze aldehyde + NAD(P)+ to carboxylate + NAD(P)H.	7.71	4.92	0.0006
IPI00218414.5	2.01	CA2	Carbonic anhydrase 2	Catalyze $H_2CO_3 = CO_2 + H_2O$	1.83	8.86	0.06
IPI00947127.1	18.31	LDHA	Lactate dehydrogenase A chain isoform 3	Glycolysis, (S)-lactate + NAD+ to pyruvate + NADH.	1.69	1.89	0
IPI00218918.5	16.15	ANXA1	Annexin A1	Calcium ion binding	1.47	12.25	0

IPI00872379.1	2	ANXA5	Annexin A5		2.28	2.25	0.01
IPI00747810.2	9.08	FSCN1	Fascin	Actin filament bundle assembly, Cell migration, invasion	5.21	3.91	0.0023
IPI00790503.3	2.22	MYH10	Isoform 3 of Myosin-10	Actin filament-based movement	3.18	1.74	0.027
IPI00007402.3	10	IPO7	Importin-7	Nuclear protein import	1.80	3.40	0.02
IPI00018352.1	5.24	UCHL1	Ubiquitin carboxyl-terminal hydrolase isozyme L1	Ubl conjugation pathway	5.01	3.40	0.015
IPI00023860.1	4.59	NAP1L1	Nucleosome assembly protein 1-like 1	Modulating chromatin formation, regulation of cell proliferation	1.40	1.75	0.004
Down-regulation in metastasis							
IPI accessions	**Unused Score**	**Gene symbols**	**Protein Name**	**Function**	**MKN7:AGS**	**AZ521:FU97**	***P* Value**
IPI00394758.1	6.01	ALDH3A2	Isoform 2 of Fatty aldehyde dehydrogenase	Catalyzes the oxidation of long-chain aliphatic aldehydes to fatty acids	0.47	0.31	0.03
IPI00219757.13	8.74	GSTP1	Glutathione S-transferase P	Conjugation of reduced glutathione to hydrophobic electrophiles	0.84	0.49	0.0003
IPI00945749.1	6.46	POR NADPH	Cytochrome P450 reductase	Catalyze NADPH + oxidized hemoprotein to $NADP^+$ + reduced hemoprotein.	0.59	0.39	0.0003
IPI00910902.1	10	NQO1	cDNA FLJ50573, highly similar to Homo sapiens NAD(P)H dehydrogenase, quinone 1 (NQO1), transcript variant 3, mRNA	Catalyze NAD(P)H + a quinone = NAD(P)+ + a hydroquinone-	0.20	0.10	0.0046
IPI00939560.1	7.55	TXNDC5	MUTED thioredoxin domain-containing protein 5 isoform 3	Cell redox homeostasis	0.50	0.51	0.0082
IPI00004669.1	6.02	GALNT2	Polypeptide N-acetylgalactosaminyltransferase 2	Post-translational protein modification	0.74	0.40	0.0003
IPI00027223.2	5.45	IDH1	Isocitrate dehydrogenase [NADP] cytoplasmic	Tricarboxylic acid cycle	0.57	0.15	0.0001

IPI00759715.1	2	FH	Isoform Cytoplasmic of Fumaratehydratase, mitochondrial		0.63	0.41	0.02
IPI00217143.3	2.15	SDHA	SDHA protein		0.44	0.35	0.015
IPI00921173.1	4	SUCLG1	SUCLG1 protein		0.72	0.61	0.0052
IPI00024993.4	2	ECHS1	Enoyl-CoA hydratase, mitochondrial	Fatty acid metabolism	0.43	0.51	0
IPI00218568.7	4.32	PCBD1	Pterin-4-alpha-carbinolamine dehydratase	Transcription regulation	0.25	0.55	0.02
IPI00016703.2	4.03	DHCR24	24-dehydrocholesterol reductase	Cholesterol metabolism	0.51	0.25	0.049
IPI00643801.1	3.67	CTSA	Cathepsin A	Lysosome function	0.67	0.40	0.0042
IPI00022334.1	3.3	OAT	Ornithine aminotransferase, mitochondrial	Amino-acid biosynthesis	0.49	0.49	0.0012
IPI00293303.1	3.16	LGMN	Legumain	Proteolysis	0.57	0.50	0.04
IPI00027444.1	4	SERPINB1	Leukocyte elastase inhibitor	Protease inhibitor	0.28	0.33	0.04
IPI00032140.4	33.2	SERPINH1	Serpin H1	Collagen biosynthetic process	0.77	0.35	0
IPI00872780.1	3	ANXA4	Annexin A4	Calcium-binding protein	0.41	0.13	0.013
IPI00295542.5	2.06	NUCB1	Nucleobindin-1		0.63	0.55	0.065
IPI00554648.3	42.5	KRT8	Keratin, type II cytoskeletal 8	Intermediate filament	0.57	0.21	0
IPI00014516.1	4.07	CALD1	Isoform 1 of Caldesmon	Actin binding	0.33	0.18	0.0006
IPI00010951.2	3.89	EPPK1	Epiplakin	Cytoskeleton protein	0.26	0.61	0.015
IPI00215611.	7.71	CRIP1	Cysteine-rich protein 1	Intracellular zinc transport	0.09	0.68	0.04

5							
IPI00027107.5	22.06	TUFM	Tu translation elongation factor, mitochondrial precursor	Protein biosynthesis	0.72	0.60	0
IPI00017283.2	10.5	IARS2	Isoleucyl-tRNAsynthetase, mitochondrial		0.64	0.41	0.0001
IPI00642984.2	6.19	BCAP31	B-cell receptor-associated protein 31 isoform a	Protein transport	0.78	0.45	0.0005
IPI00292135.1	6.18	LBR	Lamin-B receptor	Nuclear envelope inner membrane protein	0.65	0.45	0.0021
IPI00922055.1	5.5	DBI	Diazepam binding inhibitor, splice form 1G	Transport	0.63	0.47	0.0013
IPI00646182.5	18.21	ATP1A1	Sodium/potassium-transporting ATPase subunit alpha-1 isoform c	Ion transport	0.73	0.57	0
IPI00010896.3	2.83	CLIC1	Chloride intracellular channel protein 1		0.64	0.64	0.03
IPI00924436.1	2.14	HSPB1	Heat shock 27kDa protein 1	Stress resistance and actin organization	0.21	0.48	0.04
IPI00908889.1	4.62	PITRM1	cDNA FLJ54065, moderately similar to Musmusculuspitrilysinmetallepetidase 1 (Pitrm1), mRNA	Mitochondria ATP-independent protease	0.43	0.44	0.04

Table 3.1 Differentially expressed proteins, their accession numbers, gene symbols identified from the iTRAQ study. The relative expression of each protein was based on the ratio of the respective iTRAQ labels. The protein functions were extracted from the Uniprot database.

3.2 VERIFICATION OF SELECTED TARGETS WITH WESTERN BLOTTING

Several of the differentially-expressed proteins found in this iTRAQ study have been reported to be perturbed in other cancer types. The up-regulation of fascin in non-small cell lung cancer is associated with cancer malignancy (Zhao *et al*., 2010). UCHL1 plays a key role in regulating invasion and renal cell carcinoma metastasis (Kim *et al*., 2009; Seliger *et al*., 2007). Caldesmon binds to actin and has been found in the invasion front of cancer cells, while ectopic expression of caldesmon in transformed fibroblast cells reduces cancer cell invasiveness (Yoshio *et al*., 2007). In our iTRAQ data, fascin expression has been found to be high in metastasis-derived MKN7 and AZ521 compared to their primary counterparts AGS and FU97. UCHL1 is overexpressed in MKN7 and AZ521 compared to in AGS and FU97. Caldesmon has been found to be down-regulated in MKN7 and AZ521cells as compared to the primary cell counterpart AGS and FU97.

The differential expressions of these 3 proteins were verified in AGS, FU97, MKN7, and AZ521 cell lysates with western blotting (Figure 3.3). The Western blotting results were quantified with densitometry and were in agreement with the iTRAQ results.

Caldesmon and fascin are of special interest as they are both actin cytoskeleton associated proteins that have been reported to be involved in cell migration and invasion (Vignjevic *et al*., 2007; Yoshio *et al*., 2007). To study the expression level of caldesmon and fascin, we analyzed a panel of gastric cancer cell lines from primary cancer (AGS, FU97) as well as gastric cancer cell lines isolated from various metastasis status (lymph node (MKN7, AZ521), liver (MKN74, N87) and ascites (SNU16, YCC1,YCC2, YCC3, YCC9)) with Western blotting. It was observed that caldesmon expressions were higher in primary-cancer derived cell lines compared to lymph node and liver metastasis-derived

gastric cancer cell lines. Caldesmon expressions are either low or not detected in the ascites-derived cell lines. Fascin expressions are low in primary cancer cell lines AGS and FU97, and high in lymph node and liver metastasis-derived gastric cancer cell lines (MKN7, AZ521, MKN74, N87), and in 2 out of 5 ascites-derived gastric cancer cell lines (YCC2, YCC9) (Figure 3.4). The lower expression of fascin in SNU16, YCC1 and YCC3 may be attributed to inherent inter-patient variations.

(A)

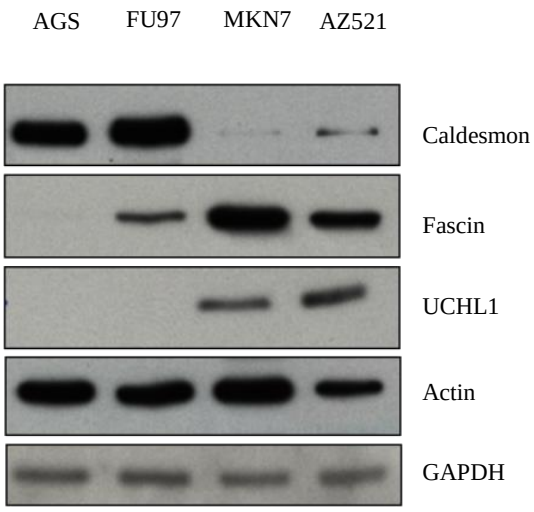

(B)

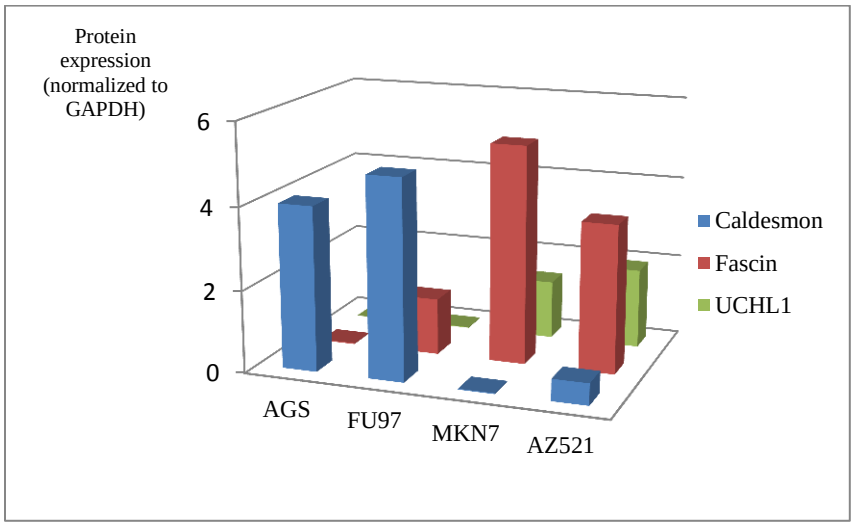

Figure 3.3 Analysis of expression levels of 3 target proteins by (A) Western blotting and (B) quantitation with densitometry in 4 gastric cell lines. Actin and GAPDH were used as loading controls. Caldesmon was down-regulated; fascin and UCHL1 were up-regulated in metastatic cell lines. Densitometry analysis of protein bands intensity was normalized to GAPDH protein bands intensity.

Figure 3.4 Western blotting showed the expression levels of caldesmon and fascin in a panel of 11 gastric cancer cell lines. Actin was used as a loading control. Caldesmon level was reduced in lymph node metastasis-derived MKN7 and AZ521, liver metastasis-derived MKN74 and N87, and ascites-derived SNU16, YCC1, YCC2, YCC3 and YCC9. Fascin expressions were low in AGS and FU97 and high in 6 out of 9 metastatic-derived gastric cancer cell lines (MKN7, AZ521, MKN74, N87, YCC2, and YCC9).

3.3 VERIFICATION OF CALDESMON AND FASCIN EXPRESSION WITH IMMUNOCYTOCHEMISTRY

Immunostaining of caldesmon and fascin in the 4 gastric cancer cell lines was carried out. The nuclei were stained blue by hematoxylin, while the target proteins were stained brown. Combining the intensity score and percentage of positively-stained cells, AGS and FU97 have stronger caldesmon expression compared to MKN7 and AZ521, and weaker fascin expression compared to MKN7 and AZ521; caldesmon and fascin were found to be localized in the cytoplasm of the cell (Figure 3.5). The results are in accord with our findings from iTRAQ and western blotting. Our results show that AZ521 cell line was partially stained. This could be due to a variably expression of caldesmon during a dynamic process of tumor heterogeneity and clonal expansion, and assessment on tissue alone may be restrictive. In future work, we can look for this marker in the circulating tumor cells.

(A)

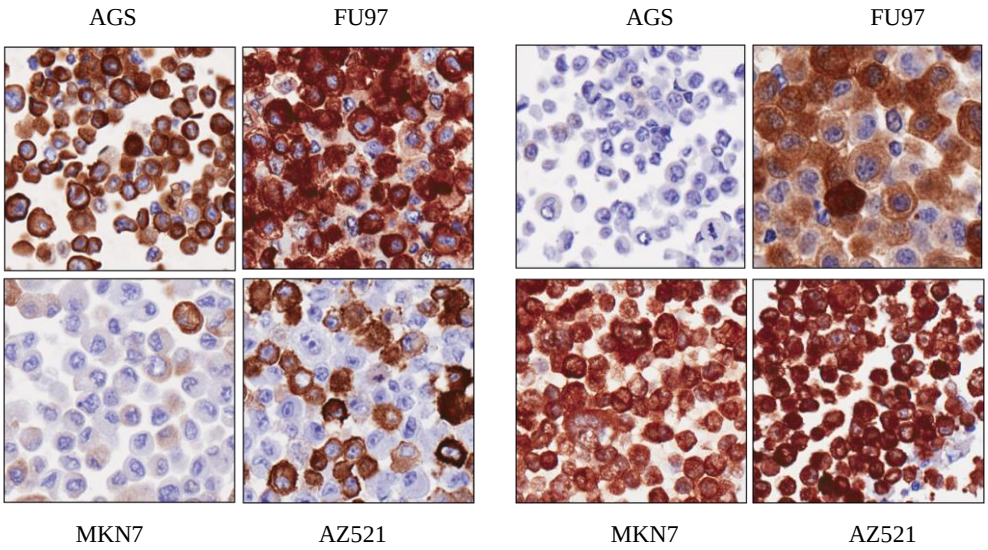

(B)

	AGS	FU97	MKN7	AZ521
Caldesmon staining score	2+, 70% positive	3+, 70% positive	1+, 10% positive	2+, 30% positive
Fascin staining score	0	2+ ,40% positive	3+, 70% positive	3+, 90% positive

Figure 3.5 (A) Immunocytochemical staining of caldesmon and fascin in cell blocks of 4 gastric cancer cell lines.
(B)The intensity scores and the percentages of positive stained cells were shown in the table. The intensity was rated from 0 to 3+; 0 represents no expression, and 3+ represents the strongest expression. Both intensity and % of positive cells were determined by a pathologist.

3.4 CALDESMON AND FASCIN EXPRESSION IN PAIRED LYMPH NODE METASTASIS AND PRIMARY GASTRIC CANCER TISSUES

We further examined the expression of caldesmon and fascin in gastric cancer tissues using immunohistochemical staining of tissues from 9 gastric cancer patients with matched primary and lymph node metastasis. As shown in Figure 3.6, caldesmon staining is high in the primary cancer cells, but decreases in tumor cells from metastatic lymph nodes. Comparing the staining index of 9 cases of lymph node metastasized tissues with matched primary cancer tissues revealed that caldesmon expression is decreased in the former (p=0.037) (Figure 3.7).

Strong staining of fascin was observed in lymph node metastasized cancer cells, compared to very low intensity of fascin in the primary tumors (Figure 3.8). The IHC staining index of 9 cases of lymph node metastasized tissues with matched primary cancer tissues revealed that fascin expression is increased in tumor cells of lymph node metastasized tissues (p=0.0071) (Figure 3.9). These results supported our iTRAQ findings which showed a down-regulation of caldesmon and up-regulation of fascin and as the gastric tumor metastasized to lymph node. In normal gastric tissues, the expression of fascin and caldesmon were both very low (data not shown).

(A)

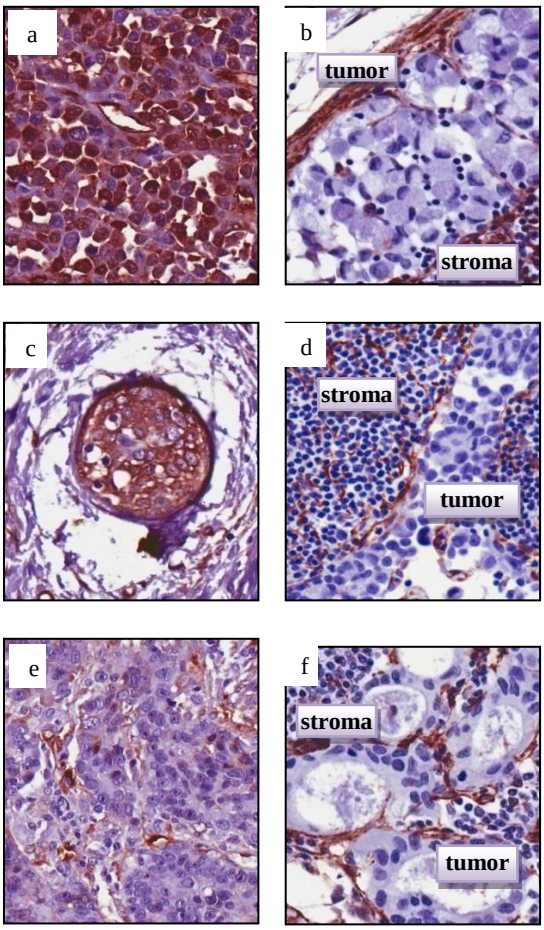

(B)

Caldesmon Intensity score	Primary tumor	lymph node metastasized tissue
	a) 2+, 80% positive	b) 1+, 10% positive
	c) 2+. 40% positive	d) 0
	e) 1+, 10% positive	f) 0

Figure 3.6(A) Immunohistochemistry of caldesmon in paired primary gastric tumor and lymph node metastasized tissues. (a) signet ring carcinoma primary tumor, (b) signet ring carcinoma lymph node metastasis, (c) poorly-differentiated gastric cancer primary tumor, (d) poorly-differentiated gastric cancer lymph node metastasis, (e) well-differentiated gastric cancer primary tumor, (f) well-differentiated gastric cancer lymph node metastasis.
(B) The intensity score and the percentages of the positive stained cells were shown in the table.

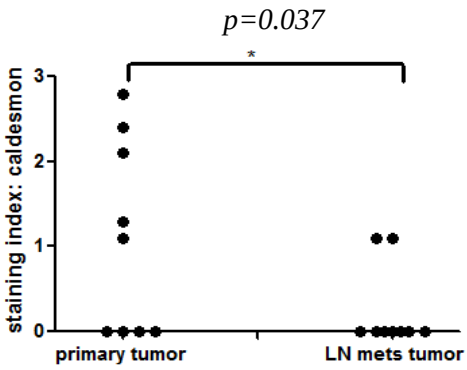

Figure 3.7 Staining index of caldesmon in lymph node metastasis was significantly decreased as compared to primary tumor. N=9. Wilcoxon signed rank test *: $p \leq 0.05$.

(A)

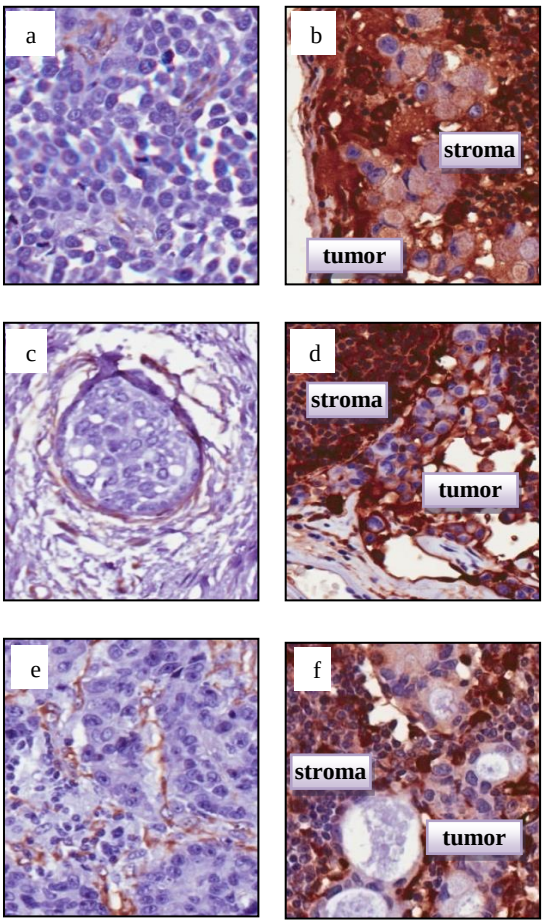

(B)

Fascin Intensity score	Primary tumor	lymph node metastasized tissue
	a) 0	b) 2+, 40% positive
	c) 0	d) 3+, 30% positive
	e) 0	f) 1+, 30% positive

Figure 3.8(A) Immunohistochemistry of fascin in paired primary gastric tumor and lymph node metastasized tissues. (a) signet ring carcinoma primary tumor, (b) signet ring carcinoma lymph node metastasis, (c) poorly-differentiated gastric cancer primary tumor, (d) poorly-differentiated gastric cancer lymph node metastasis, (e) well-differentiated gastric cancer primary tumor, (f) well-differentiated gastric cancer lymph node metastasis.
(B)The intensity score and the percentages of the positive stained cells were shown in the table.

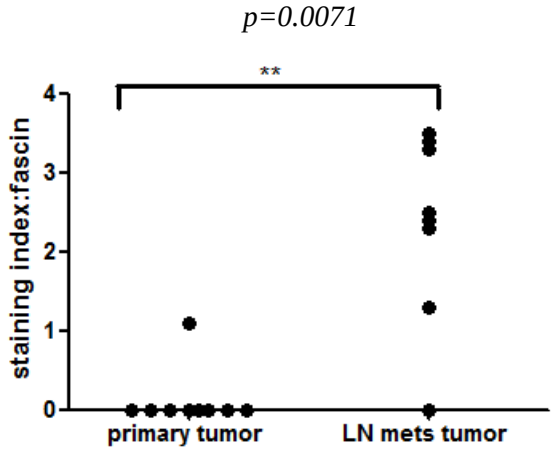

Figure 3.9 Staining index of fascin in lymph node metastasis was significantly increased as compared to primary tumor. N=9. Wilcoxon signed rank test **: $p \leq 0.01$.

3.5 TISSUE MICROARRAY ANALYSIS OF CALDESMON AND FASCIN EXPRESSION

Tissue microarrays (TMA) from gastric cancer tissues of 240 patients were constructed. The clinical features of these cases were summarized in Table 3.2. The tissue microarrays were subject to immunohistochemical analysis for caldesmon and fascin expression. Analysis of the TMA staining showed that the increased in fascin expression correlated with advanced serosal invasion and lymph node metastasis (Table 3.3). Survival analysis showed that in well/moderately-differentiated gastric cancer patients, those with fascin-negative tumors had a better clinical outcome than those with fascin-positive tumors (p=0.043) (Figure 3.10).

However, as caldesmon expression was decreased in tumor cells, we found only 14 cases of caldesmon expressed in tumor cells. In contrast, the expression of caldesmon in the tumor stroma and pericellular matrix was relatively high, and an increased pericellular expression of caldesmon was found to be associated with tumor infiltration (Table 3.3).

Clinical features	Number
Mean age (range, years)	65.2± 12.0 (27-91 years)
Gender (male/female)	148/91 (61.9%/38.1%)
Histology Subtypes	
Well/moderately differentiated	93 (39.6%)
Poorly-differentiated	122 (51.9%)
Mixed	20 (8.5%)
Serosal invasion	
absent (T1-T2)	84 (37.8%)
present (T3-T4)	138 (62.2%)
Lymph node metastasis	
absent (N0)	55 (25%)
present (N1-N3)	165 (75%)
Distant metastasis	
absent (M0)	174 (85.7%)
present (M1)	29 (14.3%)

Table 3.2 Clinical features of tumor tissues used in the TMA study. The patients' ages ranged from 27-91 years with a median age of 65.2 year. 61.9% were male and 38.1% female. Well/moderately differentiated subtypes consisted of 39.6%, poorly-differentiated 51.9% and mixed histology 8.5%. 37.8% patients have early tumor stage (T1-T2), 62.2% were in T3-T4. 25% patients had no lymph node metastasis, 75% had lymph node metastasis (N1-N3). 85.7% patients had no distant metastasis, 14.3% had distant metastasis (M1).

Serosal invasion	Fascin tumor staining index=0 N (%)	Fascin tumor staining index >0 N (%)	Fisher's exact test (two-tailed)
absent(T1-T2)	61(72.6%)	23(27.4%)	
present(T3-T4)	79(58.0%)	57(42.0%)	p=0.0315*
Lymph Node Metastasis			
absent(N0)	40(72.7%)	15(27.3%)	
present(N1-N3)	98(53.6%)	85(46.4%)	p=0.0127 *

Serosal invasion	Caldesmon pericellular staining index=0 N(%)	Caldesmon pericellular staining index >0 N(%)	Fisher's exact test (two-tailed)
absent(T1-T2)	53(63.1%)	31(36.9%)	p=0.0264 *
present(T3-T4)	65(47.1%)	73(52.9%)	

Table 3.3 Increased fascin staining index was correlated with serosal invasion and lymph node metastasis, and increased caldesmon pericellular staining index was associated with serosal invasion only. The Statistical test used was Fisher's exact test. Only 27.4% of the patients without tumor serosal invasion (T1-T2) had positive fascin IHC staining in the tumor cells, while 42% of the patients with tumor serosal invasion (T3-T4) had positive fascin stainings. Similarly, only 27.3% of the patients with no lymph node metastasis had positive stainings for fascin in the tumors, while 46.4% of the patients with lymph node metastasis had positive stainings of fascin. For caldesmon in the pericellular space of tumor, 36.9% of the patients without tumor serosal invasion had positive stainings, while 52.9% of the patients with tumor serosal invasion had positive stainings. Fisher's exact test (two-tailed): * p<0.05.

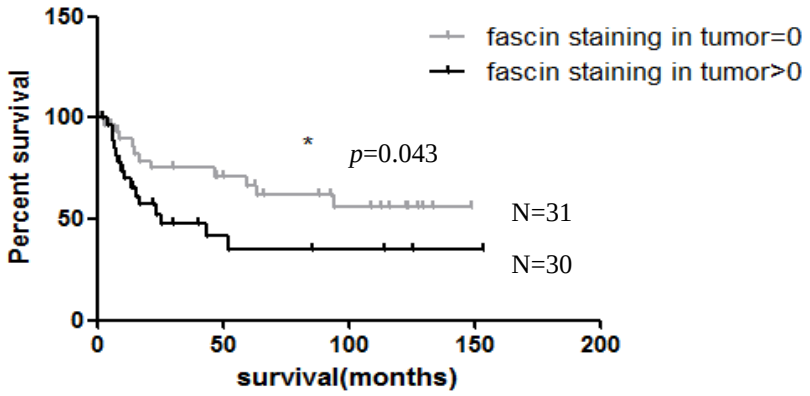

Figure 3.10 Cumulative survival curves in patients with well/moderately-differentiated gastric cancer. Patients with fascin-negative tumors had a better clinical outcome than those with fascin-positive tumors. Survival curves were plotted with the method of Kaplan and Meier. Statistical difference between two groups was compared with log-rank test * $p<0.05$.

3.6 KNOCKDOWN OF CALDESMON EXPRESSION WITH RNA INTERFERENCE

We have discovered that an increase in fascin expression in gastric cancer metastasis-derived cell lines and this increasing trend was associated with gastric cancer serosal invasion and lymph node metastasis. Fascin promoted cancer cell migration and invasion and immunohistochemical studies found that the expression of fascin in gastric cancer was associated with metastasis (Tan *et al.*, 2013). Our findings on fascin corroborated with the current understanding. A decreased caldesmon expression in gastric cancer lymph node metastasis derived cell lines was also observed. The association of caldesmon expression and gastric cancer unveiled by our proteomics study was novel, and functional studies were therefore performed to elucidate caldesmon's role in gastric metastasis.

We performed knockdown of caldesmon with siRNA in gastric cancer cells, and evaluated the migration and invasion behavior of the cancer cell. Caldesmon expression was successfully reduced after 48 hours of transfection with caldesmon-specific siRNA in AGS and FU97 cells and the knockdown effect remained till 96 hours after transfection (Figure 3.11). The growth rates of caldesmon knockdown cells were not significantly different from the control cells (Figure 3.12). Using wound healing assays, we observed a faster closure of scratch wound in the caldesmon knockdown AGS cells and FU97 cells as compared to the control cells (Figure 3.13). With transwell migration assay, we observed a significant increase in cell migration of the caldesmon knock-down cells (Figure 3.14). Using Matrigel invasion assay which mimicked tumor cells' degradation of the basement membrane (Albini & Benelli, 2007), an increased number of caldesmon knockdown tumor cells were observed invading through the Matrigel matrix as compared to the control cells (Figure 3.15). These findings from the cell assays thus proved that caldesmon played a role in suppressing gastric cancer cell migration and invasion.

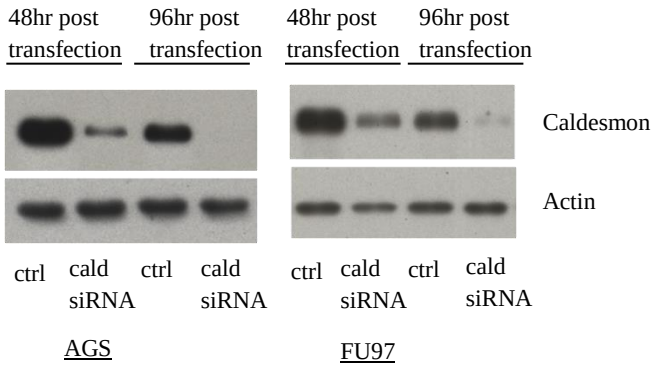

Figure 3.11 Western blot showed a decreased caldesmon protein level in AGS and FU97 cells upon transfection till 96 hours. Ctrl: control non-target siRNA transfection. Cald siRNA: caldesmon siRNA pool transfection.

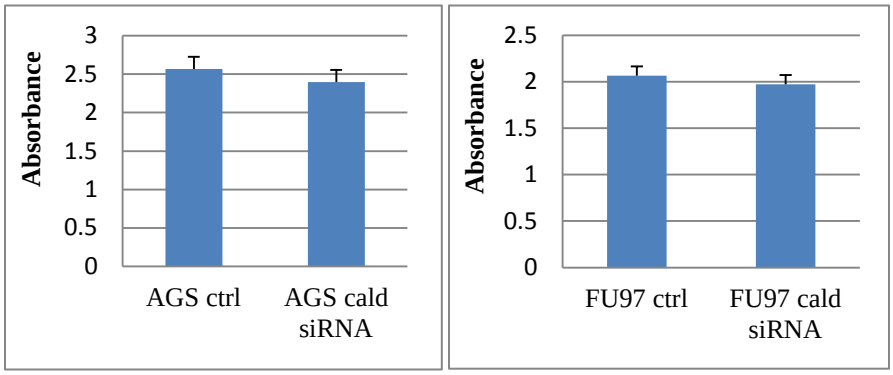

Figure 3.12 MTT assay assessing cell survival 48 hours after siRNA transfection showed no growth difference between caldesmon siRNA-transfected and control cells.

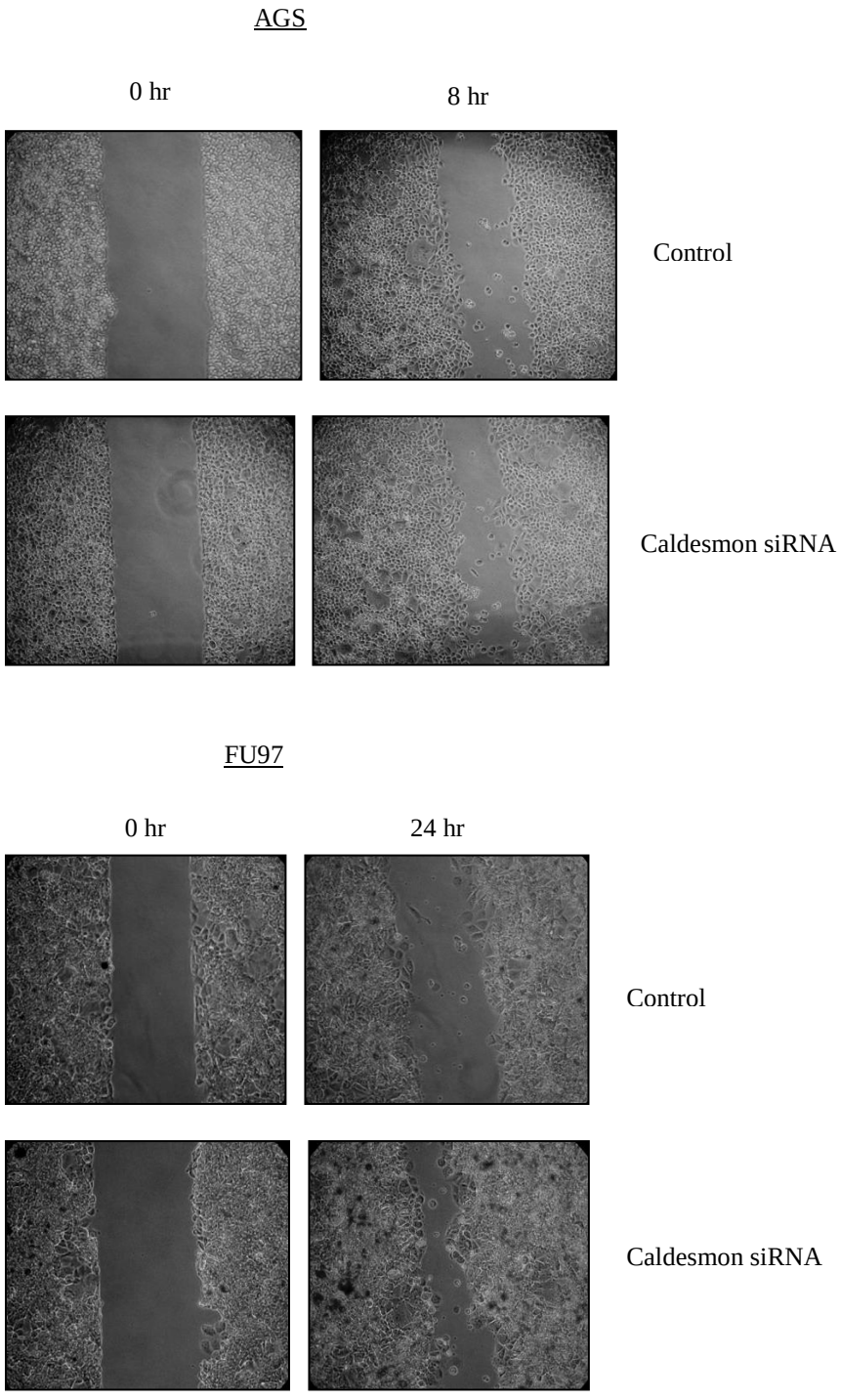

Figure 3.13 Wound healing assays showed within 8 hours, caldesmon siRNA-transfected AGS cells closed the gap faster than control cells. Wound healing assays showed within 24 hours, caldesmon siRNA-transfected FU97 cells closed the gap faster than control cells.

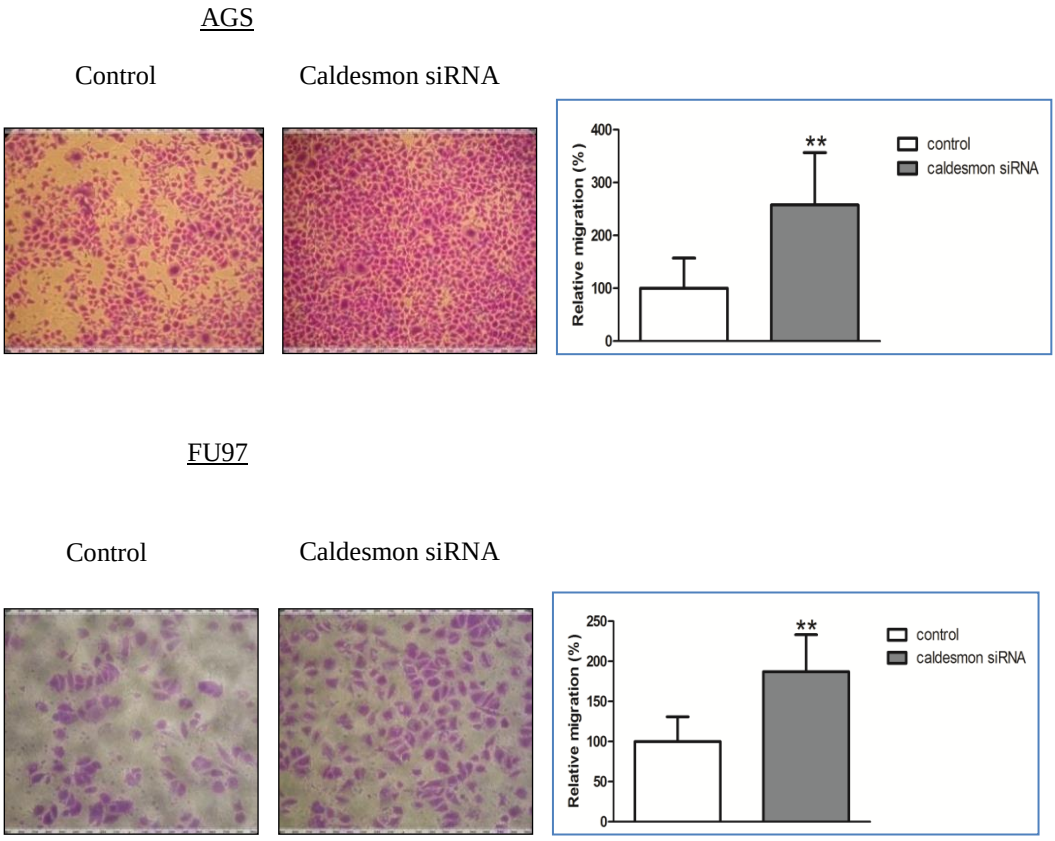

Figure 3.14 Transwell migration assay of AGS cells and FU97 cells showed an increased migration in caldesmon knock-down cells. Quantitation of migrated cells compared to control cells showed a significant increase in migration of caldesmon siRNA transfected AGS and FU97 cells (**, $p<0.01$, n=6).Error bar represents S.D.

AGS

Control Caldesmon siRNA

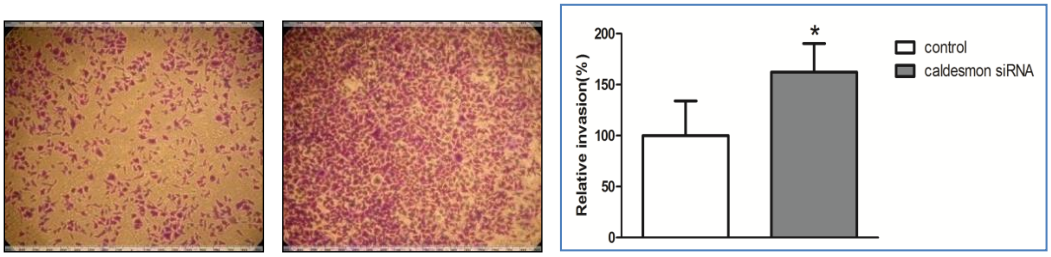

FU97

Control Caldesmon siRNA

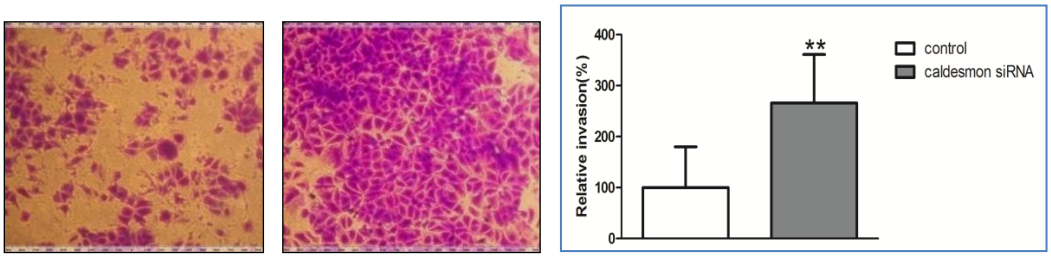

Figure 3.15 Matrigel invasion assay of AGS and FU97 cell lines with caldesmon knockdown. Caldesmon siRNA transfected AGS cells have significantly increased invasion as compared to the control cells (*, $p<0.05$, n=4). Matrigel invasion assay showed an increased invasion in caldesmon siRNA treated FU97 cells (**, $p<0.01$, n=6).

3.7 REVERSE-TRANSCRIPTION PCR IDENTIFIED CALDESMON ISOFORM 3 AS THE UBIQUITOUS EXPRESSED ISOFORM

Two high-molecular weight caldesmon (h-Cald) isoforms (expressed in muscle cells) and four low-molecular weight caldesmon (l-Cald) isoforms expressed by alternative splicing have been identified in various cell types (Figure 2.2) (Okamoto *et al*., 2000). Western blotting results revealed that the 4 gastric cancer cell lines (AGS, FU97, MKN7, AZ521) expressed l-Cald protein which was present as a band at 75 kDa (Figure 3.3). In order to determine the transcript variants of caldesmon expressed in the gastric cancer cell lines, we isolated RNA from the 4 gastric cancer cell lines, reverse-transcribed them into cDNA and identified the transcript variants using the isoform-specific primers. We first checked the presence of exon 1/exon1' with the RNA extracts from the four gastric cancer cell lines. Both exon1 and exon1' -specific forward primers yielded amplified products together with exon5-specific reverse primer (Figure 3.16). Isoform 3, 4, 5, and 6 were all likely to be present in the 4 cell lines. We further checked exon 4's presence with exon 4-specific reverse primer (P4) together with exon1- and exon1'-specific forward primer P1, P1', respectively. As shown in Figure 3.17, exon1' -specific forward primers yielded amplified products when combined with exon4-specific reverse primer with RNA isolated from AGS. Both exon 1- and exon1'-specific primer yielded amplified products combined with reverse primer P4 (exon4-specific) in the other 3 cell lines. Thus it can be inferred that caldesmon isoform 3 (NM_033157.3, cald1 transcript variant 3) was present in AGS, whereas both isoform 3 and 5 were present in the other 3 cell lines. Based on the band intensity, isoform 3 was more dominantly expressed in AZ521 and MKN7.

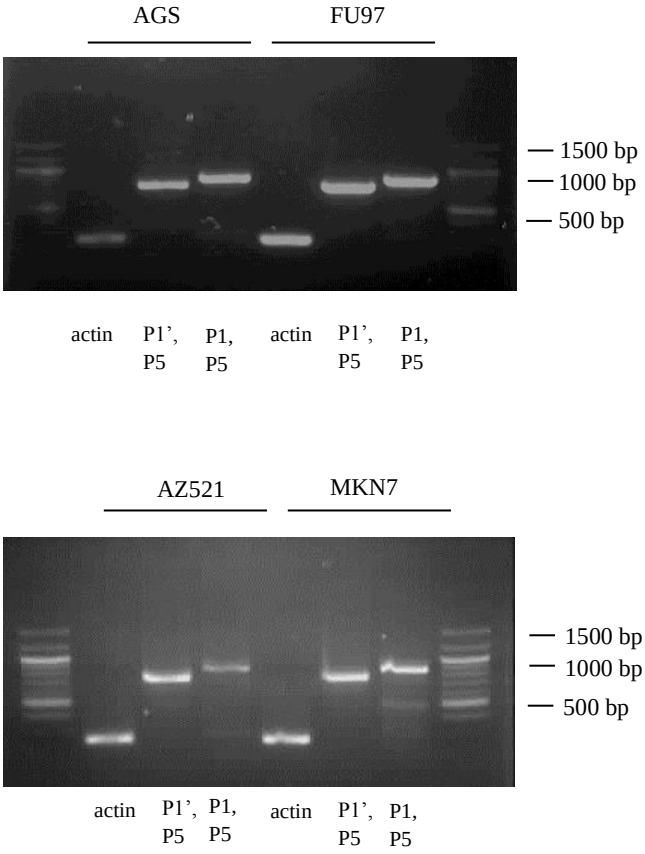

Figure 3.16 RT-PCR amplified products resolved by 1% agarose gel. Both exon1 and exon1' -specific forward primers yielded amplified products together with exon5-specific reverse primer. Isoform 3,4,5,6 were all likely to be present in the 4 cell lines.

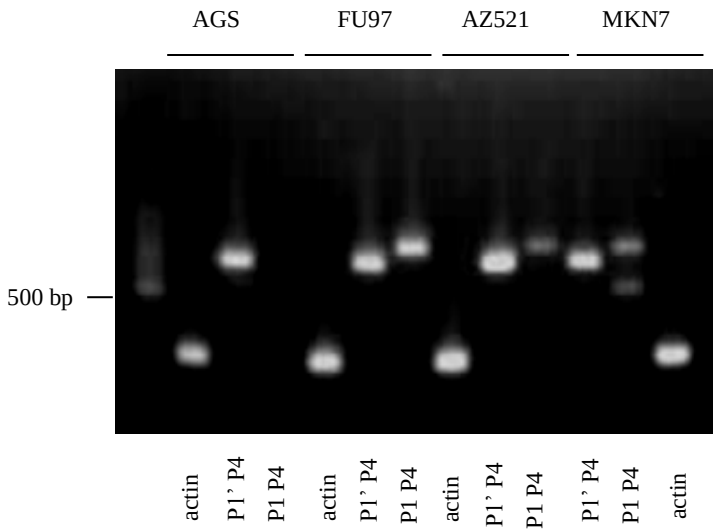

Figure 3.17 RT-PCR amplified products from 4 cell lines resolved by 1% agarose gel. Exon1' -specific forward primers yielded amplified products together with exon4-specific reverse primer with AGS RNA isolates. Both exon 1- and exon1'-specific primer yielded amplified products combined with reverse primer P4 (exon4-specific) with FU97, AZ521 and MKN7 RNA isolates. Isoform 3 was present in AGS, whereas both isoform 3 and 5 were present in the other 3 cell lines. Based on the band intensity, in AZ521 and MKN7, isoform 3 was more dominantly expressed.

3.8 STABLE OVER-EXPRESSION OF CALDESMON IN AZ521 CELL LINE

To further study the function of caldesmon in cancer metastasis, a cell line that stably over-expresses caldesmon was generated using the AZ521 cell line which has low intrinsic level of caldesmon (Figure 3.18). There is no difference in growth rate between caldesmon over-expressing cells and the control cells (Figure 3.19). We assessed the cell migration ability using the wound healing assay, and found AZ521 cells that over-expressed caldesmon closed the wound slower compared to the control cells (Figure 3.20). Using transwell cell migration assays, it was observed that caldesmon over-expression led to decreased cell migration (Figure 3.21A). A reduction in cell invasion as shown by Matrigel invasion assay (Figure 3.21B) was also noticed in the cells that over-expressed caldesmon. Caldesmon over-expressed AZ521 cells adhere stronger as compared to the control cells (Figure 3.21C). Our functional assays suggested that the observed differences in migration and invasion were due to caldesmon over-expression, and it is proposed that caldesmon, as an integral part of the cytoskeleton, may enhance the cell adherence and decrease cell migration and invasion potential in gastric cancer cells.

(A)

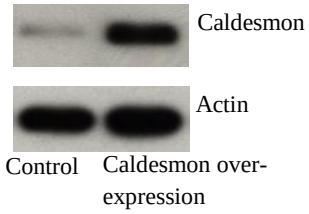

Figure 3.18 Western blotting showed AZ521 cell line that over-expressed caldesmon compared to control.

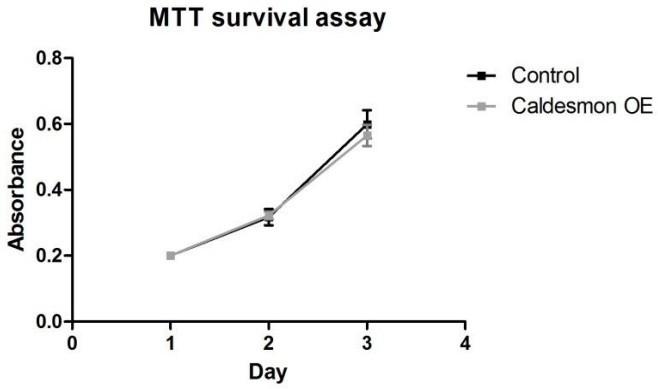

Figure 3.19 MTT survival assay showed that over 3 days, the growth rate of caldesmon over-expression AZ521 cells (Caldesmon OE) and the control cells were comparable.

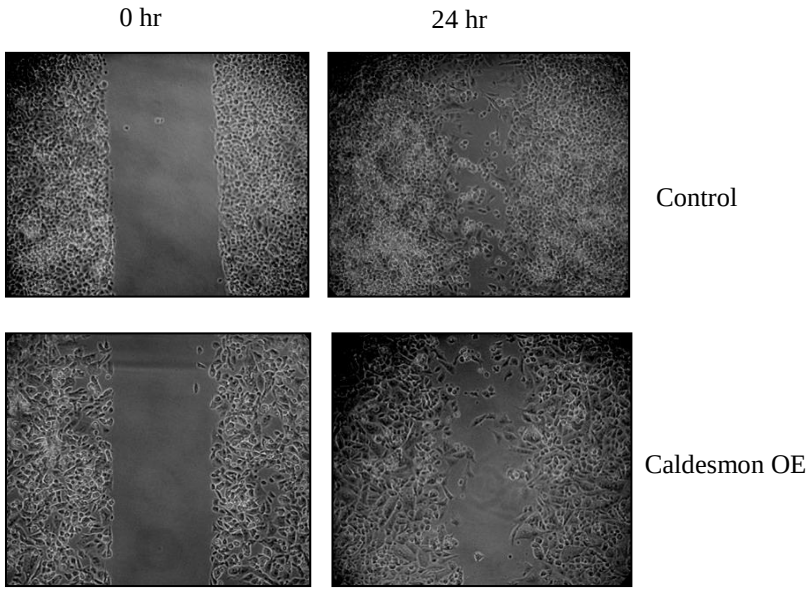

Figure 3.20 Wound healing assay showed that caldesmon-over expressing cells close the gap slower than control cells over a monitoring period of 24 hours.

(A)

Control Caldesmon OE

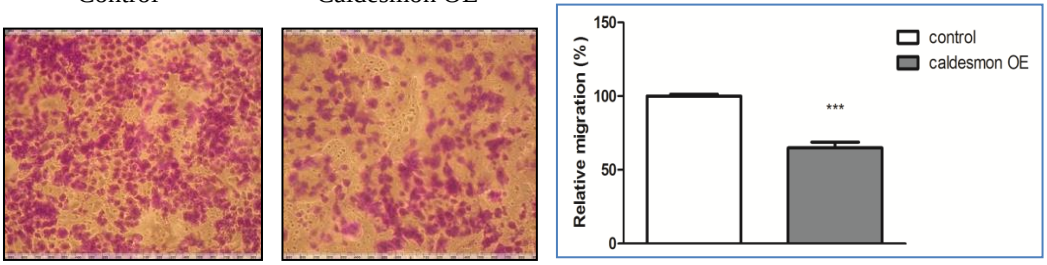

(B)

Control Caldesmon OE

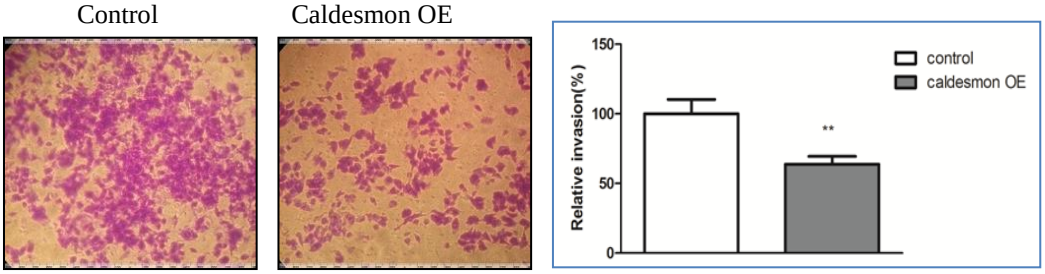

(C)

Control Caldesmon OE

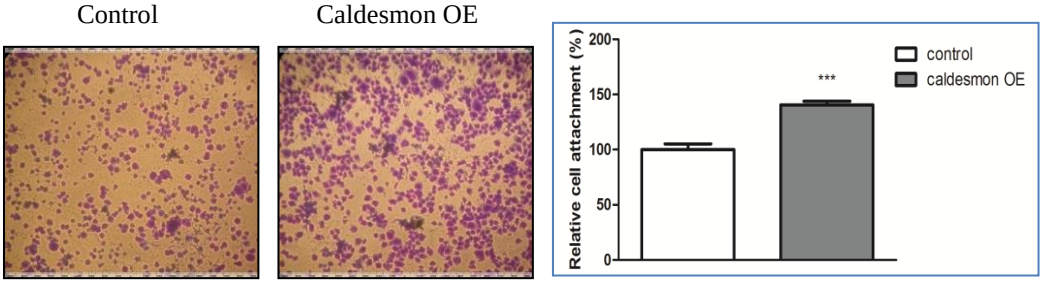

Figure 3.21 (A) Transwell migration assay of AZ521 cells showed that over-expresses caldesmon decreased cell migration (***, $p<0.001$, n=3).
(B) Matrigel invasion assay showed a decreased invasion in caldesmon-over expressing AZ521 cells (**, $p<0.01$, n=3).
(C) Cell attachment assay showed caldesmon-over expressing cells adhere stronger than control cells (***, $p<0.001$, n=3).

3.9 CO-IMMUNOPRECIPITATION IDENTIFIED CALDESMON-INTERACTING PROTEINS

Proteins that belong to the same biochemical pathways may interact and form functional clusters (Barabási *et al.*, 2011). To identify the proteins that interact with caldesmon, we used caldesmon antibody to pull down the endogenous caldesmon expressed in FU97 cells. This cell line has high level of intrinsic caldesmon expression, and was thus chosen for the co-immunoprecipitation study. A fraction of the cell lysates (input), unbound fractions, three eluates, three washes and the control eluate were resolved with SDS-PAGE and silver stained (Figure 3.22). The successful pull-down of caldesmon in the eluate was observed with Western blotting. Actin was identified in the eluate as well (Figure 3.23).

In-gel digestion was carried out to identify the potential interacting partners of caldesmon. The silver-stained bands from the eluate were excised, subject to trypsin digestion and subsequent analysis by mass spectrometry. The protein IDs that correspond to their band locations were shown in Figure 3.24 and Table 3.4. The proteins include filamin B, an actin-binding protein that played a role in TGF-β signaling and angiogenesis (Del Valle-Pérez *et al*., 2010); myosins which were known to interact with caldesmon (Lin *et al*., 2009). Structural constituent proteins of podosome like α-actinin and tropomyosins (Tanaka *et al*., 1993) were also identified to be associated with caldesmon. Proteins that regulate the filamentous actin like villin1 (dos Remedios *et al*., 2003) and F-actin capping protein (Bretscher & Lynch, 1985) were identified to be potentially associated with caldesmon. Several heat shock proteins like HSPA5 (Wang *et al*., 2009), HSPA9 (Zong *et al*., 2012), HSPD1 were detected in the eluate. The findings reflect a cytoskeleton-regulating role of caldesmon together with other structural proteins.

Among the proteins identified by mass spectrometry, myosin 10 and tropomyosins are of interest to us. Myosin and tropomyosin are involved in regulating the actin cytoskeleton. Up-regulation of myosin 10 in MKN7 and AZ521 as compared to AGS and FU97 was observed by iTRAQ. To validate that these proteins interact with caldesmon, we performed western blotting to detect myosin 10 and tropomyosin in the lysates, eluate 1 and control eluate. As shown in Figure 3.25, myosin 10 (MYH10) and low molecular weight tropomyosin (LMW TPM) were detected in the eluate, which illustrates their interactions with caldesmon.

We further probed for the expression level of myosin 10 and tropomyosin in AGS, FU97, MKN7 and AZ521 cell lysates with western blotting. As shown in Figure 3.26, in well/moderately differentiated gastric cancer metastasis *versus* primary cancer cell line (MKN7 *versus* AGS), myosin 10 expression was higher in metastasis derived MKN7 compared to its primary cancer derived counterpart AGS. Similarly, the expression of myosin 10 was higher in metastasis derived AZ521 compared to the primary cancer derived FU97 cells. The observed increased expression of myosin in metastatic gastric cancer cell lines is consistent with our findings obtained from iTRAQ.

The tropomyosin antibody used here recognized both high molecular weight (HMW) and low molecular weight (LMW) tropomyosin. As shown in Figure 3.26, HMW tropomyosin was expressed in AGS, but not detected in its metastatic counterpart MKN7. Both HMW and LMW tropomyosin were expressed in FU97, only HMW tropomyosin was detected in its metastatic counterpart AZ521. Tropomyosin expression has often been down-regulated in transformed cancer cells (Bharadwaj & Prasad, 2002). The exact roles of each tropomyosin isoform remain to be discovered.

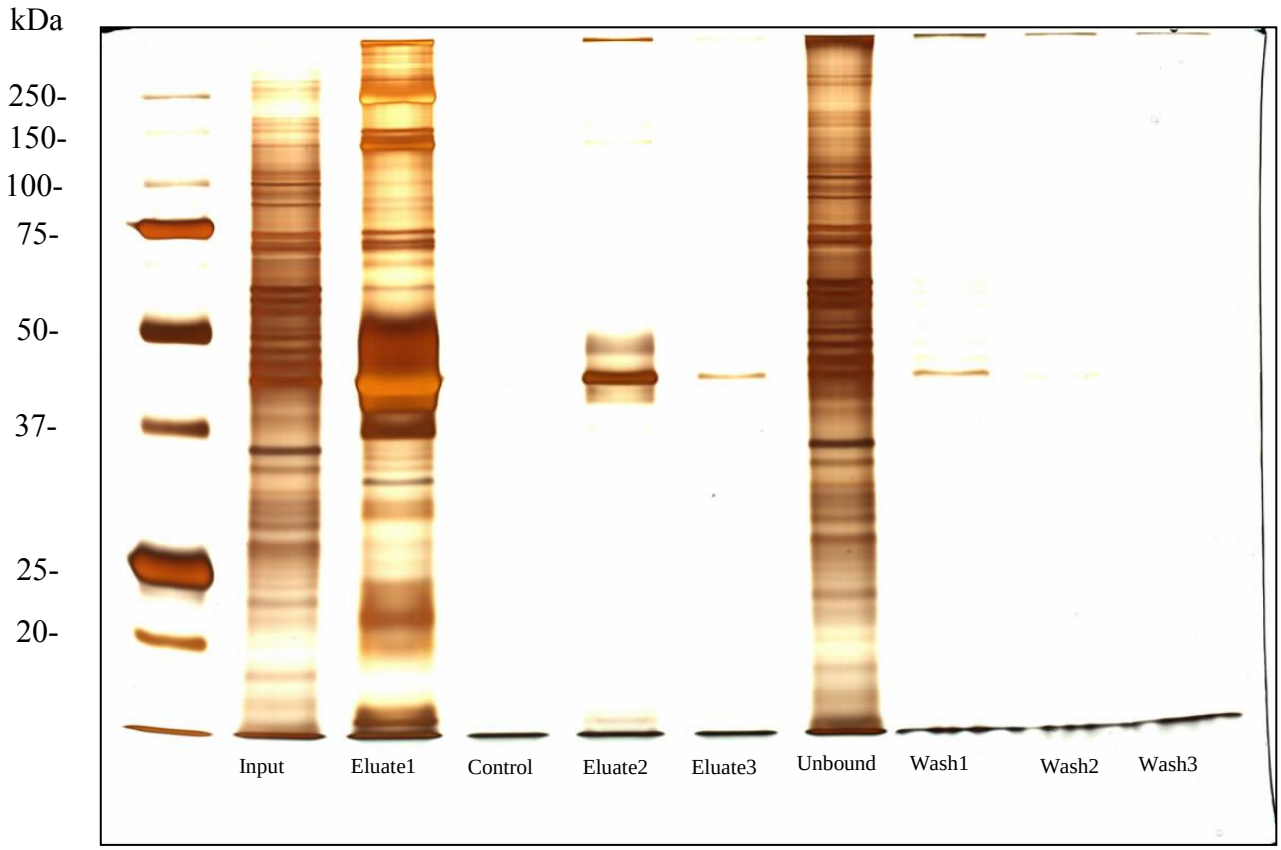

Figure 3.22 Silver staining of co-immunoprecipitation fractions: cell lysates input (1 µg), elutate 1, control eluate (with no antibody), eluate 2, eluate 3, unbound fractions, wash 1, 2 and 3 from co-immunoprecipitation experiment.

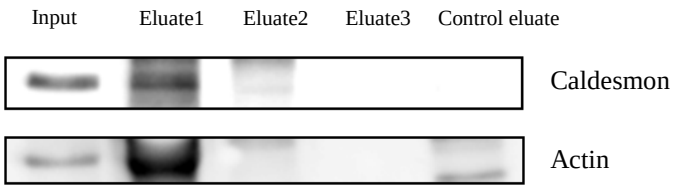

Figure 3.23 Western blotting of co-immunoprecipitation fractions showed caldesmon was pulled down in the eluate 1 fraction. The input fraction's presence of caldesmon was shown as the positive control. Actin was present in the eluate fraction as well as in input.

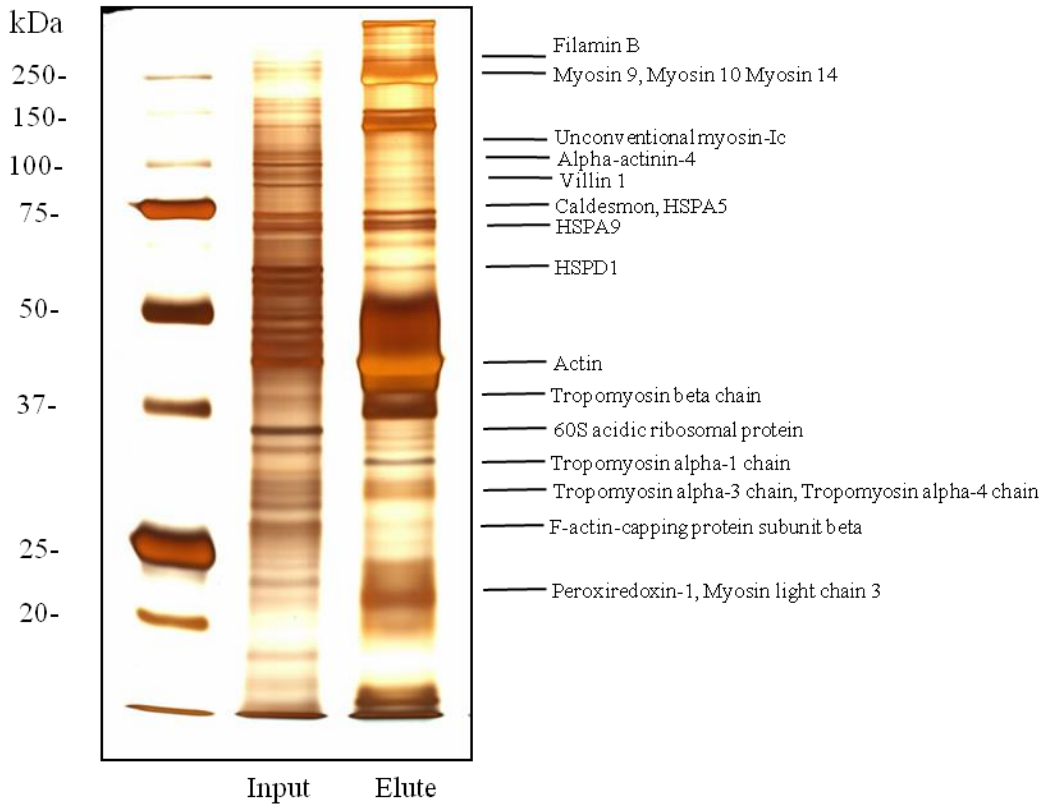

Figure 3.24 Protein identified by in-gel digestion coupled to mass spectrometry analysis. The proteins identified included filamin B, myosin 9, myosin 10, myosin 14, unconventional myosin-1c, alpha-actinin4, villin 1, caldesmon, HSPA5, HSPA9, HSPD1, actin, tropomyosin beta chain, 60S acidic ribosomal protein, tropomyosin alpha-1 chain, tropomyosin alpha-3 chain, tropomyosin alpha-4 chain, F-actin-capping protein subunit beta, peroxiredoxin-1 and myosin light chain 3.

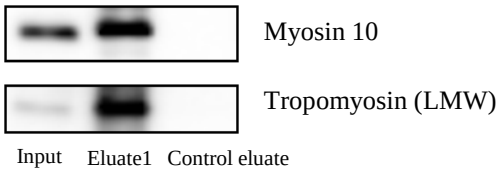

Figure 3.25 Western blotting of co-immunoprecipitation fractions. Myosin 10 and tropomyosin were pulled down in the eluate 1 fraction and they potentially interacted with caldesmon.

Figure 3.26 Western blotting of myosin 10 and tropomyosin expression levels in the 4 gastric cancer cell lines. In well/moderately differentiated gastric cancer metastasis *versus* primary cancer cell line (MKN7 *versus* AGS), myosin 10 expression was higher in MKN7 compared to AGS; whereas in poorly differentiated metastasis *versus* primary cancer cell (AZ521 *versus* FU97), the expression of myosin 10 was higher in AZ521 compared to FU97. Both high molecular weight (HMW) and low molecular weight (LMW) tropomyosin were detected here. HMW tropomyosin was expressed in AGS, but not detected in its metastatic counterpart MKN7. Both HMW and LMW tropomyosin were expressed in FU97, only HMW tropomyosin was detected in its metastatic counterpart AZ521.

UniProt Accession	Protein	MW(kDa)	Unused Score	%Cov	Function
sp|O75369|FLNB_HUMAN	Filamin-B	278	47.97	11.7	Connects cell membrane constituents to the actin cytoskeleton.
sp|P35579|MYH9_HUMAN	Myosin-9	226	442.96	77	Non-muscle cellular myosin. Play a role in cytokinesis, cell shape, secretion and capping
sp|P35580|MYH10_HUMAN	Myosin-10	229	165.55	61.6	
sp|Q7Z406|MYH14_HUMAN	Myosin-14	228	104.08	49.1	
sp|O00159|MYO1C_HUMAN	Unconventional myosin-Ic	121	13.86	8.2	Actin-based motor molecules with ATPase activity, serve in intracellular movements
sp|O43707|ACTN4_HUMAN	Alpha-actinin-4	105	30.64	27	F-actin cross-linking protein, actin filament bundle assembly
sp|P09327|VILI_HUMAN	Villin-1	93	12	8.9	Epithelial cell-specific Ca2+-regulated actin-modifying protein, modulates the reorganization of microvillar actin filaments
sp|P11021|GRP78_HUMAN	78 kDa glucose-regulated protein HSPA5	72	59.63	50.8	Facilitate the assembly of multimeric protein complexes inside the ER.
sp|Q05682|CALD1_HUMAN	Caldesmon	75	38.41	21.2	Regulation of actomyosin interactions. Stimulates actin binding of tropomyosin which increases the stabilization of actin filament structure
sp|P38646|GRP75_HUMAN	Stress-70 protein, mitochondrial HSPA9	73	66.08	47.6	Implicated in the control of cell proliferation and cellular aging. May also act as a chaperone
sp|P10809|CH60_HUMAN	60 kDa heat shock protein, mitochondrial HSPD1	60	17.89	21.6	Implicated in mitochondrial protein import and macromolecular assembly. May facilitate the correct folding of imported proteins

sp|P63261|ACTG_HUMAN	Actin, cytoplasmic 2	42	197.96	94.7	Actins are highly conserved proteins that are involved in various types of cell motility and are ubiquitously expressed in all eukaryotic cells.
sp|P07951|TPM2_HUMAN	Tropomyosin beta chain	33	47.13	61.6	Binds to actin filaments in muscle and non-muscle cells.
sp|P05388|RLA0_HUMAN	60S acidic ribosomal protein P0	34	14.93	38.5	Ribosomal protein
sp|P09493|TPM1_HUMAN	Tropomyosin alpha-1 chain	33	53.97	65.1	Binds to actin filaments in muscle and non-muscle cells.
sp|P67936|TPM4_HUMAN	Tropomyosin alpha-4 chain	28	42	66.9	
sp|P06753|TPM3_HUMAN	Tropomyosin alpha-3 chain	33	24.68	49.3	
sp|P47756|CAPZB_HUMAN	F-actin-capping protein subunit beta	31	6.07	22.7	Bind in a Ca2+-independent manner to the fast growing ends of actin filaments (barbed end) thereby blocking the exchange of subunits at these ends
sp|Q06830|PRDX1_HUMAN	Peroxiredoxin-1	22	15.01	52.8	Involved in redox regulation of the cell.
sp|P08590|MYL3_HUMAN	Myosin light chain 3	22	14.73	61.5	Regulatory light chain of myosin.

Table 3.4 Proteins identified from in-gel digestion of co-immunoprecipitation eluate. MW represents the theoretical molecular weight extracted from UniProt. The unused score is a measurement of all the peptide evidence for a protein that is not better explained by a higher ranking protein. It is the true indicator of protein confidence; with a high unused score, protein is identified with more confidence. % Cov showed the percentage of matching amino acids from identified peptides having confidence greater than 0 divided by the total number of amino acids in the sequence. The functions of the proteins were extracted from the UniProt database.

CHAPTER 4 DISCUSSION

4.1 GASTRIC CANCER CELL LINES AS MODEL FOR PROTEOME PROFILING

Proteins constituted the major players in the signaling pathways and various cellular processes, thus proteomics profiling is a valid approach in addressing many biological questions (Nishizuka *et al*., 2003). In our study, the proteins expressed by a panel of four gastric cancer cell lines were profiled. Cancer cell lines were utilized as disease model for proteomics profiling in many studies as cell lines are highly homogeneous compared to tissue samples, and can be easily cultured for protein harvesting.

Our four gastric cancer cell lines consisted of two derived from primary cancer and two from lymph node metastasis with matched histopathologic subtypes. With 8-plex iTRAQ labeling technology, the four cell lines with their technical replicates were incorporated, allowing us to compare the protein expressions between metastasis and primary cancer in both poorly-differentiated and well/moderately-differentiated gastric cancer subtype. The technical replicates provided assurance for the robustness of iTRAQ labeling. Furthermore, the incorporation of four cell lines allowed us to cross-compare protein expressions among poorly- and well/moderately-differentiated gastric cancer cell lines. In previous cell line-based gastric cancer proteomics studies, only two cell lines were compared (Chen *et al*., 2006; Takikawa *et al*., 2006); the targets they identified may be confined to certain cell lines which may represent only one subtype of the disease.

We have also verified the differentially expressed proteins caldesmon and fascin discovered by the proteomics method with other gastric cancer cell lines as well as in the clinical samples. The verification proved that our discovery based on cell lines can be extended with clinical relevance.

4.2 DIFFERENTIALLY EXPRESSED PROTEINS IN GASTRIC CANCER METASTASIS

Comparing the cellular proteome of gastric cancer cell lines, we identified 19 proteins were up- and 33 were down-regulated in both poorly- and well/moderately-differentiated metastatic gastric cancer cells. As shown in Table 3.1, the differentially expressed proteins covered a wide spectrum of functions and were potentially associated with cancer progression as many of them were also found to be dysregulated in other types of cancer. The proteins that were over-expressed in metastatic gastric cancer cell lines belong to functional groups such as protein biosynthesis/transcription regulation (EEF1D, EIF5A2, EEF1G, EIF5A2), ribosomal proteins (RPL7A, RPL26, RPL32, RPL23A) protein chaperones (HSP90AB1), glycolytic enzymes (LDHA), calcium binding protein (ANXA1,ANXA5), protein involved in ubiquitin conjugation pathway (UCHL1), actin cytoskeleton proteins (FSCN1,MYH10).

4.2.1 Up-Regulated Protein Functional Groups

(1) Protein biosynthesis, transcription regulation. In our study, up-regulation of eukaryotic elongation factor 1-delta (EEF1D) and eukaryotic initiation factor 5A2 (EIF5A2) in metastatic cell lines which are involved in protein synthesis were observed. In oesophageal carcinoma, higher expression of EEF1D mRNA is associated with lymph node metastases, advanced disease stages and poor prognosis (Ogawa *et al*., 2004). Over-expression of EIF5A2 is correlated with advanced stage of ovarian cancer (Guan *et al*., 2004).

(2) Chaperone protein. Heat-shock protein 90 (Hsp90) has been involved in stabilization of multiple signaling proteins involved in oncogenesis (Kamal *et al*, 2004). It has also been shown to be involved in regulating cell adhesion, cell

motility and angiogenesis and inhibition of Hsp90 led to anti-metastatic effect (Tsutsumi *et al.*, 2009).

(3) Glycolytic enzymes. Lactate dehydrogenase A (LDHA), which converted lactate from glucose metabolism to pyruvate, is up-regulated in metastatic gastric cancer cell lines in our study. In colorectal cancer, the level of serum lactate dehydrogenase and glycolysis are correlated with tumor angiogenesis and the expression of VEGFA and VEGFR (Azuma *et al*., 2007). Furthermore, knockdown of LDHA induced oxidative stress and inhibited tumor progression in human lymphoma (Le *et al*., 2010).

(4) Proteins involved in calcium binding. Annexin A5 was up-regulated in metastatic gastric cancer cell lines found in our study. Expression of Annexin A5 in colorectal cancer was associated with advanced cancer stage and poor prognosis (Xue *et al*., 2009). Knockdown of Annexin A5, a Ca^{2+} -binding protein in oral carcinoma cells led to decreased cell migration and invasion (Wehder *et al*., 2009).

(5) Proteins involved in ubiquitin-mediated protein degradation. The increased expression of UCHL1 was identified in renal cell carcinoma and non-small lung cancer cells (Kim *et al*., 2009; Seliger *et al*., 2007). In non-small lung cancer cells, UCHL1 regulates tumor cell invasion by upstream activation of Akt (Kim *et al*., 2009).

(6) Proteins regulating actin cytoskeleton. Fascin and myosin 10 were up-regulated in metastasis-derived cancer cells. Fascin is involved in bundling of actin filament in cell migration and invasion, and it is over-expressed in advanced stage cancer (Darnel *et al*., 2009). Myosin 10 participates in maintaining cell shape and generates contraction forces for cell migration (Vicente-Manzanares *et al*., 2009). The up-regulation of these proteins may reflect increased cell motility during metastasis.

4.2.2Down-Regulated Protein Functional Groups

The proteins which are down-regulated in metastasis-derived gastric cancer cells involve in a plethora of cellular functions: cell redox homeostasis (GSTP1), cytoskeleton (especially intermediate filament) proteins (EPPK1, KRT8, CALD1), extracellular matrix synthesis enzyme (SERPINH1), protein degradation/turnover (SERPINB1, LGMN, CTSA), ion transporters (CRIP1) *etc*.

(1) Proteins involved in cell redox homeostasis. A down-regulation of glutathione S-transferase P (GSTP1) was observed in the metastasis derived gastric cancer cells. GSTP conjugated reduced glutathione to a the electrophilic centers of a spectrum of molecules, detoxifying their potential carcinogenic effect (Tew *et al*., 2011). A down-regulation of GSTP1 mRNA expression was observed in esophageal adenocarcinoma (Brabender *et al*., 2002). The expression level of GSTP1 were also lower in metastatic gastric carcinoma compared to the primary cancer found by tissue microarrays in 250 pairs of primary and metastatic gastric cancer tissues (Kim *et al*., 2009).

(2) Cytoskeletal proteins. Epiplakin (EPPK1), keratin 8 (KRT8), caldesmon, are found to be down-regulated in metastasis-derived gastric cancer cells. EPPK1 has been found to be a regulator of the intermediate filament (IF) network. Knockdown of epiplakin disrupted the IF networks in epithelial cells (Jang *et al.*, 2005). Keratin 8 is also a component of intermediate filament. Loss of keratin 8 expression is associated with tumor metastasis and epithelial-mesenchymal transition (Fortier *et al.*, 2013). Caldesmon interacts with cytoskeleton proteins actin, myosin, calmodulin and tropomyosin. Over-expression of caldesmon suppresses cancer cell invasiveness (Wang, 2008).

(3) Protein involved in extracellular matrix synthesis. Serpin H1 (SERPINH1) is involved in collagen synthesis progress, and a decreased expression of SERPINH1 was observed in metastasis derived gastric cancer cells.

(4) Proteins involved in protein degradation and turnover. Leukocyte elastase inhibitor (SERPINB1) is a serine protease inhibitor. The expression of SERPINB1 is down-regulated in gastric cancer tissues identified by microarray analysis (Wang *et al*., 2006). Cysteine protease legumain (LGMN) and serine protease cathepsin A (CTSA) are both found to be down-regulated in metastasis-derived gastric cancer cells. These proteins are involved in lysosome-mediated protein degradation and participate in regulating apoptosis (Kirkegaard & Jäättelä, 2009).

(5) Ion transporters. Cysteine-rich protein 1(CRIP1) which is involved in intracellular zinc transport, has found to be down-regulated in metastasis-derived gastric cancer cells. Low CRIP1 expression in breast cancer is correlated with poor prognosis (Ludyga *et al*., 2013). Similarly, expression of CRIP1 in osteosarcoma patients indicates a better survival (Baumhoer *et al.*, 2011).

A wide range of protein expressions are perturbed when we compared metastasis-derived to primary cancer-derived gastric cancer cells, which indicates that metastasis progression affects global proteome expression and multiple cellular events and signaling pathways. From the functions of these dysregulated proteins, we may infer that an increased energy demand via glycolysis, a change in protein degradation and cytoskeleton modification are taking place in the metastasis progress.

4.3 FASCIN UP-REGULATION IN GASTRIC CANCER METASTASIS

Of the differentially expressed proteins in metastasis-derived gastric cancer cells, fascin is worth noting because it is an actin cytoskeleton-associated protein and may play a role in regulating cell motility during the metastasis progression. With Western blotting (Figure 3.3, 3.4) and immunocytochemical (Figure 3.5) approaches, we observed that fascin was over-expressed in a panel of metastasis-derived gastric cancer cell lines isolated from lymph nodes, liver metastasis and ascites. To extrapolate these findings from cell line models to clinical relevance, we analyzed the expressions of fascin with primary gastric cancer and their matching lymph node metastasis tissues (Figure 3.8, 3.9). The expression of fascin was found to be up-regulated when the tumor progressed from primary site to lymph node. Tumor invasion of lymph node is one of the critical events in gastric cancer metastasis, and it is the most important prognosis factor for patient survival (Coburn, 2009). We have discovered the expression level of fascin altered with regard to the lymph node metastasis of the tumors. Tissue microarray analysis confirmed that the expression of fascin is correlated with tumor serosal invasion and lymph node metastasis (Table 3.3), and in well/moderately differentiated gastric cancer patients, those with no expression of fascin have better survival compared to those with positive expression of fascin (Figure 3.10). These results obtained with clinical samples have established fascin as a protein of which the expression is correlated with gastric cancer metastasis, and it could possibly be served as a prognostic marker in gastric cancer patients

Fascin is a 55 kDa actin-bundling protein. It is found to be up-regulated in ovarian, breast, thyroid and prostate cancers (Darnel *et al*., 2009). The elevated expression level of fascin is associated with advanced gastric cancer stage and poor prognosis (Hashimoto *et al*., 2004). Fascin is localized at the filopodia and regulates the number and morphology of filopodia (Vignjevic *et al*., 2006). It also plays a role in stabilizing the invadopodia, the invasive front for extracellular matrix degradation, and potentiated cell invasion. In fascin knockdown cells,

fewer invadopodia were formed with smaller size(Li *et al*., 2010). Knockdown of fascin with siRNA in gastric cancer cells decreased cell proliferation and cell migration (Fu *et al*., 2009). Recently migrastatin, an anti-cancer compound secreted by *Streptomyces* was found to inhibit fascin bundling of actin by competing with one of its actin-binding sites (Chen *et al*., 2010). Upstream signaling molecules including galectin-3 and TGF-β regulate fascin expressions. High expression of both galectin-3 and fascin were identified in gastric cancer tissues. Galectin-3 was found to be interacting with β-catenin/TCF and mediating the translocation of this complex into the nucleus, which subsequently promoted the expression of fascin (Kim *et al*., 2010). TGF-β-mediates fascin expression via JNK and ERK signaling and induces gastric cancer cell invasion and metastasis (Fu *et al*., 2009). Our proteomics and tissue immunohistochemistry results identified up-regulation of fascin which could be potentially associated with gastric cancer metastasis, and the findings agree with the above literature. However, since the current research on fascin in gastric cancer has been quite extensive, further functional studies of fascin were not continued in this study.

4.4 CALDESMON DOWN-REGULATION IN GASTRIC CANCER METASTASIS

The proteomics study has identified caldesmon expression decreased in gastric cancer metastasis-derived cell lines (Figure 3.3). Caldesmon was found to be down-regulated in a panel of lymph node metastasis, liver metastasis, and ascites metastasis-derived gastric cancer cells compared to the primary cancer-derived cells with Western blotting and immunocytochemistry (Figure 3.4, 3.5). An analysis of tumor tissues (matched primary cancer and lymph node metastasis) observed the decreased expression of caldesmon when the tumor developed lymph node metastasis (Figure 3.6, 3.7). In tissue microarray analysis, caldesmon expression was found in a small proportion of gastric tumor we examined, and most of the tumor cells didn't express caldesmon. This could possibly mean that loss of caldesmon is an early stage event in gastric cancer.

We have discovered the novel association of caldesmon expression with gastric cancer metastasis but the role of caldesmon in gastric cancer was unknown. Thus we performed functional studies of caldesmon using gastric cancer cell lines. Knockdown of caldesmon, which mimicked the advanced gastric cancer stage, has resulted in increased cell migration and invasion (Figure 3.13-3.15). Over-expression of caldesmon, however, decreased the motility and invasiveness of gastric cancer cells (Figure 3.20, 3.21). These functional assays showed that the expression levels of caldesmon have an impact on the motility and invasiveness of gastric cancer cells, possibly exerting these effects by regulating the actin cytoskeleton. The effect of caldesmon in gastric cancer *in vivo* has not been studied yet. It is hypothesized that when the primary gastric cancer cells progressed into metastasis, the down-regulation of caldesmon will help the cancer cells gain more motility and cellular invasiveness which will facilitate metastasis progression.

Caldesmon is an actin-binding protein which localized to structures including stress fibers, membrane ruffles, podosome *etc*. Studies have found that caldesmon competes with Arp2/3 complex for actin binding and inhibites the formation of podosomes in RSV-transformed fibroblast cells (Hai & Gu, 2006).In transformed cells and cancer cells like human colon carcinoma (HCA7) and murine melanoma (B16F10) cell line, reduced caldesmon expression has been observed (Yoshio *et al*., 2007). In advanced stage breast cancer cell lines, caldesmon expression is reduced identified by a proteomics-based study (Geiger *et al*., 2012). Caldesmon down-regulation in the gastric tumor compared to adjacent normal tissue was identified with genomic profiling(Lee *et al*., 2003). Besides expression in tumor cells, caldesmon was found to be expressed in stroma vasculatures of various tumor types like glioma, stomach cancer, colon cancer *etc*., but not in normal blood vessels (Zheng *et al*., 2005). Caldesmon's expression is observed in colon cancer stroma although its expression levels were not different between primary tumor and lymph node metastasis (Köhler, 2011). Knockdown of caldesmon in breast cancer and colon cancer cell line promoted cell invasion (Yoshio *et al*., 2007), while over-expression of caldesmon in cancer and fibroblast cells reduced podosome formation and subsequent decreased cell invasion (Lin *et al*., 2009). The factors that regulated caldesmon activity include various kinases and tumor suppressor gene p53. Cdk5 reduces caldesmon activity and subsequently promotes cancer cell invasion (Quintavalle *et al*., 2011). PFTK1, a CDC-2 related kinase, phosphorylates caldesmon, leading to its dissociation from actin and subsequent increase in hepatocellular carcinoma (HCC) cell migration (Leung *et al*., 2011). PKGIβ, a cGMP-dependent protein kinase, phosphorylates caldesmon and relieves its inhibition effect on myosin ATPase activity, resulting in increased breast cancer cell migration and invasion (Schwappacher *et al*., 2012). p53 up-regulates caldesmon expression, leading to the inhibition of podosome formation (Mukhopadhyay *et al*., 2009). Correlating the current literature with our findings, we proposed that caldesmon may be a potential metastasis repressor, and its role in gastric metastasis progression remains to be fully elucidated.

4.5 CALDESMON IN TUMOR STROMA OF GASTRIC CANCER PATIENTS

In our immunohistochemical study, caldesmon expression is decreased in lymph node metastasis compared to its primary cancer counterparts (Figure 3.6, 3.7). The expression of caldesmon has also been observed in the tumor stroma as well as net-like pericellular space. Tissue microarray analysis showed that the expression of caldesmon in pericellular space is positively correlated with tumor infiltration (Table 3.3). The role of caldesmon in tumor stroma remains to be determined.

Tumor cells interact closely with their microenvironment - the tumor stroma which has a supportive role in carcinogenesis. The stroma includes inflammatory cells, cancer-associated fibroblasts (CAFs) which are responsible for the synthesis and modeling of the extracellular matrix (ECM) (Tlsty & Coussens, 2006) and cells that constitute the vasculature (Bhowmick & Moses, 2005). During the carcinogenesis progression, the stromal is altered in response to the tumor, and an acquisition of α-smooth muscle actin, vimentin, smooth muscle myosin, calponin, tenascin and desmin expression has been found in tumor stroma. These proteins are often expressed as a response to wound healing or inflammation (Tlsty & Coussens, 2006). In pancreatic ductal adenocarcinoma (PDA), the host stromal response to an invasive tumor, including proliferation of the fibrotic tissue, and altered ECM conducive to the progression of tumor involves several key molecules including collagen type I, fibronectin, laminin, matrix metalloproteinases (MMPs), tissue inhibitors of MMP (TIMPs), TGF-β, platelet-derived growth factor (PDGF), chemokines, integrins *etc.*(Mahadevan & Von Hoff, 2007). These molecules could potentially be used in tumor diagnosis and targeted therapy. Of these molecules, MMPs' increased expression was correlated with tumor invasion (Deryugina & Quigley, 2006). An immunohistochemical study using gastric cancer tissues revealed that the expression of MMP2and MMP9 were higher in malignant glands, and the

increased expressions are correlated with tumor recurrence and distant metastasis (Josson *et al*., 2010). Another study has identified in gastric cancer tissues, the tumor cells express PDGF-β, whereas the stromal cells (cancer-associated fibroblasts, pericytes, endothelial cells) express PDGF receptors (PDGFR-β). The administration of PDGFR tyrosine kinase inhibitor and cytotoxic drug decrease tumor growth and metastasis (Kitadai *et al*., 2011). The tumor stroma may also contribute to drug resistance. An impaired function of p53 in tumor stroma in a tumor xenograft model may be responsible for the tumor's resistance to anti-cancer drugs and contributed to stromal cell survival (Dudley *et al.*, 2008).

Caldesmon plays a part in the synthesis or modification of ECM (Ross *et al*., 2000). In colon cancer tissues, caldesmon expression was observed by immunohistochemistry in the stroma of primary tumor and metastases, and the expression was associated with proliferating cancer-associated fibroblasts (CAFs) (Köhler, 2011). The expression of caldesmon in pericellular space and stroma may have a different role compared to the role of caldesmon in tumor cells thus an expression variance was observed here. The role of caldesmon in tumor stroma may be studied with co-culturing of tumor cells with stromal cells which over-expressed caldesmon.

4.6 CALDESMON MAY BE INVOLVED IN GASTRIC CANCER METASTASIS BY REGULATING THE ACTIN CYTOSKELETON AND INVADOPODIA

With functional study coupled to cell assays, we have identified a decreased level of caldesmon expression promoted gastric cancer cell migration and invasion, and an increased expression of caldesmon inhibited the migration and invasion. Co-immunoprecipitation experiment discovered that caldesmon interacted with actin, myosin and tropomyosin which were involved in regulating the cytoskeleton, cell tension and invasion front such as invadopodia formation (Figure 3.9.3, 3.9.4, Table 3.4).

A proposed model of caldesmon's involvement in regulating the actin filaments is shown in Figure 4.1. Caldesmon, as an actin-binding protein, increases the cell rigidity via F-actin cross-linking (Greenberg *et al.*, 2008). Caldesmon is found to be associated with invadopodia (an actin-enriched cellular protrusion which degrades the extracellular matrix), and negatively regulates invadopodia formation (Hai & Gu, 2006). The molecular mechanism of this regulation may be involving other actin-binding proteins including Arp2/3, myosin and tropomyosin. Caldesmon inhibits the binding of Arp2/3 complex which promotes actin polymerization and membrane protrusions (Yamakita *et al*., 2003). Caldesmon also inhibites myosin (detected at invadopodia) binding to actin (Linder *et al*., 2011). The binding of myosin II to F-actin facilitates the cell contraction, which is critical for cell morphology reorganization and ECM remodeling (Olson & Sahai, 2009). Inhibition of myosin II activity with a chemical inhibitor blebbistatin results in abrogation of invadopodia-associated ECM degradation (Alexander *et al*., 2008). It is postulated that the actomyosin contraction may be involved in regulation of invadopodia and its associated mechanosensing (Linder *et al*., 2011). Caldesmon may inhibit invadopodia formation via interfering with myosin-mediated cell contraction.

Cellular protrusions like lamellipodia, filopodia and invadopodia are assembled by the actin filaments (Chhabra & Higgs, 2007). The invadopodia have a central core of F-actin with surrounding actin-binding proteins like Wiskott-Aldrich syndrome protein (WASP) and WASP-interacting protein (WIP) (García *et al*., 2012), lipid raft-associated protein caveolin-1, membrane-binding matrix metalloproteinases MT1-MMP (Yamaguchi & Oikawa, 2010), vinculin, talin, α-actinin, Src, gelsolin, Arp2/3 complex etc. (Buccione *et al*., 2004).Actin-binding proteins have important structural and functional roles in the cell such as maintaining cell shape and modulating cell movement. In carcinogenesis, the actin cytoskeleton has been altered (Wang & Coluccio, 2010) and the expressions of many actin-binding proteins are perturbed via signaling proteins such as Rac, Rho, and CDC42 which further induced changes in cell morphology and motility (Rao & Li, 2004). These proteins function as regulator of actin polymerization and assembly, or actin bundling/cross-linking (Rao & Li, 2004). Caldesmon may be one of these actin-binding proteins involved in regulating the cell dynamics.

Invadopodia has been identified in numerous cancer cell lines derived from melanoma, breast cancer, glioma and head and neck squamous cell carcinoma (Stylli *et al*., 2008). In cancer cells, the ability of forming these invasive membrane protrusions is critical for the dissemination of cancer cells during the metastatic cascade (Klemke, 2012). These ventral cell protrusions adhere to and degrade the extracellular matrix with MMPs, thus facilitate cancer cell invasion (Yamaguchi & Oikawa, 2010). Unlike focal adhesions which cultured cells develop as organized sites of contact with substrate, invadopodia are more dynamic in formation and contain MMP for proteolytic degradation of ECM constituents (Buccione *et al*., 2004). Many factors regulate invadopodia formation. Growth factors such as PDGF, TGF-β and EGF induce invadopodia formation in cancer cells (Murphy & Courtneidge, 2011). Transcription factors like Twist induced PDGFRα expression which activates Src signaling and subsequent invadopodia formation (Eckert *et al*., 2011).It has been discovered that caldesmon may act downstream of p53 which suppresses invadopodia formation and extracellular matrix degradation (Mukhopadhyay *et al*., 2010).

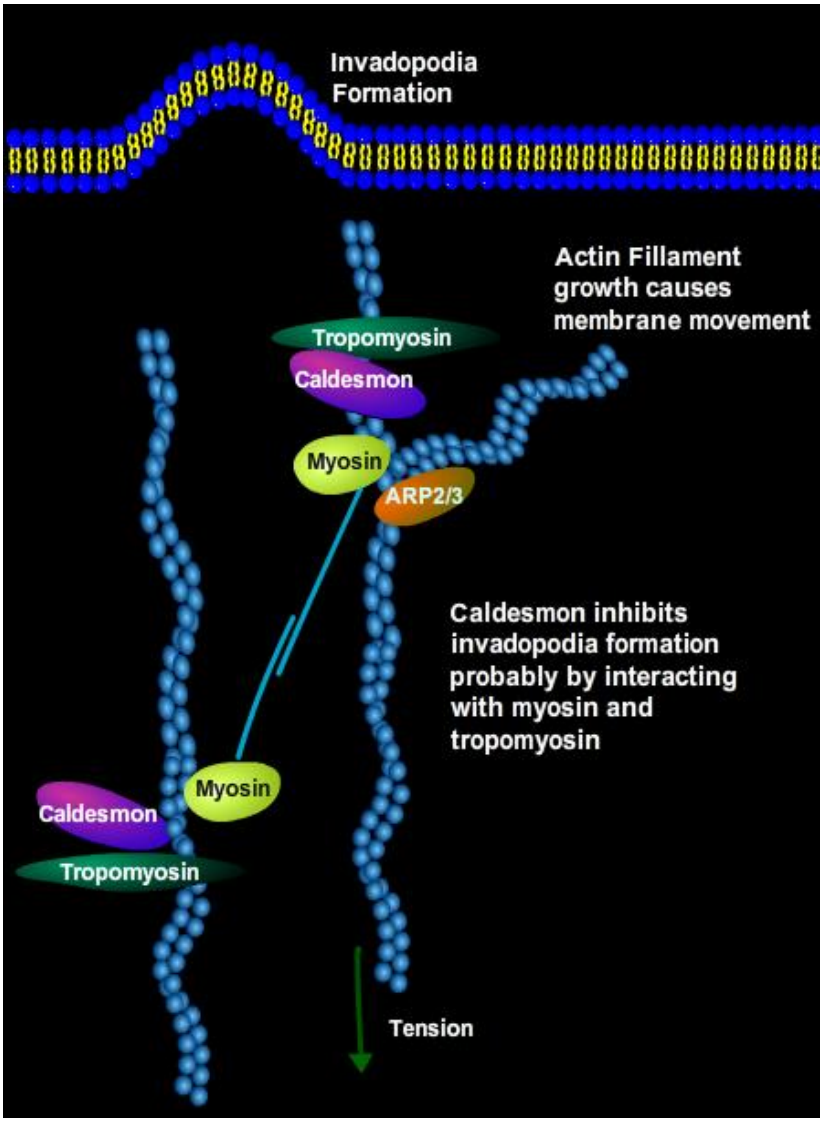

Figure 4.1 A proposed model for caldesmon, myosin, tropomyosin and Arp2/3 in regulating the actin filaments, cell contraction and invadopodia formation. Caldesmon probably suppresses cancer cell migration and invasion by inhibiting with myosin-induced cell contraction and subsequent invadopodia formation. This figure was adapted from (Pawlak & Helfman, 2001) and created with tools from (www.proteinlounge.com).

4.7 CALDESMON INTERACTING PROTEINS IDENTIFIED BY CO-IMMUNOPRECIPITATION

The proteins that potentially interact with caldesmon have been identified by co-immunoprecipitation (Table 3.4). Many of these proteins are involved in regulating the actin cytoskeleton or cancer progression. We constructed an interaction network (Figure 4.2) based on the caldesmon-interacting proteins identified with STRING database (Szklarczyk *et al*., 2011). The network functions as actin cytoskeleton regulation. Tropomyosins, actin and myosins are directly linked to caldesmon in the network. Besides, the associations of the rest of the proteins with caldesmon are novel findings and the functional significance remains to be discovered.

Many of the interacting proteins are involved in mediating cancer cell migration. Among these proteins, myosin and tropomyosin have been shown in the previous literature to be interacting directly with caldesmon (Wang, 2008). We performed Western blotting with the co-immunoprecipitation eluate, and verified caldesmon interacted with myosin10 and tropomyosin in gastric cancer cells. An over-expression of myosin10 was observed in the metastasis-derived gastric cancer cells. The loss of expression of low molecular weight tropomyosin in AZ521 and the loss of expression of both high and low molecular weight tropomyosin in MKN7 has been observed. The increased expression of myosin, the decreased expression of caldesmon and tropomyosin in cancer cells isolated from gastric cancer lymph node metastasis led us to postulate that caldesmon may co-operate with tropomyosin and oppose myosin's pro-migratory activity in the metastasis progression.

An increased myosin expression in gastric cancer metastasis-derived cell lines has been observed in our study. Non-muscle myosin II expresses in epithelial cells, encoded by MYH9, MYH10 and MYH14, has been involved in generating cytoskeleton tension (Clark *et al., 2007*), regulating cell polarity, cell

migration and cell-cell adhesion (Conti & Adelstein, 2008; Vicente-Manzanares *et al.*, 2009). In fibroblast cells, myosin induces cell contraction which is inhibited by caldesmon (Helfman *et al*., 1999). Knockdown of myosin 9 and myosin 10 with siRNA in breast cancer cells decreases cell migration (Betapudi *et al.*, 2006). It has been proposed that the over-expression of myosin is correlated with gastric cancer cell migration.

A plethora of tropomyosin isoforms are expressed in epithelial cells which are encoded by 4 genes tropomyosin α, β, γ and δ (Gunning *et al.*, 2005). Tropomyosins protects actin filaments from been severed by gelsolin and cofilin (Wang & Coluccio, 2010). Tropomyosin is shown to be co-operatively binding to caldesmon, which promotes its association with the actin filaments (O'Neill *et al.*, 2008). In transformed cells, tropomyosin expression is down-regulated (Bharadwaj & Prasad, 2002). The down-regulation of tropomyosin in breast cancer may destabilize the structure of actin cytoskeleton and confer resistance to anoikis, which promotes the malignant growth of tumor (Raval *et al*., 2003). Our findings confirm tropomyosin's interaction with caldesmon and they share the same down-regulation trend in metastasis-derived gastric cancer cell lines.

Besides actin, myosin and tropomyosin which are shown to be interacting with caldesmon, novel targets including actin filaments regulating proteins and mechanosensor filamin B, invadopodia protein α-actinin, F-actin capping protein subunit beta (CAPZB), chaperone protein HSPA9 were identified to be potentially caldesmon-binding. These novel proteins identified here may play a role in gastric cancer metastasis via involving in the network that regulates the migration/invasion of gastric cancer cells together with caldesmon.

Filamin B, which connects the plasma membrane with the actin filaments, is potentially involved in metastasis. Filamins are mechanosensors, and regulator of cell-cell adhesion and receptor-mediated signalling (Stevenson *et al.*, 2012). In TGF-β induced epithelial-mesenchymal transition (EMT) in human lung cancer cells, the expression of filamin B, an actin polymerization regulator is up-

regulated (Keshamouni *et al*., 2006). Knockdown of filamin B with siRNA in endothelial cells decreases cell migration ability (Del Valle-Pérez *et al*., 2010).

α-actinin, an actin cross-linking protein, is localized to invadopodia (Schoumacher *et al.*, 2010) and along stress fibers. In absence of α-actinin, the actin filaments are short and less organized (Vicente-Manzanares *et al*., 2009). α-actinin is co-localized with tropomyosin and caldesmon (Bretscher & Lynch, 1985). Knockdown of α-actinin-4 expression results in decreased cell migration, cell spreading and cell proliferation (Shao *et al.*, 2010).

F-actin capping protein subunit beta (CAPZB) is a regulator of filamentous actin growth. CAPZB stabilizes the length of actin filament by capping the barbed end (fast growing) of actin filament. The expression of CAPZB is down-regulated in 5-FU treated gastric cancer cells (Tseng *et al*., 2011).

Stress-70 protein, mitochondrial, also known as HSPA9 or mortalin, is over-expressed in human lung squamous carcinoma with early recurrence (Zong *et al*., 2012) and advanced stage liver cancer. It may act as a protein chaperone, interacting with various key signaling proteins including p53, fibroblast growth factor-1 *etc.* (Yi *et al*., 2008).

Identifying these interacting partners of caldesmon in gastric cancer metastasis reaffirmed the role of caldesmon as a potential regulator of cell migration and invasion by modulating the actin cytoskeleton dynamics with its interacting partners. The novel targets identified here may be studied further for their roles in actin cytoskeleton regulation and gastric cancer metastasis.

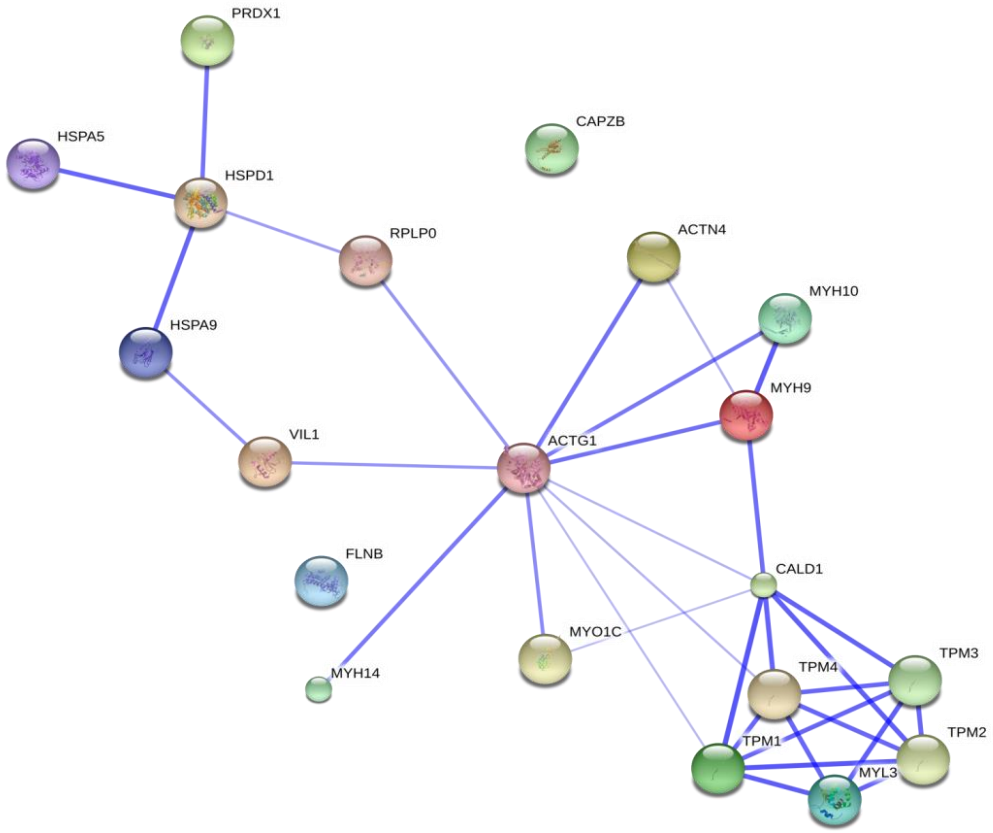

Figure 4.2 Interaction network formed by caldesmon-interacting proteins identified. The network functions as actin cytoskeleton regulation. Stronger associations were represented by thicker lines in the figure as defined by STRING database.

CHAPTER 5 CONCLUSION

In this study, we used iTRAQ-based quantitative proteomics approach to profile the protein expression in a panel of 4 gastric cancer cell lines. Proteins that are differentially expressed among metastasis *versus* primary gastric cancer comprise of a spectra of cellular event: protein biosynthesis, transcription regulation, structural constituent of ribosome, RNA binding proteins, molecular chaperone, enzymes involved in glycolysis, TCA cycle, fatty acid metabolisms, actin cytoskeleton regulators, transporter proteins, calcium regulators *etc*. Among these proteins, fascin is over-expressed in metastasis-derived gastric cancer cell lines. The over-expression of fascin in gastric tumor tissues is correlated with advanced tumor stage and metastasis, and associated with poorer survival in patients with well/moderately differentiated gastric cancer.

Caldesmon is down-regulated in metastasis-derived gastric cancer cell lines. Its expression in tumor cells decreases in lymph node metastasis tumor tissues compared to their primary tumor counterparts. The expression of caldesmon is also found in tumor stroma and its expression is associated with advanced tumor stage.

Functional studies of caldesmon were performed in gastric cancer cell lines. Knockdown of caldesmon with siRNA in two primary cancer-derived cell lines increased the migration and invasion capacity of these cells. Over-expression of caldesmon in metastasis-derived cell line impaired cell migration and invasion, and increased the adhesion ability of cancer cells to the matrix.

To discover proteins interacting with caldesmon, co-immunoprecipitation experiment was performed. We found that caldesmon interacted with actin, myosins, tropomyosins and other cytoskeleton-related proteins, protein chaperones to regulate the actin cytoskeleton. We propose that caldesmon could be potentially associated with gastric cancer metastasis by negatively regulating

the motility of cancer cells. Further functional analysis will be performed to elucidate the significance of the interactions.

CHAPTER 6 FUTURE STUDIES

Despite the declining global incidence rates, gastric cancer still remains a health burden in Asia. Identification of metastasis-associated proteins is critical for understanding the molecular mechanisms underlying metastasis and early diagnosis of malignant progression. Our study has established caldesmon's role as a potential player in gastric cancer metastasis. A functional cluster that interacted with caldesmon and regulated the actin cytoskeleton has been identified with co-immunoprecipitation. Further studies to elucidate the role of caldesmon and to understand gastric cancer metastasis mechanism will be performed. Future work will involve (a) investigating caldesmon's role in invadopodia formation with fluorescent gelatin degradation assay, (b) *in vivo* study of caldesmon's role in tumor formation, (c) functional study of the caldesmon-interacting proteins myosins and tropomyosins with knockdown and over-expression.

(a) Fluorescent gelatin degradation assay for invadopodia visualization

Caldesmon may regulate the ECM-degrading cell protrusion called invadopodia. Proteolytic degradation occurred at these protrusions through matrix metalloproteinases, facilitating cancer cell invasion. The ECM degradation via invadopodia of cells that over-expressed caldesmon can be compared to control cells via plating cells on fluorescence-labeled gelatin matrix and visualizing the matrix degradation (non-fluorescence). The total degradation area may be quantified and compared.

(b) *In vivo* study of caldesmon's role in tumor formation

The role of caldesmon in tumor formation may be studied *in vivo.* Cells that over-expressed caldesmon may be injected into nude mice, and the tumor size and metastatic potential may be affected by the over-expression of caldesmon. By comparing the tumor formation of caldesmon over-expression cells *versus* control, the role of caldesmon *in vivo* may be elucidated.

(c) Functional study of the caldesmon-interacting proteins myosins and tropomyosins

Co-immunoprecipitation has identified myosin and tropomyosins as interacting partners of caldesmon in regulating the actin cytoskeleton. The functional role of myosin and tropomyosin may be studied with knockdown and over-expression experiments. Cell migration/invasion assays may be performed to assay for the change in cell motility upon the expression level alteration of these proteins.

REFERENCES

Albini, A., & Benelli, R. (2007). The chemoinvasion assay: a method to assess tumor and endothelial cell invasion and its modulation. *Nat Protoc*, *2*(3), 504–11.

Areia, M., Carvalho, R., Cadime, A. T., Rocha Gonçalves, F., & Dinis-Ribeiro, M. (2013). Screening for Gastric Cancer and Surveillance of Premalignant Lesions: a Systematic Review of Cost-Effectiveness Studies. *Helicobacter*, *18*(5), 325-37.

Azuma, M., Shi, M., Danenberg, K. D., Gardner, H., Barrett, C., Jacques, C. J., Lenz, H.-J. (2007). Serum lactate dehydrogenase levels and glycolysis significantly correlate with tumor VEGFA and VEGFR expression in metastatic CRC patients. *Pharmacogenomics*, *8*(12), 1705–13.

Barabási, A.-L., Gulbahce, N., & Loscalzo, J. (2011). Network medicine: a network-based approach to human disease. *Nat Rev Genet*, *12*(1), 56–68.

Baumhoer, D., Elsner, M., Smida, J., & Zillmer, S. (2011). CRIP1 expression is correlated with a favorable outcome and less metastases in osteosarcoma patients. *Oncotarget*, *2*(12), 970–975.

Bertuccio, P., Rosato, V., Andreano, A., Ferraroni, M., Decarli, A., Edefonti, V., & La Vecchia, C. (2013). Dietary patterns and gastric cancer risk: a systematic review and meta-analysis. *Ann Oncol*, *00*, 1–9.

Betapudi, V., Licate, L. S., & Egelhoff, T. T. (2006). Distinct roles of nonmuscle myosin II isoforms in the regulation of MDA-MB-231 breast cancer cell spreading and migration. *Cancer Res*, *66*(9), 4725–33.

Bharadwaj, S., & Prasad, G. L. (2002). Tropomyosin-1, a novel suppressor of cellular transformation is downregulated by promoter methylation in cancer cells. *Cancer Lett*, *183*(2), 205–13.

Bhatia, V. N. *et al*. (2009). Software Tool for Researching Annotations of Proteins : Open-Source Protein Annotation Software with Data Visualization. *Anal. Chem.*, *81*(23), 9819–9823.

Bhowmick, N. A, & Moses, H. L. (2005). Tumor-stroma interactions. *Curr Opin Gen & Develop*, *15*, 97–101.

Brabender, J., Lord, R. V, Kumari Wickramasinghe, R. M., Schneider, P. M., Park, J.-M., Hölscher, A. H., & Tom R DeMeester, Kathleen D Danenberg, P. V. D. (2002). Glutathione S-transferase-pi expression is downregulated in patients with Barrett's esophagus and esophageal adenocarcinoma. *J Gastrointest Surg.*, *6*(3), 359–67.

Bravo-Cordero, J. J., Hodgson, L., & Condeelis, J. (2012). Directed cell invasion and migration during metastasis. *Curr Opin Cell Biol*, *24*(2), 277–83.

Brenner, H., Rothenbacher, D., & Arndt, V. (2009). Epidemiology of Stomach Cancer. *Methods Mol Biol*.;472:467-77.

Bretscher, A., & Lynch, W. (1985). Identification and localization of immunoreactive forms of caldesmon in smooth and nonmuscle cells: a comparison with the distributions of tropomyosin and alpha-actinin. *J Cell Biol*, *100*(5), 1656–63.

Broders, A. C. (1925). The grading of carcinoma. *Minn Med*, *8*, 726–730.

Brooks, S. A., Lomax-Browne, H. J., Carter, T. M., Kinch, C. E., & Hall, D. M. S. (2010). Molecular interactions in cancer cell metastasis. *Acta Histochem*, *112*, 3–25.

Catalano, V., Labianca, R., Beretta, G. D., Gatta, G., de Braud, F., & Van Cutsem, E. (2009). Gastric cancer. *Crit Rev Oncol Hematol*, *71*(2), 127–64.

Chaerkady, R., & Pandey, A. (2007). Quantitative proteomics for identification of cancer biomarkers. *Proteomics Clin Appl. 1*(9), 1080–9.

Chaffer, C. L., & Weinberg, R. A. (2011). A Perspective on Cancer. *Science*, *331*, 1559–1564.

Chen, C., Wang, C., Huang, Y., Chien, K., Liang, Y., Chen, W., & Lin, K. (2007). Overexpression of CLIC1 in human gastric carcinoma and its clinicopathological significance. *Proteomics*, *7*, 155–167.

Chen, E. I., & Yates, J. R. (2007). Cancer proteomics by quantitative shotgun proteomics. *Mol Oncol*, *1*(2), 144–159.

Chen, J.-L., Tang, H., Hu, J.-D., Fan, J., Hong, J., & Gu, J.-Z. (2010). Metabolomics of gastric cancer metastasis detected by gas chromatography and mass spectrometry. *World J Gastroenterol.*, *16*(46), 5874–5880.

Chen, L., Yang, S., Jakoncic, J., Zhang, J. J., & Huang, X.-Y. (2010). Migrastatin analogues target fascin to block tumour metastasis. *Nature*, *464*(7291), 1062–6.

Chen, Y., Juan, H., Huang, H., Huang, H., Lee, Y., Liao, M., Chen, Y. (2006). Quantitative Proteomic and Genomic Profiling Reveals Metastasis-Related Protein Expression Patterns in Gastric Cancer Cells research articles. *J Proteome Res*, 5, 2727 – 2742.

Cheng, L. L., Itahana, Y., Lei, Z. D., Chia, N.-Y., Wu, Y., Yu, Y., Tan, P. (2012). TP53 genomic status regulates sensitivity of gastric cancer cells to the histone methylation inhibitor 3-deazaneplanocin A (DZNep). *Clin Cancer Res*, *18*, 4201–4212.

Chhabra, E. S., & Higgs, H. N. (2007). The many faces of actin: matching assembly factors with cellular structures. *Nat Cell Biol*, *9*(10), 1110–21.

Chiodoni, C., Colombo, M. P., & Sangaletti, S. (2010). Matricellular proteins: from homeostasis to inflammation, cancer, and metastasis. *Cancer Metastasis Rev.*, *29*, 295–307.

Cho, H. J., Baek, K. E., Park, S., Kim, I., Choi, Y., Cho, H., Yoo, J. (2009). Human Cancer Biology RhoGDI2 Expression Is Associated withT umor Growth and Malignant Progression of Gastric Cancer. *Human Cancer Biol*, *15*(8), 2612–2619.

Cho, W. C. S. (2007). Contribution of oncoproteomics to cancer biomarker discovery. *Mol Cancer*, *6*(25), 1–13.

Chou, H.-C., & Chan, H.-L. (2012). Targeting proteomics to investigate metastasis-associated mitochondrial proteins. *J Bioenerg Biomembr*, *44*, 629–634.

Chua, T. C., & Merrett, N. D. (2012). Clinicopathologic factors associated with HER2-positive gastric cancer and its impact on survival outcomes--a systematic review. *Intel J Cancer*, *130*(12), 2845–56.

Clark, K., Langeslag, M., Figdor, C. G., & van Leeuwen, F. N. (2007). Myosin II and mechanotransduction: a balancing act. *Trends Cell Biol*, *17*(4), 178–86.

Coburn, N. G. (2009). Lymph nodes and gastric cancer. *J Surg Oncol*, *99*(4), 199–206.

Conti, M. a., & Adelstein, R. S. (2008). Nonmuscle myosin II moves in new directions. *J Cell Sci*, *121*(3), 404–404.

Darnel, A. D., Behmoaram, E., Vollmer, R. T., Corcos, J., Bijian, K., Sircar, K., Bismar, T. a. (2009). Fascin regulates prostate cancer cell invasion and is associated with metastasis and biochemical failure in prostate cancer. *Clin Cancer Res*, *15*(4), 1376–83.

Del Valle-Pérez, B., Martínez, V. G., Lacasa-Salavert, C., Figueras, A., Shapiro, S. S., Takafuta, T., Viñals, F. (2010). Filamin B plays a key role in vascular endothelial growth factor-induced endothelial cell motility through its interaction with Rac-1 and Vav-2. *J Biol Chem.*, *285*(14), 10748–10760.

Deryugina, E. I., & Quigley, J. P. (2006). Matrix metalloproteinases and tumor metastasis. *Cancer Metastasis Rev*, *25*(1), 9–34.

Ding, L., Ellis, M. J., Li, S., Larson, D. E., Chen, K., Wallis, J. W., Fulton, L. L. (2010). Genome remodelling in a basal-like breast cancer metastasis and xenograft. *Nature*, *464*(7291), 999–1005.

Dos Remedios, C. G., Chhabra, D., Kekic, M., Dedova, I. V, Tsubakihara, M., Berry, D. A., & Nosworthy, N. J. (2003). Actin binding proteins: regulation of cytoskeletal microfilaments. *Physiol Rev*, *83*(2), 433–73.

Dudley, A., Shih, S.-C., Cliffe, a R., Hida, K., & Klagsbrun, M. (2008). Attenuated p53 activation in tumour-associated stromal cells accompanies decreased sensitivity to etoposide and vincristine. *British J Cancer*, *99*(1), 118–25.

Duffy, M. J., & Crown, J. (2008). A personalized approach to cancer treatment: how biomarkers can help. *Clin Chem*, *54*(11), 1770–9.

Enomoto, S., Maekita, T., Ohata, H., Yanaoka, K., Oka, M., & Ichinose, M. (2010). Novel risk markers for gastric cancer screening: Present status and future prospects. *World J Gastrointest Endosc*, *2*(12), 381–7.

Fortier, A. M., Asselin, E., & Cadrin, M. (2013). Keratin 8 and 18 loss in epithelial cancer cells increases collective cell migration and cisplatin sensitivity through claudin1 up-regulation. *J Biol Chem*, *288*(16), 11555–71.

Fu, H., Hu, Z., Wen, J., Wang, K., & Liu, Y. (2009). TGF-b promotes invasion and metastasis of gastric cancer cells by increasing fascin1 expression via ERK and JNK signal pathways. *Acta Biochim Biophys Sin*, *41*(8), 648 – 656.

Fu, H., Wen, J.-F., Hu, Z.-L., Luo, G.-Q., & Ren, H.-Z. (2009). Knockdown of fascin1 expression suppresses the proliferation and metastasis of gastric cancer cells. *Pathology*, *41*(7), 655–60.

Ganesan, K., Ivanova, T., Wu, Y., Rajasegaran, V., Wu, J., Lee, M. H., Tan, P. (2008). Inhibition of gastric cancer invasion and metastasis by PLA2G2A, a novel beta-catenin/TCF target gene. *Cancer Res*, *68*(11), 4277–86.

Garcia M, Jemal A, Ward EM, Center MM, Hao Y, Siegel RL, Thun MJ. *Global Cancer Facts & Figures 2007*. Atlanta, GA: American Cancer Society, 2007

Geiger, T., Madden, S. F., Gallagher, W. M., Cox, J., & Mann, M. (2012). Proteomic portrait of human breast cancer progression identifies novel prognostic markers. *Cancer Res*, *72*(9), 2428–39.

Gherardi, E., Birchmeier, W., Birchmeier, C., & Vande Woude, G. (2012). Targeting MET in cancer: rationale and progress. *Nat Rev Cancer*, *12*(2), 89–103.

Glen, A., Evans, C. a, Gan, C. S., Cross, S. S., Hamdy, F. C., Gibbins, J., Rehman, I. (2010). Eight-plex iTRAQ analysis of variant metastatic human prostate cancer cells identifies candidate biomarkers of progression: An exploratory study. *Prostate*, *70*(12), 1313–32.

Görg, A., Obermaier, C., Boguth, G., Harder, A., Scheibe, B., Wildgruber, R., & Weiss, W. (2000). The current state of two-dimensional electrophoresis with immobilized pH gradients. *Electrophoresis*, *21*(6), 1037–1053.

Gravalos, C., & Jimeno, a. (2008). HER2 in gastric cancer: a new prognostic factor and a novel therapeutic target. *Ann Oncol*, *19*(9), 1523–9.

Guan, X., Fung, J., Ma, N., Lau, S., & Tai, L. (2004). Oncogenic role of eIF-5A2 in the development of ovarian cancer. *Cancer Res*, *64*, 4197–4200.

Gunning, P. W., Schevzov, G., Kee, A. J., & Hardeman, E. C. (2005). Tropomyosin isoforms: divining rods for actin cytoskeleton function. *Trends Cell Biol*, *15*(6), 333–41.

Hai, C. M., & Gu, Z. (2006). Caldesmon phosphorylation in actin cytoskeletal remodeling. *Europ J Cell Biol*, *85*, 305–309.

Hanahan, D., & Weinberg, R. A. (2011). Hallmarks of Cancer: The Next Generation. *Cell*, *144*(5), 646–674.

Hartgrink, H. H., Jansen, E. P. M., van Grieken, N. C. T., & van de Velde, C. J. H. (2009). Gastric cancer. *Lancet*, *374*(9688), 477–90.

Haruma, K. (1991). Evaluation of tumor growth rate in patients with early gastric carcinoma of the elevated type. *Gastrointest Radiol.*, *16*, 289–292.

Hashimoto, Y., Shimada, Y., Kawamura, J., Yamasaki, S., & Imamura, M. (2004). The prognostic relevance of fascin expression in human gastric carcinoma. *Oncology*, *67*, 262–270.

He, Q., Cheung, Y. H., Leung, S. Y., Yuen, S. T., Chu, K., & Chiu, J. (2004). Diverse proteomic alterations in gastric adenocarcinoma. *Proteomics*, *4*, 3276–3287.

He, Q.-Y., & Chiu, J.-F. (2003). Proteomics in biomarker discovery and drug development. *J Cellular Biochem*, *89*(5), 868–886.

Helfman, D. M., Levy, E. T., Berthier, C., Shtutman, M., Riveline, D., Grosheva, I., Bershadsky, a D. (1999). Caldesmon inhibits nonmuscle cell contractility and interferes with the formation of focal adhesions. *Mol Biol Cell*, *10*(10), 3097–112.

Hou, Q., Tan, H. T., Lim, K. H., Lim, T. K., Khoo, A., Tan, I. B. H., Chung, M. C. M. (2013). Identification and functional validation of caldesmon as a potential gastric cancer metastasis-associated protein. *J Proteome Res*, *12*(2), 980–90.

Hsieh, H., Yu, J., Ho, L., Chiu, S., & Harn, H. (1999). Molecular studies into the role of CD44 variants in metastasis in gastric cancer. *Mol Pathol*, *52*(1), 25.

Hsu, K.-W., Hsieh, R.-H., Huang, K.-H., Fen-Yau Li, A., Chi, C.-W., Wang, T.-Y., Yeh, T.-S. (2012). Activation of the Notch1/STAT3/Twist signaling axis promotes gastric cancer progression. *Carcinogenesis*, *33*(8), 1459–67.

Hu, B., El Hajj, N., Sittler, S., Lammert, N., Barnes, R., & Meloni-Ehrig, A. (2012). Gastric cancer: Classification, histology and application of molecular pathology. *J Gastrointest Oncol*, *3*(3), 251–61.

Hwang, T.-L., Lee, L.-Y., Wang, C.-C., Liang, Y., Huang, S.-F., & Wu, C.-M. (2012). CCL7 and CCL21 overexpression in gastric cancer is associated with lymph node metastasis and poor prognosis. *World J Gastroenterol*, *18*(11), 1249–56.

Sobin LH, Wittekind C. (2002) International union against cancer TNM classification of malignant tumours. 6th ed.. Hoboken, NJ: John Wiley & Sons.

Ito, M., Takata, S., Tatsugami, M., Wada, Y., Imagawa, S., Matsumoto, Y., Chayama, K. (2009). Clinical prevention of gastric cancer by Helicobacter pylori eradication therapy: a systematic review. *J Gastroenterol*, *44*(5), 365–71.

Jang, S.-I., Kalinin, A., Takahashi, K., Marekov, L. N., & Steinert, P. M. (2005). Characterization of human epiplakin: RNAi-mediated epiplakin depletion leads to the disruption of keratin and vimentin IF networks. *J Cell Science*, *118*, 781–93.

Jemal, A., Center, M. M., DeSantis, C., & Ward, E. M. (2010). Global patterns of cancer incidence and mortality rates and trends. *Cancer Epidemiol Biomarkers Prev.*, *19*(8), 1893–907.

Josson, S., Matsuoka, Y., Chung, L. W. K., Zhau, H. E., & Wang, R. (2010). Tumor-stroma co-evolution in prostate cancer progression and metastasis. *Sem Cell Dev Biol*, *21*(1), 26–32.

Kamal, A., Boehm, M. F., & Burrows, F. J. (2004). Therapeutic and diagnostic implications of Hsp90 activation. *Trends Mol Med.*, *10*(6), 283–90.

Katoh, M. (2005). Epithelial-mesenchyal transition in gastric cancer(review). *Int J Oncol.*, *27*(6), 1677–1683.

Kersey, P. J., Duarte, J., Williams, A., Karavidopoulou, Y., Birney, E., & Apweiler, R. (2004). The International Protein Index: an integrated database for proteomics experiments. *Proteomics*, *4*(7), 1985–8.

Keshamouni, V. G., Michailidis, G., Grasso, C. S., Anthwal, S., Strahler, J. R., Walker, A., Omenn, G. S. (2006). Differential protein expression profiling by iTRAQ-2DLC-MS/MS of lung cancer cells undergoing epithelial-mesenchymal transition reveals a migratory/invasive phenotype. *J Proteome Res*, *5*(5), 1143–54.

Kim, H. J., Kim, Y. M., Lim, S., Nam, Y. K., Jeong, J., Kim, H., & Lee, K. (2009). Ubiquitin C-terminal hydrolase-L1 is a key regulator of tumor cell invasion and metastasis. *Oncogene*, *28*, 117–127.

Kim, J., Kim, M., Lee, H., & Kim, W. (2009). Comparative analysis of protein expressions in primary and metastatic gastric carcinomas. *Hum Pathol.*, *40*(3), 314–322.

Kim, S.-J., Choi, I.-J., Cheong, T.-C., Lee, S.-J., Lotan, R., Park, S. H., & Chun, K.-H. (2010). Galectin-3 increases gastric cancer cell motility by up-regulating fascin-1 expression. *Gastroenterol*, *138*(3), 1035–45.e1–2.

Kirkegaard, T., & Jäättelä, M. (2009). Lysosomal involvement in cell death and cancer. *Biochim Biophys Acta*, *1793*(4), 746–54.

Kitadai, Y., Kodama, M., & Shinagawa, K. (2011). Stroma-Directed Molecular Targeted Therapy in Gastric Cancer. *Cancers*, *3*(4), 4245–4257.

Klemke, R. L. (2012). Trespassing cancer cells: "fingerprinting" invasive protrusions reveals metastatic culprits. *Curr Opin Cell Biol*, *24*(5), 662–9.

Knight, G., Earle, C. C., Cosby, R., Coburn, N., Youssef, Y., Malthaner, R., & Wong, R. K. S. (2013). Neoadjuvant or adjuvant therapy for resectable gastric cancer: a systematic review and practice guideline for North America. *Gastric cancer*, *16*(1), 28–40.

Köhler, C. (2011). Histochemical localization of caldesmon isoforms in colon adenocarcinoma and lymph node metastases. *Virchows Archiv*, *459*(1), 81–9.

Lauren, P. (1965). The two histological main types of gastric carcinoma: diffuse and so-called intestinal-type carcinoma. *Acta Pathol Microbiol Scand*, *64*, 31–49.

Le, A., Cooper, C. R., Gouw, A. M., Dinavahi, R., Maitra, A., Deck, L. M., & Royer, R. E. (2010). Inhibition of lactate dehydrogenase A induces oxidative stress and inhibits tumor progression. *PNAS*, *107*(5), 2037–2042.

Lee, J.-Y., Eom, E.-M., Kim, D.-S., Ha-Lee, Y. M., & Lee, D.-H. (2003). Analysis of gene expression profiles of gastric normal and cancer tissues by SAGE. *Genomics*, *82*(1), 78–85.

Leung, W. K. C., Ching, A. K. K., & Wong, N. (2011). Phosphorylation of Caldesmon by PFTAIRE1 kinase promotes actin binding and formation of stress fibers. *Mol Cell Biochem*., 350(1-2):201-6

Leung, W. K., Wu, M., Kakugawa, Y., Kim, J. J., Yeoh, K., Goh, K. L., others. (2008). Screening for gastric cancer in Asia: current evidence and practice. *Lancet Oncol*, *9*(3), 279–287.

Li, A., Dawson, J. C., Forero-Vargas, M., Spence, H. J., Yu, X., König, I., Machesky, L. M. (2010). The actin-bundling protein fascin stabilizes actin in invadopodia and potentiates protrusive invasion. *Current Biol.*, *20*(4), 339–45.

Lilley, K. S., Razzaq, A., & Dupree, P. (2001). Two-dimensional gel electrophoresis: recent advances in sample preparation, detection and quantitation. *Curr Opin Chem Biol*, *6*, 46–50.

Lin, J. J. C., Li, Y., Eppinga, R. D., Wang, Q., & Jin, J. P. (2009). Roles of caldesmon in cell motility and actin cytoskeleton remodeling. *Intel Rev Cell Mol Biol*, *274*, 1–68.

Look, M., Gao, F., Low, C. H., & Nambiar, R. (2001). Gastric cancer in Singapore. *Gastric cancer*, *4*(4), 219–22.

Ludyga, N., Englert, S., Pflieger, K., Rauser, S., Braselmann, H., Walch, A., Aubele, M. (2013). The impact of Cysteine-Rich Intestinal Protein 1 (CRIP1) in human breast cancer. *Mol Cancer*, *12*, 28.

M.J.Greenberg, C.-L.A.Wang, Lehman, W., & J.R.Moore. (2008). Modulation of actin mechanics by caldesmon and tropomyosin. *Cell Motil Cytoskeleton.*, *65*(2), 156–164.

Ma, J.-L., Zhang, L., Brown, L. M., Li, J.-Y., Shen, L., Pan, K.-F., Gail, M. H. (2012). Fifteen-year effects of Helicobacter pylori, garlic, and vitamin treatments on gastric cancer incidence and mortality. *J Natl Cancer Instit*, *104*(6), 488–92.

Mahadevan, D., & Von Hoff, D. D. (2007). Tumor-stroma interactions in pancreatic ductal adenocarcinoma. *Mol Cancer Ther*, *6*(4), 1186–97.

Marcato, P., Dean, C. A., Pan, D., Araslanova, R., Gillis, M., Joshi, M. (2011). Aldehyde dehydrogenase activity of breast cancer stem cells is primarily due to isoform ALDH1A3 and its expression is predictive of metastasis. *Stem Cells*, *29*(1), 32–45.

Ming, S. C. (1977). Gastric carcinoma: a pathobiological classification. *Cancer*, *39*(6), 2475–2485.

Mortz, E. *et al*. (2001). Improved silver staining protocols for high sensitivity protein identification using matrix-assisted laser desorption / ionization-time of flight analysis. *Proteomics*, *1*, 1359–1363.

Mukhopadhyay, U.K., Mooney, P., Jia, L., Eves, R., Raptis, L., & Mak, A. S. (2010). Doubles Game: Src-Stat3 *versus* p53-PTEN in Cellular Migration and Invasion. *Mol Cell Biol*, *30*(21), 4980–4995.

Mukhopadhyay, Utpal K, Eves, R., Jia, L., Mooney, P., & Mak, A. S. (2009). p53 suppresses Src-induced podosome and rosette formation and cellular invasiveness through the upregulation of caldesmon. *Mol Cell Biol*, *29*(11), 3088–98.

Nishizuka, S., Charboneau, L., Young, L., Major, S., Reinhold, W. C., Waltham, M., Weinstein, J. N. (2003). Proteomic profiling of the NCI-60

cancer cell lines using new high-density reverse-phase lysate microarrays. *PNAS*, *100*(24), 14229–34.

O'Neill, G. M., Stehn, J., & Gunning, P. W. (2008). Tropomyosins as interpreters of the signalling environment to regulate the local cytoskeleton. *Sem Cancer Biol*, *18*(1), 35–44.

Ogawa, K., Utsunomiya, T., Mimori, K., Tanaka, Y., Tanaka, F., Inoue, H., Mori, M. (2004). Clinical significance of elongation factor-1 delta mRNA expression in oesophageal carcinoma. *Br J Cancer*, *91*(2), 282–6.

Okamoto, K., Kashihara, N., Yamasaki, Y., Kanao, K., Maeshima, Y., Sekikawa, T., Makino, H. (2000). Caldesmon isoform associated with phenotypic modulation of mesangial cells. *Exp Nephrol*, *8*(1), 20–7.

Pani, G., Galeotti, T., & Chiarugi, P. (2010). Metastasis: cancer cell's escape from oxidative stress. *Cancer Metastasis Rev*, *29*(2), 351–78.

Pawlak, G., & Helfman, D. M. (2001). Cytoskeletal changes in cell transformation and tumorigenesis. *Curr Opin Gen Develop*, *11*(1), 41–7.

Peleteiro, B., Lopes, C., Figueiredo, C., & Lunet, N. (2011). Salt intake and gastric cancer risk according to Helicobacter pylori infection, smoking, tumour site and histological type. *Br J Cancer*, *104*(1), 198–207.

Piazuelo, M., Epplein, M., & Correa, P. (2010). Gastric cancer: an infectious disease. *Infect Dis Clin North Am.*, *24*(4), 853–869.

Polk, D. B., & Peek, R. M. (2010). Helicobacter pylori: gastric cancer and beyond. *Nat Rev Cancer*, *10*(6), 403–14.

Poon, T. C. W., Sung, J. J. Y., Chow, S. M., Ng, E. K. W., Yu, A. C. W., Chu, E. S. H., Leung, W. A. I. K. (2006). Diagnosis of Gastric Cancer by Serum Proteomic Fingerprinting. *Gastroenterol*, *130*, 1858 –1864.

Quintavalle, M., Elia, L., Price, J. H., Heynen-Genel, S., & Courtneidge, S. a. (2011). A Cell-Based High-Content Screening Assay Reveals Activators and Inhibitors of Cancer Cell Invasion. *Science Signaling*, *4*(183), ra49–ra49.

Raval, G. N., Bharadwaj, S., Levine, E. a, Willingham, M. C., Geary, R. L., Kute, T., & Prasad, G. L. (2003). Loss of expression of tropomyosin-1, a novel class II tumor suppressor that induces anoikis, in primary breast tumors. *Oncogene*, *22*(40), 6194–203.

Ren, J.-S., Kamangar, F., Forman, D., & Islami, F. (2012). Pickled food and risk of gastric cancer--a systematic review and meta-analysis of English and Chinese literature. *Cancer Epidemiol Biomarkers Prev*, *21*(6), 905–15.

Rüschoff, J., Hanna, W., Bilous, M., Hofmann, M., Osamura, R. Y., Penault-Llorca, F., Viale, G. (2012). HER2 testing in gastric cancer: a practical approach. *Modern Pathol*, *25*(5), 637–50.

Ryu, H. S., Park, D. J., Kim, H. H., Kim, W. H., & Lee, H. S. (2012). Combination of epithelial-mesenchymal transition and cancer stem cell-like phenotypes has independent prognostic value in gastric cancer. *Human Pathology*, *43*(4), 520–8.

Sadowski, P. G., Dunkley, T. P. J., Shadforth, I. P., Dupree, P., Bessant, C., Griffin, J. L., & Lilley, K. S. (2006). Quantitative proteomic approach to study subcellular localization of membrane proteins. *Nat Protoc*, *1*(4), 1778–89.

Saghier, A. Al, Kabanja, J. H., Afreen, S., & Sagar, M. (2013). Gastric Cancer: Environmental Risk Factors, Treatment and Prevention. *J Carcinogene Mutagene*, *S14*: 008.

Schoumacher, M., Goldman, R. D., Louvard, D., & Vignjevic, D. M. (2010). Actin, microtubules, and vimentin intermediate filaments cooperate for elongation of invadopodia. *J Cell Biol*, *189*(541-556).

Schwappacher, R., Rangaswami, H., Su-yuo, J., Hassad, A., Spitler, R., & Casteel, D. E. (2012). cGMP-dependent protein kinase Ibeta regulates breast cancer migration and invasion via a Novel Interaction with the Actin / Myosin-associated Protein Caldesmon. *J Cell Science*. 126(Pt 7):1626-36.

Seliger, B., Fedorushchenko, A., Brenner, W., Ackermann, A., Atkins, D., Hanash, S., & Lichtenfels, R. (2007). Ubiquitin COOH-terminal hydrolase 1: a biomarker of renal cell carcinoma associated with enhanced tumor cell proliferation and migration. *Clin Cancer Res. ,13*(1), 27–37.

Shao, H., Wang, J. H.-C., Pollak, M. R., & Wells, A. (2010). A-Actinin-4 Is Essential for Maintaining the Spreading, Motility and Contractility of Fibroblasts. *PloS one*, *5*(11), e13921.

Sleeman, J., & Steeg, P. S. (2010). Cancer metastasis as a therapeutic target. *Eur J Cancer*, *46*(7), 1177–80.

Spano, D., Heck, C., De Antonellis, P., Christofori, G., & Zollo, M. (2012). Molecular networks that regulate cancer metastasis. *Sem Cancer Biol*, *22*(3), 234–249.

Stevenson, R. P., Veltman, D., & Machesky, L. M. (2012). Actin-bundling proteins in cancer progression at a glance. *J Cell Sci*, *125*(Pt 5), 1073–9.

Stoecklein, N. H., & Klein, C. A. (2010). Genetic disparity between primary tumours, disseminated tumour cells, and manifest metastasis. *Int J. Cancer*, *126*(3), 589–98.

Stylli, S. S., Kaye, A. H., & Lock, P. (2008). Invadopodia: at the cutting edge of tumour invasion. *J Clin Neurosci*, *15*(7), 725–37.

Szklarczyk, D., Franceschini, A., Kuhn, M., Simonovic, M., Roth, A., Minguez, P., von Mering, C. (2011). The STRING database in 2011: functional interaction networks of proteins, globally integrated and scored. *Nucleic Acids Res*, 39(Database issue):D561-8.

Tahara, E. (2004). Genetic pathways of two types of gastric cancer. *IARC Sci Publ*, *157*, 327–349.

Tainsky, M. A. (2009). Genomic and proteomic biomarkers for cancer: a multitude of opportunities. *Biochimica et biophysica acta*, *1796*(2), 176–93.

Takikawa, M., Akiyama, Y., Maruyama, K., Suzuki, A., Feng, L., Tai, S., others. (2006). Proteomic analysis of a highly metastatic gastric cancer cell line using two-dimensional differential gel electrophoresis. *Oncol Rep*, *16*(4), 705–711.

Talmadge, J. E., & Fidler, I. J. (2010). AACR centennial series: the biology of cancer metastasis: historical perspective. *Cancer Res*, *70*(14), 5649–69.

Tan, H. T., Tan, S., Lin, Q., Lim, T. K., Hew, C. L., & Chung, M. C. M. (2008). Quantitative and temporal proteome analysis of butyrate-treated colorectal cancer cells. *Mol Cell Proteomics*, *7*(6), 1174–85.

Tan, I. B., Ivanova, T., Lim, K. H., Ong, C. W., Deng, N., Lee, J., Tan, P. (2011). Intrinsic subtypes of gastric cancer, based on gene expression pattern, predict survival and respond differently to chemotherapy. *Gastroenterol*, *141*(2), 476–485.e11.

Tan, V. Y., Lewis, S. J., Adams, J. C., & Martin, R. M. (2013). Association of fascin-1 with mortality, disease progression and metastasis in carcinomas: a systematic review and meta-analysis. *BMC Med*, *11*(1), 52.

Tanaka, J., Watanabe, T., Nakamura, N., & Sobue, K. (1993). Morphological and biochemical analyses of contractile proteins (actin, myosin, caldesmon and tropomyosin) in normal and transformed cells. *J Cell Sci*, *104*, 595.

Tew, K. D., Manevich, Y., Grek, C., Xiong, Y., Uys, J., & Townsend, D. M. (2011). The role of glutathione S-transferase P in signaling pathways and S-glutathionylation in cancer. *Free Radic Biol Med*, *51*(2), 299–313.

The Gene Ontology Consortium. (2000). Gene ontology: tool for the unification of biology. *Nat. Genet.*, *25*(1), 25–29.

Tlsty, T. D., & Coussens, L. M. (2006). Tumor stroma and regulation of cancer development. *Annu Rev Pathol Mech Dis*, *1*, 119–50.

Tseng, C.-W., Yang, J.-C., Chen, C.-N., Huang, H.-C., Chuang, K.-N., Lin, C.-C., Juan, H.-F. (2011). Identification of 14-3-3β in human gastric cancer cells and its potency as a diagnostic and prognostic biomarker. *Proteomics*, *11*(12), 2423–39.

Tsukuma, H., Oshima, A., Narahara, H., & Morii, T. (2000). Natural history of early gastric cancer: a non-concurrent, long term, follow up study. *Gut*, *47*(5), 618–21.

Tsutsumi, S., Beebe, K., & Neckers, L. (2009). Impact of heat-shock protein 90 on cancer metastasis. *Future Oncol*, *5*(5), 679–88.

Vicente-Manzanares, M., Ma, X., Adelstein, R. S., & Horwitz, A. R. (2009). Non-muscle myosin II takes centre stage in cell adhesion and migration. *Nat Rev Mol Cell Biol*, *10*(11), 778–90.

Vignjevic, D., Kojima, S., Aratyn, Y., Danciu, O., Svitkina, T., & Borisy, G. G. (2006). Role of fascin in filopodial protrusion. *J Cell Biol*, *174*(6), 863–75.

Vignjevic, D., Schoumacher, M., Gavert, N., Janssen, K.-P., Jih, G., Laé, M., Robine, S. (2007). Fascin, a novel target of beta-catenin-TCF signaling, is expressed at the invasive front of human colon cancer. *Cancer Res*, *67*(14), 6844–53.

Voulgari, A., & Pintzas, A. (2009). Epithelial-mesenchymal transition in cancer metastasis: mechanisms, markers and strategies to overcome drug resistance in the clinic. *Biochim Biophys Acta*, *1796*, 75–90.

Wagner, A. D., Unverzagt, S., Grothe, W., Kleber, G., Grothey, A., Haerting, J., & We, F. (2010). Chemotherapy for advanced gastric cancer (Review). *Cochrane Database Syst Rev*, 3, CD004064.

Wang, C. A., & Coluccio, L. M. (2010). New Insights into the Regulation of the Actin Cytoskeleton by Tropomyosin. *Int Rev Cell Mol Biol.* 281:91-128.

Wang, C.-L. A. (2008). Caldesmon and the Regulation of Cytoskeletal Functions. *Adv Exp Med Biol.*, *644*, 250–272.

Wang, L., Zhu, J.-S., Song, M.-Q., Chen, G.-Q., & Chen, J.-L. (2006). Comparison of gene expression profiles between primary tumor and metastatic lesions in gastric cancer patients using laser microdissection and cDNA microarray. *World J Gastroenterol*, *12*(43), 6949–54.

Wang, P., Bouwman, F. G., & Mariman, E. C. M. (2009). Generally detected proteins in comparative proteomics--a matter of cellular stress response? *Proteomics*, *9*(11), 2955–66.

Wehder, L., Arndt, S., Murzik, U., Bosserhoff, A. K., Kob, R., von Eggeling, F., & Melle, C. (2009). Annexin A5 is involved in migration and invasion of oral carcinoma. *Cell Cycle*, *8*(10), 1552–8.

Wu, W. W., Wang, G., Baek, S. J., & Shen, R. (2006). Comparative Study of Three Proteomic Quantitative Methods , DIGE , cICAT , and iTRAQ , Using 2D Gel- or LC-MALDI TOF / TOF. *J Proteome Res*, 5(3), 651–658.

www.proteinlounge.com.

Xue, G., Hao, L.-Q., Ding, F.-X., Mei, Q., Huang, J.-J., Fu, C.-G., Sun, S.-H. (2009). Expression of annexin a5 is associated with higher tumor stage and poor prognosis in colorectal adenocarcinomas. *J Clin Gastroenterol*, *43*(9), 831–7.

Yang, Y., Toy, W., Choong, L. Y., Hou, P., Ashktorab, H., Smoot, D. T., Lim, Y. P. (2012). Discovery of SLC3A2 cell membrane protein as a potential gastric cancer biomarker: implications in molecular imaging. *J Proteome Res*, *11*(12), 5736–47.

Yasui, W., Oue, N., Aung, P. P., Matsumura, S., Shutoh, M., & Nakayama, H. (2005a). Molecular-pathological prognostic factors of gastric cancer: a review. *Gastric cancer ,8*(2), 86–94.

Yi, X., Luk, J. M., Lee, N. P., Peng, J., Leng, X., Guan, X.-Y., Fan, S.-T. (2008). Association of mortalin (HSPA9) with liver cancer metastasis and prediction for early tumor recurrence. *Mol Cell Proteomics*, *7*(2), 315–25.

Yonemura, Y., Endo, Y., & Fujita, H. (1999). Role of vascular endothelial growth factor C expression in the development of lymph node metastasis in gastric cancer. *Clin Cancer Res*, *5*, 1823–1829.

Yonemura, Y., Endou, Y., & Kimura, K. (2000). Inverse expression of S100A4 and E-cadherin is associated with metastatic potential in gastric cancer. *Clin Cancer Res*, *6*, 4234–4242.

Yoshio, T., Morita, T., Kimura, Y., Tsujii, M., Hayashi, N., & Sobue, K. (2007). Caldesmon suppresses cancer cell invasion by regulating podosome/invadopodium formation. *FEBS Lett*, *581*(20), 3777–82.

Yu, E. J., Lee, Y., Rha, S. Y., Kim, T. S., Chung, H. C., Oh, B. K., Jeung, H. C. (2008). Angiogenic factor thymidine phosphorylase increases cancer cell invasion activity in patients with gastric adenocarcinoma. *Mol Cancer Res*, *6*(10), 1554.

Zhao, J., Zhou, Y., Zhang, Z., Tian, F., Ma, N., Liu, T., Wang, Y. (2010). Upregulated fascin1 in non-small cell lung cancer promotes the migration and invasiveness, but not proliferation. *Cancer letters*, *290*(2), 238–47.

Zheng, H., Shah, P. K., & Audus, K. L. (1996). Evaluation of antiulcer agents with a human adenocarcinoma cell line (AGS). *Intl J Pharmaceutics*, *129*, 103–112.

Zheng, P.-P., van der Weiden, M., & Kros, J. M. (2005). Differential expression of Hela-type caldesmon in tumour neovascularization: a new marker of angiogenic endothelial cells. *J Pathol*, *205*(3), 408–14.

Zong, J., Guo, C., Liu, S., Sun, M.-Z., & Tang, J. (2012). Proteomic research progress in lymphatic metastases of cancers. *Clin Transl Oncol*, *14*(1), 21–30.